

**PREPARATION AND CHARACTERISATION OF  
ZEOLITIC MATERIALS FROM AHOKO CLAY**

**By**

**MOHAMMED, SIDI ALI  
(M.ENG/SEET/2004/921)**

**A THESIS SUBMITTED TO THE POSTGRADUATE SCHOOL,  
FEDERAL UNIVERSITY OF TECHNOLOGY, MINNA**

**IN PARTIAL FULFILMENT OF THE REQUIREMENTS FOR THE  
AWARD OF MASTER OF ENGINEERING DEGREE (M. ENG) IN  
CHEMICAL ENGINEERING,**

**DEPARTMENT OF CHEMICAL ENGINEERING,  
SCHOOL OF ENGINEERING AND ENGINEERING TECHNOLOGY,  
FEDERAL UNIVERSITY OF TECHNOLOGY, MINNA**

**MAY, 2011**

## DECLARATION

I, hereby declare that this thesis titled "PREPARATION AND CHARACTERISATION OF ZEOLITIC MATERIALS FROM AHOKO CLAY" is a record of my own research findings. It has not been presented partially or wholly on any previous work for the award of any degree. Any quotations and sources of information are acknowledged by means of reference.



MOHAMMED SIDI ALI

07-06-2011


DATE



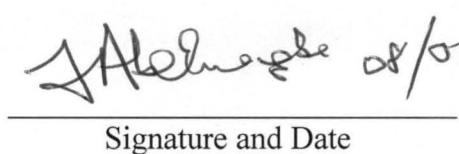
## CERTIFICATION

This is to certify that the thesis titled "PREPARATION AND CHARACTERISATION OF ZEOLITIC MATERIALS FROM AHOKO CLAY" by MOHAMMED SIDI ALI (M.ENG/SEET/2004/921) meet the regulations governing the award of Master Degree in Chemical Engineering of the Federal University of Technology, Minna is approved for its contribution to scientific knowledge and literary presentation.

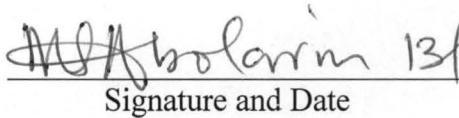
Dr. M. O. Edoga  
Project Supervisor

 07-06-11  
Signature and Date

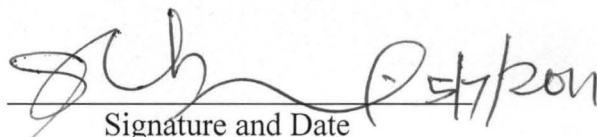
Prof. F. Aberuagba  
H. O. D., Chemical Engineering

 08/06/11  
Signature and Date

Prof. M. S. Abolarin  
Dean, School of Engineering  
And Engineering Technology

 13/06/11  
Signature and Date

Prof. (Mrs.) S. N. Zubairu  
Dean, Post Graduate School

 05/07/2011  
Signature and Date

## **DEDICATION**

This thesis is dedicated to the Almighty Allah for seeing me through this work.

## ACKNOWLEDGEMENTS

My sincere thanks and gratitude go to the Almighty Allah for seeing me through this programme.

I wish to express my indebtedness to my supervisor, Dr. M. O. Edoga who kept on encouraging me to continue with the work despite all frustrations and other odds especially that of lack of equipment for the research work. His contributions by way of attention, advice and constructive criticisms cum comments throughout the period of the research were immeasurable in spite of his tight schedules and commitment as the Head of Department.

My sincere gratitude goes to my late father, Alhaji Muhammadu Mamman Bawan Allah, the late Agankyu of Kakanda, Budon for giving me the opportunity to be educated, and my immediate family for the inconveniences caused to them during this program.

My appreciation goes to the following individuals and organizations: Alhaji Suleiman B. Mohammed of Bank PHB for his financial support; Saka A. Abdulkareem; the management and staff of School of Chemical and Metallurgical Engineering, University of Witwatersrand, Johannesburg, South Africa for carrying out the XRD and adsorption analyses on the samples, and Ashaka Cement Plc for determining the Chemical composition of the samples using their XRF equipment.

## ABSTRACT

The process steps followed to achieve the development of zeolitic materials were beneficiation, calcination, formulation (reactant composition), aging and crystallization. The methods of X-ray fluorescence (XRF) for chemical composition, X - ray diffraction (XRD) for crystal phase identification patterns, and adsorption and desorption data for surface area, pore volume and average pore diameters of the zeolite samples were investigated. Presence of Zeolite Y samples with  $\text{SiO}_2/\text{Al}_2\text{O}_3$  molar ratios of 3.72 and 2.57 were developed from Ahoko clay (kaolin) in Kogi State, Nigeria, under hydrothermal conditions and autogenous pressure using an autoclave. The X - ray diffraction (XRD) analysis revealed that there are possibly about five zeolites of interest that can be developed from the Ahoko clay namely zeolite 5A for sample ZY1, synthesized zeolite ZSM-10 for ZY2 and ZY3, synthesized zeolite Y and dealuminated zeolite Y otherwise known as USY zeolite for samples ZY4 and ZY5. Presence of potassium in Ahoko clay had inhibited the growth of these zeolites and therefore the need for its removal in future research works in this area. However, the crystal phases were reduced in ZY6 and ZY7 samples on dealumination as it eliminated the framework and non-framework aluminum hence it resulted in pure quartz ( $\text{SiO}_2$ ). The Brunauer, Emmett, and Teller (BET) surface areas of the samples varied from 0.9-91.8  $\text{m}^2/\text{g}$  and that for Langmuir varied from 1.0-104.1  $\text{m}^2/\text{g}$  while the total pore volume varied from 0.01-0.14  $\text{cm}^3/\text{g}$ . A constant porosity of 0.5 determined was an indication of consistency in the crystal structure. ZY4 and ZY5 samples were supported on zirconium and used to investigate the conversion of Petroleum Gas Oil (PGO) to distilled fuels. The hydrocracking reaction was carried out in a microreactor at a reaction temperature of 450 °C, contact time of 90 minutes at a catalyst to gas oil ratio of 0.04. It was found that samples ZY4/Zirconium and ZY5/Zirconium catalysts gave a total conversion and total distilled fuels of 44.91 wt. % & 35.48 wt. %, and 45.73 wt. % & 39.39 wt. % respectively, compared to 47.81 wt. % and 36.58 wt. % over unloaded USY zeolite. The hydrocracking activity of ZY5/Zirconium was more than that of ZY4/Zirconium.

## TABLE OF CONTENTS

	PAGE
Title page	i
Declaration	ii
Certification	iii
Dedication	iv
Acknowledgements	v
Abstract	vi
Table of Contents	vii
List of Tables	xi
List of Figures	xii
<b>CHAPTER ONE</b>	
<b>1.0 INTRODUCTION</b>	1
1.1 Molecular Sieves and Zeolites	1
1.2 Aim	3
1.3 Objectives	3
1.4 Approach	3
1.5 Justification	4
1.6 Research Constraints	4
<b>CHAPTER TWO</b>	
<b>2.0 LITERATURE REVIEW</b>	5
2.1 Historical Development of Zeolite	5
2.2 Zeolite Composition and Structure	7
2.2.1 Zeolite Surface Chemistry	12
2.3 Zeolite Synthesis	16
2.3.1 General Conditions for Hydrothermal Zeolite Synthesis	17
2.3.2 Conventional Zeolite Synthesis	17
2.3.3 Clay Conversion Processes	21
2.3.4 Kaolin Transitions	22
2.3.5 Industrial Manufacture of Zeolite	24

2.3.6	Synthesis Mechanism	25
2.3.7	Factors that affect Zeolite Crystallization	31
2.3.8	Dealumination of Zeolites	34
2.4	Properties of Zeolites	37
2.4.1	Adsorption and Molecular Sieve Effects	37
2.4.2	Water Sorption/Desorption	38
2.4.3	Silicon to Aluminum Ratio/Ion Exchange	39
2.4.4	Catalytic Properties	40
2.5	Zeolite Characterization	41
2.5.1	X – Ray Fluorescence Spectroscopy (XRF)	43
2.5.2	X – Ray Diffraction Spectroscopy (XRD)	45
2.6	Adsorption Phenomena	48
2.6.1	Classification of Adsorption Processes	49
2.6.2	Adsorption Isotherms	52
2.6.3	The Brunauer, Emmett and Teller (BET) Isotherm	52
2.6.4	Physical Characteristics of Zeolite Catalyst	60
2.7	Application and Practical Utilization of Zeolites	69
2.7.1	Petroleum Refining Processes for the Production of Fuels	70
2.7.2	Petrochemicals Processing for Aromatics Production and Derivatives	75
2.7.3	Disproportionation of Toulene and Transalkylation of Toulene and Trimethylbenzenes	77
2.7.4	Petrochemicals Processing for Olefins Production	78
2.7.5	Petrochemicals Processing for Detergents Production	79
2.7.6	Separation and Purification Process Applications	81
2.7.7	Manufacturing Industries and Consumer Products Application	81
2.7.8	Environmental Protection Application	81
2.8	Chemistry of Catalytic Processes	82
2.8.1	Types of Cracking Processes	83
2.8.2	Hydrocracking Catalysts	84
2.8.3	Hydrocracking Process	87



2.8.4	Hydrocracking Reactions and Mechanisms	88
2.8.5	Coke Formation	93
<b>CHAPTER THREE</b>		
<b>3.0</b>	<b>MATERIALS AND METHODS</b>	94
3.1	Materials and Equipment	94
3.2	Experimental Procedure	96
3.2.1	Procurement and Pretreatment of the Ahoko Clay	96
3.2.2	Beneficiation of the Clay	96
3.2.3	Centrifugation of the Clay	97
3.2.4	Calcination of the Clay	97
3.2.5	Preparation of Sodium Aluminate for Zeolite Y Synthesis	97
3.3	Preparation of Zeolitic Materials	98
3.3.1	Synthesis of Zeolitic Materials	98
3.3.2	Preparation of Zeolite Y	101
3.3.3	Dealumination and Catalyst enhancement for Evaluation	103
3.4	Characterization of the Developed Samples	103
3.4.1	Determination of Chemical Composition of Raw Materials and Products	103
3.4.2	X – Ray Diffraction (XRD) Analysis	104
3.4.3	Nitrogen Adsorption Measurement	104
3.5	Catalytic Activity	105
<b>CHAPTER FOUR</b>		
<b>4.0</b>	<b>RESULTS</b>	109
<b>CHAPTER FIVE</b>		
<b>5.0</b>	<b>DISCUSSION, CONCLUSION AND RECOMMENDATION</b>	123
5.1	Discussion of Results	123
5.1.1	Chemical and Structural Composition of Kaolin Clay	123
5.1.2	Chemical Composition of Developed Zeolite Samples	123
5.1.3	Diffraction Peaks/Identified Phases of XRD Patterns	124
5.1.4	Analysis of Adsorption Measurement	125
5.1.5	Product Evaluations	128



5.2	Conclusions	129
5.3	Recommendations	130
	<b>REFERENCES</b>	131
	<b>APPENDICES</b>	

## LIST OF TABLES

Table	Page
2.1: Pore Size Classification of Zeolites	13
2.2: Clay Conversion Processes	23
3.1: List of Materials used for the Experiment	94
3.2: List of Equipment used for the Experiment	95
3.3: Reaction Mixture Composition of Zeolitic Materials	100
3.4: Reaction Mixture Composition of Zeolite Y Catalyst	102
4.1: The Chemical Composition of Ahoko Clay in Mass Percentage	109
4.2: The Chemical Composition of Developed Zeolite Samples	110
4.3: XRD Analysis of Developed Zeolite Samples and Reference Sample	112
4.4: Identified Phases of XRD Patterns	113
4.5: Surface Area and Pore Size Distribution	121
4.6: Testing Conditions	122
4.7: Product Distribution of Gas Oil Hydrocracking over ZY4 and ZY5	122

## LIST OF FIGURES

Figure	Page
2.1: Schematic Representation of Zeolite T – Site	9
2.2: Primary Building Blocks (PBUs) of Zeolites	10
2.3: Secondary Building Units (SBUs) found in Zeolite- like Molecular Sieve Structures	11
2.4a: Neutral All – Silica Framework	15
2.4b: Neutral Sodium Balanced Zeolite Framework	15
2.4c: Neutral Calcium Balanced Zeolite Framework	15
2.4d: Schematic Representation of Protonic or Solid Acid form of Zeolite	15
2.4e: Schematic Representation of a Bronsted Acid Site Formation due to Si/Al Substitution in a Zeolite Framework (Neutral Hydrogen Balanced Zeolite Framework)	15
2.4f: Bronsted and Lewis Acid Site	15
2.5: Schematic Representation of Synthesis Methods for Zeolite	20
2.6: Flowsheet for Zeolite Processing	26
2.7: The S – Shaped Crystallization Curve of a Molecular Sieve	30
2.8: Reactant, Product and Restricted Transition – State Shape Selectivity	42
2.9: The Principle of XRF and the Typical Detection Arrangement	44
2.10: Adsorption Isotherm	57
2.11: BET Plot of Gas Phase Adsorption Isotherm	59
2.12: Adsorption Isotherm in Mesoporous solids	65

2.13:	Hydrocracking Mechanism of n-paraffins	90
2.14:	Generally Accepted Desulphurization Mechanism	91
2.15:	Typical Mechanisms of Hydrodenitrogenation	92
3.1:	Synthesis of Zeolitic Materials	99
3.2:	Schematic Representation of Microreactor Configured for a Fixed Catalytic Bed Operation	106
4.1:	Graphical Representation of XRD Pattern for ZY1 – ZY7	111
4.2a:	Plot of Adsorption – Desorption Isotherm for ZY1	114
4.2b:	Plot of Adsorption – Desorption Isotherm for ZY2	115
4.2c:	Plot of Adsorption – Desorption Isotherm for ZY3	116
4.2d:	Plot of Adsorption – Desorption Isotherm for ZY4	117
4.2e:	Plot of Adsorption – Desorption Isotherm for ZY5	118
4.2f:	Plot of Adsorption – Desorption Isotherm for ZY6	119
4.2g:	Plot of Adsorption – Desorption Isotherm for ZY7	120

## CHAPTER ONE

### 1.0

### INTRODUCTION

The demand for gasoline has grown rapidly since 1940, requiring increase in conversion capacity to crack heavier oil fractions. There are many significant efforts being made to increase the conversion of heavier oil fractions to gasoline by cracking (Mu & Mya, 2008).

Zeolites have found wide industrial applications in molecular sieving (separation and purification process), manufacturing industries and consumer products (gas separation process), environmental protection (ion exchange process), and in petroleum refining and petrochemical processing (catalysis) (Sherman, 1999). The catalytic application of zeolites is only a small segment (Natural zeolites, 18%; Adsorbents, 6%; Detergents, 68% and Catalysts, 8%) but has more than 55% of the market on a cash basis. This is because the products obtained by using these catalysts have a value, which are of several magnitudes higher than the catalysts and therefore represent the largest market for zeolites.

There is a strong economic and strategic desire to convert crude petroleum oil to more gallons of gasoline or diesel fuel using zeolite for petroleum cracking thus making them extremely important for many processes. In our quest for industrialization and the presence of refineries, petrochemicals and other manufacturing industries, it therefore requires the setting up of synthetic zeolite production plants in Nigeria since the raw materials are locally available. This will create employment opportunities for our people, reduce our dependence on imported zeolites and at the same time conserve our foreign exchange earnings.

#### 1.1 Molecular Sieves and Zeolites

The term “molecular sieve” is generally used to describe a class of materials that exhibit selective adsorption properties capable of separating components of a mixture based on

differences in molecular sizes and shapes (McBain, 1932). In this context, the term molecular sieve will be used to describe microporous crystalline materials such as clays, aluminosilicates otherwise known as zeolites, silica molecular sieves, aluminophosphates and other related materials.

Zeolites are three dimensional, microporous, crystalline solids with well-defined structures that contain aluminum, silicon, and oxygen in their regular framework. The silicon and aluminium atoms are tetrahedrally connected to each other through the shared oxygen atoms. Thus, the framework of every zeolite is constructed from tetrahedral building blocks ( $TO_4$ ), where T is a tetrahedral coordinated atom. They are a family of complex aluminosilicates that are built from an infinitely extending three-dimensional network of  $AlO_4^{-5}$  and  $SiO_4^{-4}$  tetrahedral linked to each other by the sharing of oxygen atoms (Breck, 1974). Each  $AlO_4$  tetrahedron in the framework bears a negative charge that is balanced by a cation, normally from the group I or II. The framework contains channels and interconnected voids, which are occupied by the cation and water molecules. The cations are mobile and may usually be exchanged by other cations. The water in many zeolites may be removed reversibly leaving intact a crystalline host structure permeated by micropores and voids which make up to 20 – 50% of the total crystal volume of most dehydrated zeolites. The Si/Al ratio is an important characteristic of zeolite. The charge imbalance due to the presence of aluminium in the zeolite framework determines the ion exchange properties of zeolites and induces potential acidic sites. As the Si/Al ratio increases, the cation content decreases, the thermal stability increases and the surface selectivity changes from hydrophilic to hydrophobic and may have no ion exchange or catalytic properties (Tosheva, 1999).



A representative empirical formula for a zeolite written in an oxide form would appear as:

$$M_x/nO \cdot Al_2O_3 \cdot xSiO_2 \cdot yH_2O \quad (1)$$

Where, M – represents the exchangeable cation of valence n (oxidation state of cation). It is monovalent (Group I - Na, K, Li) and/or bivalent (Group II - Ca, Mg, Ba etc).

x – is generally equal to or greater than two.

y – is the degree of hydration (i.e. the number of water molecules in the voids).

Zeolites are usually synthesized under hydrothermal conditions in a period from few hours to days from solutions of sodium aluminate, sodium silicate in the presence of sodium hydroxide and/or organic bases (Dwyer, 1984). Zeolites are desired catalysts because of their high concentration of active acid sites, their high thermal/hydrothermal stability, and size /shape selectivity hence high surface area.

## 1.2 Aim

The main goal of this work therefore was to develop zeolitic material catalysts for petroleum hydrocarbon cracking.

## 1.3 Objectives

Specifically, the objective is to develop process technology (preparative procedures) for synthesis of zeolitic material catalysts under hydrothermal conditions and to characterize the synthesized catalysts using both instrumental and specific performance tests.

## 1.4 Approach

To achieve the above objective of preparing zeolitic material catalysts using locally sourced material typical of Ahoko clay include the following:

- Procurement of the clay from its natural deposit in Ahoko village, Kogi L.G.A of Kogi State, Nigeria;



- Beneficiation and calcination of the kaolin clay, and subsequent formulation of the beneficiated calcined clay into zeolite Y with the other necessary chemical components;
- Characterization of the prepared zeolite samples using appropriate techniques such as X – Ray Fluorescence Spectroscopy (XRF), X – Ray Diffraction Spectroscopy (XRD), and
- A Laboratory Microreactor attached to a Gas Chromatograph (GC) equipped with Thermal Conductivity Detector (TCD) and a Flame Ionization Detector (FID).

### **1.5 Justification**

Presently, zeolites are imported into the country for the local industries that use them. For example, Kaduna Refinery and Petrochemical Company, a subsidiary of the Nigerian National Petroleum Company alone imports about 500 metric tonnes annually (KRPC, Kaduna). This preponderance is expected to increase geometrically in the future with the Federal Government anticipation to expand refineries in line with vision 20 – 2020. Hence, there is a need to develop process technology with a view to putting up a zeolite plant that would create employment and conserve our foreign exchange earnings. Previous research work carried out by Kovo (2006) resulted in the production of zeolite A and D.

### **1.6 Research Constraints**

Though the practical aspect of the preparation was done in Nigeria, the major constraint encountered during the course of this research work was the non – availability of analytical equipment such as XRD and BET isotherms hence the samples had to be sent to South Africa for analysis.

## CHAPTER TWO

### 2.0 REVIEW OF RELATED LITERATURE

#### 2.1 Historical Development of Zeolite

The word zeolite is Greek in origin, emanating from the words Zeo and Lithos meaning to boil and rock, respectively. In 1756, the Swedish mineralogist A. F. Cronstedt discovered that the first zeolite mineral (Stilbite) visibly lost water when heated (Cronstedt, 1756). Subsequent discoveries of zeolites and other porous materials using charcoal by adsorption process in 1777, natural leucynite in 1825, dehydration of zeolites in 1840 and natural faujasite in 1842 (Breck, 1974). Attempts to synthesize silicates under hydrothermal conditions began with experiments by Schafhäutle, who in 1845 reported the preparation of quartz by heating "gel" silica with water in an autoclave. Reversible ion exchange of certain zeolites in 1858 for purification and removal of substances and in 1862, St. Claire Deville reported the synthesis of "Levynite" by heating aqueous solutions of potassium silicate and sodium aluminate in glass tubes at 170°C. Discovery of natural mordenite was in 1864. De Schulten reported the synthesis of "analcime" in 1882. Discovery of natural erionite was in 1890. By 1925, the zeolite researchers became interested in the characterization of zeolites of which the adsorption characteristics of chabazite were attributed to tiny pores ( $< 5 \text{ \AA}$  in diameter) that allowed small molecules to enter but excluded larger ones, hence the term "molecular sieve effect" (Mc Bain, 1932). Even then, there was little interest in zeolites until the late 1930s when the modern founder of zeolite chemistry, Barrer began the characterization of zeolite structure and chemistry.

By 1945, Barrer classified zeolite minerals into three classes depending on the size of the molecules adsorbable rapidly, slowly or not appreciably at room temperature or above (Barrer, 1945). However, zeolites did not find any significant commercial use until synthetic zeolites

were discovered and developed. Barrer's 1948 synthesis of small-pore mordenite at high temperatures and pressures heralded the era of synthetic zeolites (Barrer, 1948). The discovery of zeolites by laboratory synthesis from silicate alumina gels, the changes that occur upon ion exchange and their use as strong environmentally friendly, shape selective catalyst sparked huge interest in companies such as Union Carbide and Mobil. Between 1949 through 1964, Milton and Breck at the Tonawanda, New York, Laboratories of the Linde Air Products Division of Union Carbide Corporation discovered the commercially significant zeolites Linde A, X and Y for separation and purification of air. These zeolites were synthesized from readily available raw materials at much lower temperature and pressure than used earlier. Many of the new synthetic zeolites had larger pore size than most of the known natural zeolites, allowing applications involving larger molecules. In addition, many had larger pore volume, giving higher capacity.

In 1953, Linde type A zeolite became the first synthetic zeolite to be commercialized as an adsorbent to remove O<sub>2</sub> impurity from argon at a Union Carbide plant (Milton, 1968). Union Carbide introduced synthetic zeolites as a new class of industrial adsorbents in 1954 and as hydrocarbon conversion catalysts in 1959. New zeolites and new uses appeared steadily through the 1960s. In 1962, zeolite-based cracking catalysts were introduced and Mobil Oil Corporation synthesized highly siliceous zeolites (ZSM-5, ZSM-8). In 1975 and 1978, ZSM-5 catalysts were used in ethyl benzene production and oil dewaxing respectively. An explosion of new molecular sieve structures and compositions occurred in the 1980s and the 1990s. High resolution electron microscopy and nuclear magnetic resonance (NMR) applied to zeolite in 1980 through 1986 from the synthesis of aluminosilicate zeolites to the microporous silica polymorphs to the microporous aluminophosphate – based polymorphs and metallo – silicate compositions (Flanigen, 1991).

The zeolite cracking catalysts are unique among the many commercial oxide catalysts in that they are crystalline. More than sixty three natural zeolites and over one hundred and fifty synthetic zeolite types are known. Molecular sieves now serve the petroleum refinery, petrochemical industry and other chemical process industries as selective catalysts, adsorbents and ion exchangers (Sherman, 1999).

## 2.2 Zeolite Composition and Structure

Silicon and aluminium are the main tetrahedrally co-ordinated atoms i.e. T-atoms or T-sites in aluminosilicate as shown in Figure 2.1. Aluminosilicate zeolites consist of silicon cations ( $\text{Si}^{4+}$ ) and Aluminum cations ( $\text{Al}^{3+}$ ) that are surrounded by four oxygen anions ( $\text{O}^{2-}$ ). Each oxygen anion connects two cations and this yields a microporous crystalline solid of three dimensional (3D) framework. Each silicon ion has its +4 charge balanced by the four tetrahedral  $\text{O}_2$  and the silica tetrahedral is therefore electrically neutral. Each alumina tetrahedron has a residual charge of -1 since the trivalent aluminium is bonded to four  $\text{O}_2$  anions. The negative charge arises from the difference in formal valency between the silicon and aluminum cations and will be located on one of the oxygen anions connected to an aluminum cation. Therefore, each alumina tetrahedron requires a +1 charge from a cation in the structure to maintain electrical neutrality. The balancing cations can be a metal, non-metal and organic.

The negative charge is compensated by additional non-framework cations like sodium which is generally present after the synthesis of the zeolite. However, for catalysis applications, sodium ions are mostly replaced by ion exchange. They are replaced by protons ( $\text{H}^+$ ) that form a bond with the negatively charged oxygen anions of the zeolite. This results in Bronsted OH acid sites as shown in the figure 2.1 that have proven to be highly active in catalyzing cracking and isomerization reactions. Ion exchange represents the most direct and useful method for the

alteration of zeolite properties (Gates et al., 1979). This ion exchange property gives zeolite the ability to act as selective adsorbents and catalysts in industrial processes.

Zeolite Y exhibits the FAU (faujasite) structure. It has a 3-dimensional pore structure with pores running perpendicular to each other in the x, y, and z planes similar to Linde Type A (LTA), and is made of secondary units 4, 6, and 6-6. The pore diameter is as large as  $7.4\text{\AA}$ , since the aperture is defined by a 12 member oxygen ring, and leads into a larger cavity of diameter  $12\text{\AA}$ .

The fundamental building block of all zeolites is a tetrahedron of four  $\text{O}_2$  anions surrounding a smaller silicon or aluminium ion. These tetrahedrons are arranged so that each of the four oxygen anions is shared in turn with another silica or alumina tetrahedron. The crystal lattice extends in 3 – dimension and the -2 oxidation state of each oxygen can be accounted for. The structural framework can be visualized as  $\text{SiO}_4$  and  $\text{AlO}_4$  tetrahedra called Primary Building Units (PBUs) as shown in Figure 2.2. The PBU of a molecular sieve is the individual tetrahedral unit.

These tetrahedral units are linked together into simple geometrical forms called Secondary Building Units (SBUs) as shown in Figure 2.3. The tetrahedra are arranged so that the zeolites have an open framework structure, leading to a series of pores and channels with high surface area (Breck, 1974).

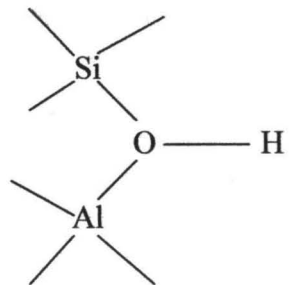
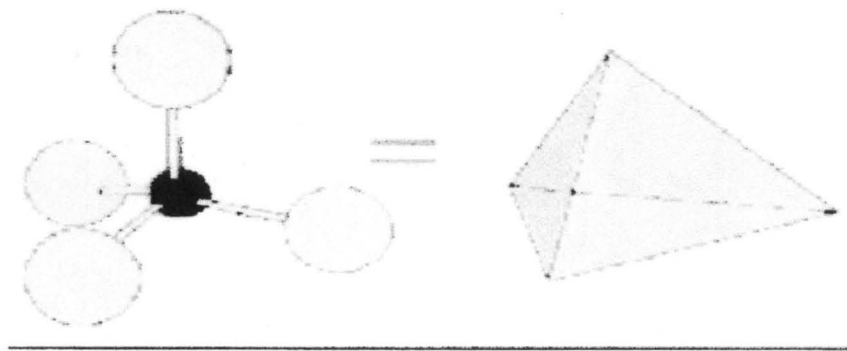


**Figure 2.1: Schematic Representation of Zeolite T - Site**

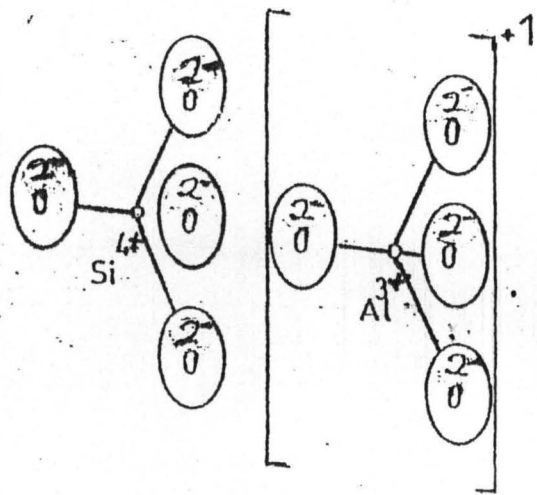


Figure 2.2: Primary Building Blocks (PBUs) of Zeolites



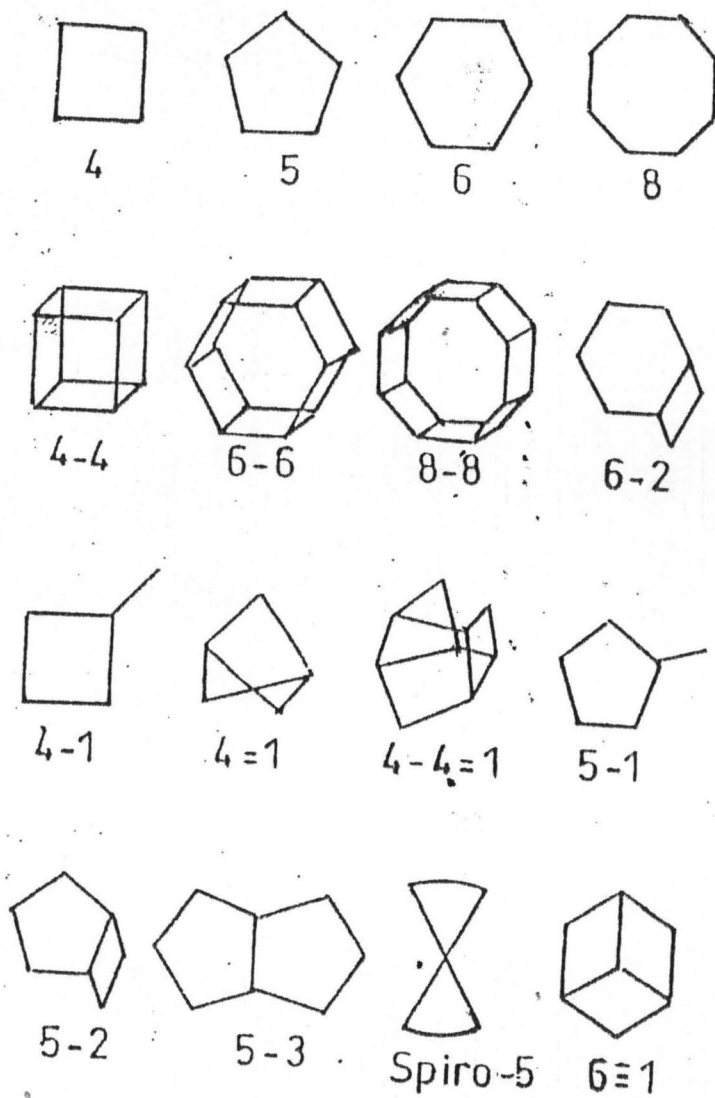


Figure 2.3: Secondary Building Units (SBUs) found in Zeolite – like Molecular Sieve Structures

In all zeolites, the free aperture resulting from 4-, 6-, 8-, 10- or 12- membered rings of oxygen atoms determines pore diameters, and these have maximum values calculated to be 2.6, 3.6, 4.2, 6.3 and 7.4 Å respectively as in Table 2.1 (Barrer, 1968, Breck, 1974). Only zeolites with 8 – and 12 – membered oxygen rings have found major catalytic applications. The smaller apertures place unacceptable size limitations on the molecules to be adsorbed. The zeolites of industrial importance, which are used as catalysts in cracking and related reactions, are zeolites A, X and Y, erionite and mordenite are the only ones of importance (Gates et al., 1979).

### 2.2.1 Zeolite surface chemistry

One of the most important roles of zeolites is as solid acid catalysts for petrochemical processes (being solid they are easily removable from products and therefore environmentally friendly). Each zeolite has an all silica polymorph; in all silica frameworks, there is charge neutrality due to a 4<sup>+</sup> charge on the Si atoms and two O<sup>-</sup> with a 2<sup>+</sup> charge per Si. Zeolites are crystalline solids made up of SiO<sub>4</sub> building blocks. These tetrahedral units join together to form several different ring and cage structures as shown in Figure 2.4a (Windsor, 1998). The standard synthesis techniques generally use sodium and calcium for charge compensation. The surface of the zeolite structure can be schematically represented for sodium form as shown in Figure 2.4(b). If Ca<sup>2+</sup> is replaced by Na<sup>+</sup>, the structure is shown in Figure 2.4(c). The single calcium ion balances the charges of two AlO<sub>4</sub> groups. In the true structure, the negative charge is not localized on one tetrahedron but is at least partially distributed over a number of oxygen anions, which interact through either 6- or 12-fold co-ordination with a cation.

**TABLE 2.1: Pore Size Classification of Zeolites**

<b>Designation of Pore</b>	<b>Pore diameter A<sup>o</sup></b>	<b># Os in Pore opening</b>	<b>Example</b>
Small	3 – 5	8	Erionite Linde type A (LTA) Sodalite Zeolite A
Medium	5 – 6	10	Pentasil, Silicate and ZSM – 5
Large	6 – 9	12	Zeolite $\beta$ , X, Y
	cages:12 - 13	(or 18)	MOR
Extra Large	> 20		MCM – 41

(Susan, 2003)

The completed sodium form of the zeolite is then stirred in a solution of  $\text{NH}_4^+$ , which replaces the sodium ion ( $\text{Na}^+$ ) at the cation exchange sites in the zeolite. Once all the sodium has been replaced by ammonium, the zeolite is dried and calcined to liberate ammonia. The formation of the resultant zeolite (hydrogen Y zeolite) by ion exchange with ammonium salt to replace the  $\text{Na}^+$  followed by heating to decompose the  $\text{NH}_4^+$  into  $\text{NH}_3$  and  $\text{H}^+$  (now in its protonic or solid acid form) is shown schematically in Figure 2.4(d). The characteristic that separates zeolites and their related mineral counterparts from all silica minerals, is the substitution of metals (Al, Ga, Ti, Zr, V, Fe, Sn etc) other than silicon into the crystalline framework (aluminum in the case of zeolites). The addition or substitution of aluminum, a tri-valent cation into the framework generates a -ve charge in the crystal that must be compensated for with a +ve charge. This charge compensation (cation) in zeolite chemistry being the proton, however, in order to be of catalytic interest, that cation should be hydrogen. The protons probably bond immediately with one of the lattice oxygen to give OH groups as shown in figure 2.4(e). The acid sites represent potential Bronsted proton donating acid site, as shown later to have strong Bronsted acidity. Upon further heating to temperatures exceeding  $450^\circ\text{C}$ , dehydroxylation of the above structure occurs as shown in figure 2.4(f).

These structural considerations suggest that two Bronsted acid sites are lost for every Lewis acid site generated and that acid - base and positive - negative site pairs are generated. The dehydroxylation can be reversed if water is added back, starting at the highest temperature of dehydroxylation, and cooling is done in the presence of water vapour (Bolton & Lanewala, 1970).

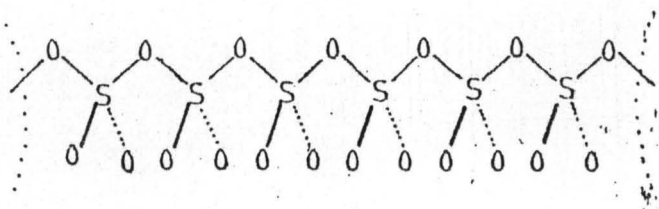


Figure 2.4(a): Neutral All – Silica Framework

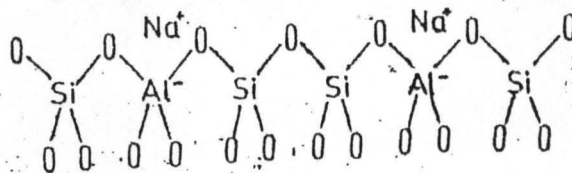


Figure 2.4(b): Neutral Sodium Balanced Zeolite Framework

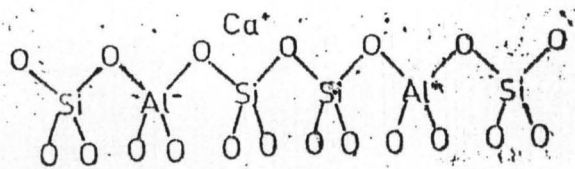


Figure 2.4(c): Neutral Calcium Balanced Zeolite Framework

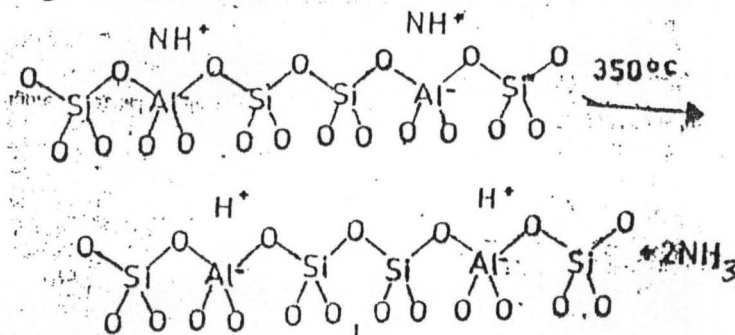


Figure 2.4(d): Schematic Representation of Protonic or Solid Acid form of Zeolite

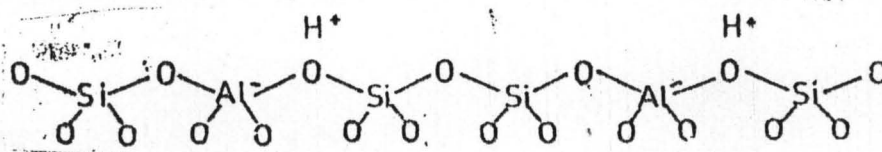


Figure 2.4(e): Schematic of a Bronsted Acid Site Formation due to Si/Al Substitution in a Zeolite Framework (Neutral Hydrogen Balanced Zeolite Framework)

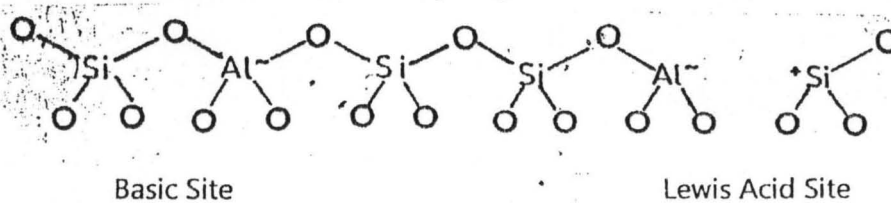


Figure 2.4(f): Bronsted and Lewis Acid Site

The highly acidic sites, combined with high selectivity arising from shape selectivity and large internal surface area makes the zeolite an ideal industrial catalyst. The zeolitic proton has been used as an efficient solid acid catalyst in several industrial reactions, a major advantage being the heterogeneity of the catalyst and reactant/products allowing easy catalyst recovery. The introduction of the solid acid Y zeolite and fluid catalytic cracking (FCC) revolutionized the process of cracking petroleum, where raw feed stock are pressurized and heated causing large hydrocarbons to break into lighter more useful compounds. This replaced the inefficient free radical based on homogeneous thermal process (which produces excessive amounts of coke and light gases) with a heterogeneous process based on carbocation chemistry reminiscent of the liquid phase. In addition to the solid acid nature of the catalyst, the pore system is vital in the manipulation of selectivity of acid catalyzed reactions. While liquid phase acid catalyzed reactions allow the formation of essentially any transition state, the pore system containing the acid site requires the transition state to be able to fit in the pore system. Any transition state that are too bulky are not formed e.g. formation of some types of coke in ZSM - 5 which are too large to form within the pore system, are not formed (Bradley, 2004).

### **2.3 Zeolite Synthesis**

Zeolites are hydrated aluminosilicates formed in a closed hydrothermal system typically under mild conditions. The term hydrothermal is used in a broad sense to describe zeolite synthesis; however, zeolite synthesis involves the crystallization of reactive aluminosilicate gels or solutions in a basic environment. This goes an inch to explain the crystallization of zeolites from aqueous systems (reaction mixtures) which contain the necessary chemical components in amount corresponding to the composition of the desired product. The nature of the zeolite obtained is determined by the synthesis conditions namely reactant concentrations, pH, time,



temperature, and the nature and concentration of added promoters. Zeolite synthesis involves the crystallization of reactive aluminosilicate gels or solutions in a basic environment (Breck, 1974).

### **2.3.1 General conditions for hydrothermal zeolite synthesis**

The conditions that are usually employed in synthesizing zeolites hydrothermally include the following:

- Amorphous starting reactants containing silica and alumina are mixed together with a cation source, usually high pH introduced in the form of basic medium (alkali metal hydroxide or strong base – alkaline ion etc) are used;
- The aqueous reaction mixture is aged at room temperature and then heated at reaction temperatures above 100°C in a sealed autoclave with low autogeneous pressure at saturated vapour pressure of water;
- The reactants remain amorphous after raising the synthesis temperature for some time;
- After the induction period, a high degree of super-saturation of the components of the gel leading to the nucleation of a large number of zeolite crystals, and time required for crystallization varies from a few hours to several days; and
- All amorphous materials are gradually replaced by an approximately equal mass of zeolite crystals recovered by filtration, washing and drying (Breck & Flanigen, 1968, Barrer, 1968).

### **2.3.2 Conventional zeolite synthesis**

The synthesis of cation aluminosilicates may be performed by

- a) Gel or hydrogel process
- b) Clay reaction process

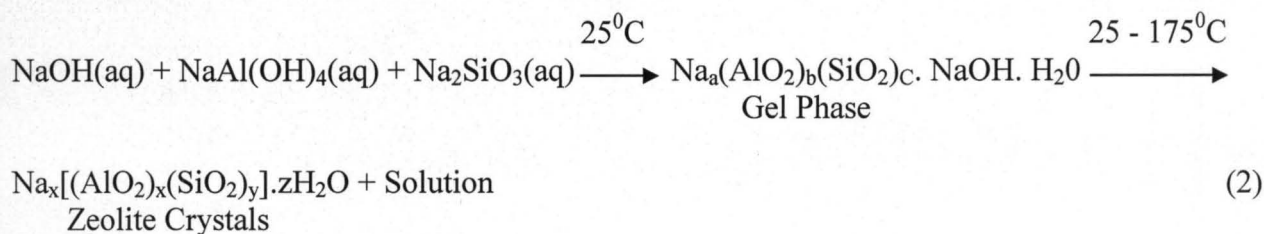
A gel is defined as a hydrous metal aluminosilicate, which is prepared from aqueous solutions, reactive solids, colloidal sols, or reactive aluminosilicates such as the residue structure



of metakaolin (derived from kaolin clay by dehydroxylation) and glasses. Reactions in aqueous systems at temperature of 100°C or less, in general, which form gels prior to crystallization are termed Gel process while the term clay reaction process is the name given to the aqueous, atmospheric pressure process of silicification of cations with a clay mineral at elevated pressures and temperatures (greater than 100°C), the synthesis is called hydrothermal. These gels are formed upon mixing typical reactants: a silica source (sodium silicate), an aluminate source (sodium aluminate solution) in the presence of alkali hydroxide source (sodium hydroxide and/or organic bases), the latter being used mainly to control pH as shown in Figure 2.5.

The gels are crystallized in a closed hydrothermal system at temperatures varying from room temperature to elevated temperatures (usually 300°C). The pressure is generally the autogeneous pressure, which is approximately equivalent to the saturated vapour pressure (SVP) of water at temperature designated. The time required for crystallization varies from a few hours to several days.

Many of the phases formed are not equilibrium phases, but only metastable ones, which in time are converted to other more stable zeolitic phases. When prepared, the aluminosilicate gels differ greatly in appearance from a stiff translucent nature to opaque gelatinous precipitates, to heterogeneous mixtures of an amorphous solid dispersed in an aqueous solution (Zhdanov, 1968). The sequence of gel preparation and crystallization involves the formation of a hydrous aluminosilicate gel from typical reactants such as sodium aluminate, sodium silicate, silicic acid and sodium hydroxide. The latter being used to control the pH and the crystallization of the gel is done under carefully controlled conditions to give the desired zeolitic phase using the  $\text{Na}_2\text{O}-\text{Al}_2\text{O}_3-\text{SiO}_2-\text{H}_2\text{O}$  as shown by the chemical Equation (2).



The gel is probably produced by the copolymerization of the individual silicate and aluminate species by a condensation polymerization mechanism. The gel composition and structure appear to be controlled by the size and structure of the polymerizing species. The resultant zeolite must be removed from the mother liquor at the proper time and must be thoroughly washed with distilled water to remove sodium silicate from the pore structure.

The reaction mixture is first aged at ambient temperature and then subsequently heated at higher temperature, usually at  $100^{\circ}\text{C}$ . *Aging time* (AT) is defined as a period between the mixing of reagents and the onset of heating to the crystallization temperature. After the initial gel formation, the aging step is necessary to equilibrate the heterogeneous gel mixture with the solution. It is known that aging causes the duration of crystallization, the induction period and the size of crystals in the final products to be gradually reduced and therefore room temperature equilibration or aging reduces the  $\text{SiO}_2/\text{Al}_2\text{O}_3$  ratio in the gel necessary to form zeolite Y. The formation of the zeolites from gels based on reactive colloidal forms of silica is very dependent upon the base concentration, which determines the solubility of the silica in the system. The activity of  $\text{SiO}_2$  in the mixture depends upon the  $[\text{OH}^-]$ . The higher the  $[\text{OH}^-]$ , the lower the activity; thus synthesis of zeolites with high  $\text{SiO}_2/\text{Al}_2\text{O}_3$  requires lower  $[\text{OH}^-]$ . The use of a more reactive amorphous silica is important in the synthesis of the high silica-zeolites e.g. zeolite Y.

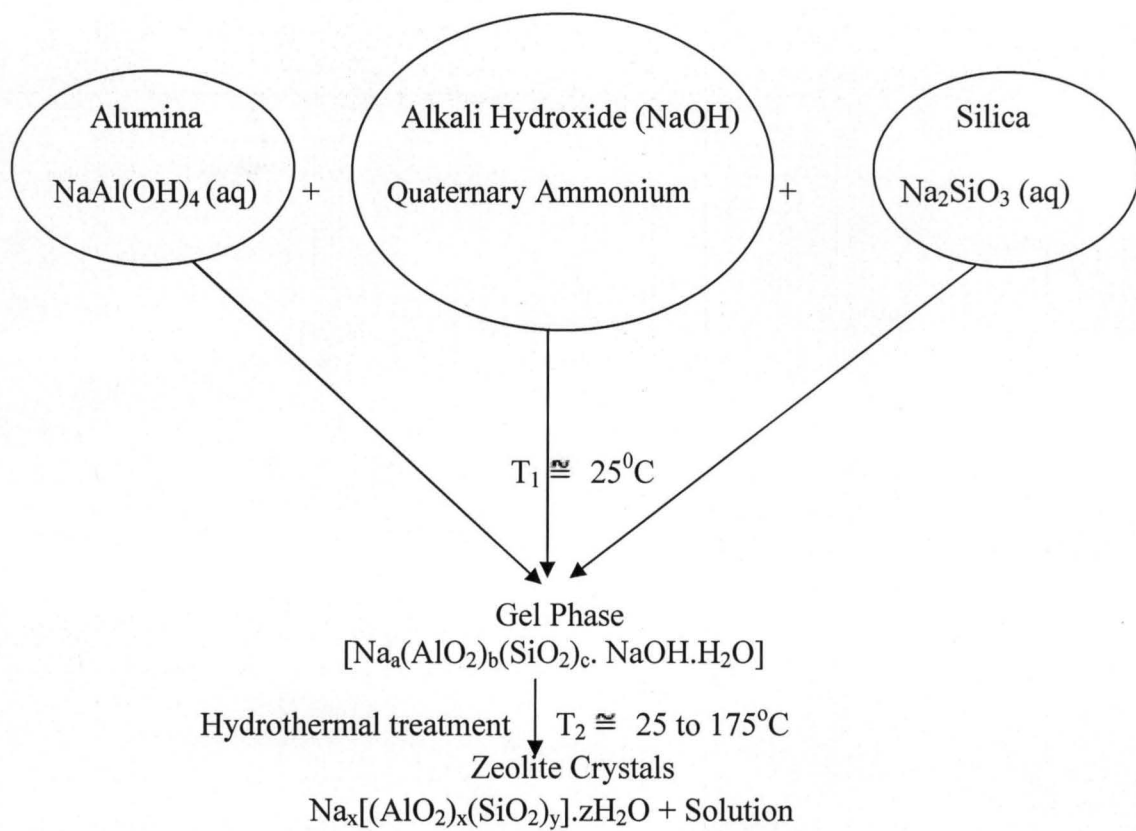
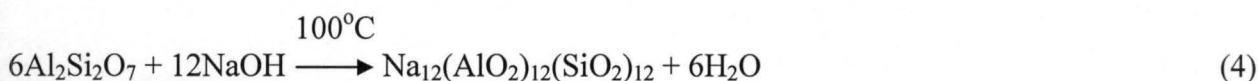
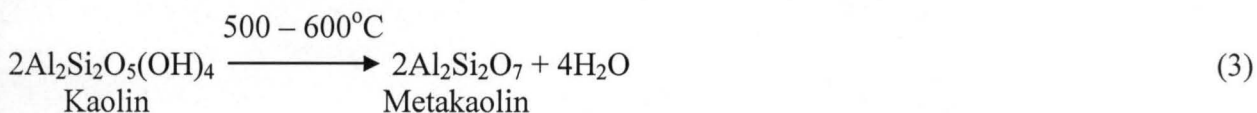


**Figure 2.5: Schematic Representation of Synthesis Methods for Zeolite**

The effect of temperature on the time required for crystallization of the most reactive gels e.g. zeolite X crystallizes in 800 hr at 25°C and in approximately 6 hrs at 100°C. At low temperatures, the more complex and more easily nucleated zeolite Y or X are formed whereas increasing the temperature of crystallization favours the formation of zeolite P followed by analcime. At ambient temperature, the composition is dominated by zeolites Y, A and X. Above 150°C zeolite P is the dominant phase along with zeolite A and analcime (Breck & Flanigen, 1968).

### 2.3.3 Clay conversion processes

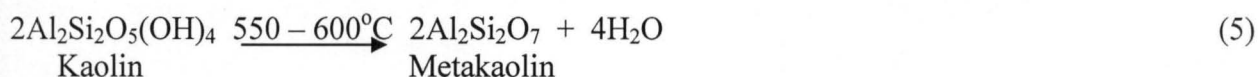
The major clay type starting material used in the manufacture of molecular sieves zeolite is of kaolin group, chemically represented as  $\text{Al}_2\text{O}_3 \cdot 2\text{SiO}_2 \cdot 2\text{H}_2\text{O}$ . In order to “activate” the clay for the reaction to occur, the kaolin is usually converted or dehydroxylated to metakaolin. The dehydroxylation of kaolin is generally accomplished by thermal treatment (air calcination) at temperatures of about 600°C. This amorphous material, commonly referred to as metakaolin is then treated with aqueous alkali metal hydroxide solutions at a convenient temperature of about 100°C. A product is obtained which may be more or less suitable for conversion to a zeolite. The zeolite formed depends upon the composition of the reaction mixture. For example, if only NaOH is added to the metakaolin, then zeolite A is formed according to reaction schemes 3 and 4.



The pulverized clay material is mixed with the aqueous base (NaOH or KOH) for periods of 1–5 hrs at pressures ranging from atmospheric to 200 Kg/cm<sup>3</sup>, and then heated in a steam autoclave. The mixture is filtered and the residue and filtrate are analyzed. If the solid residue weighs more than the starting clay, it is an indication that Na<sub>2</sub>O and H<sub>2</sub>O were incorporated into the clay. At times, the raw clay material is calcined at temperatures ranging from 500 – 1260°C before the hydrothermal treatment.

### 2.3.4 Kaolin Transitions

In general, two types of calcined kaolin have been used namely metakaolin, calcined at 550°C and kaolin calcined at 925°C as shown in Table 2.2. Kaolin type of clays when heated at 550–600°C undergoes dehydration (endothermic dehydroxylation) to produce disordered metakaolin phase according to the reaction in chemical Equation 5.



The theoretical weight loss for this change is 13.95%. After forming the initial metakaolin slurry, a low temperature, aging treatment improves the conversion of the clay to zeolite. Additional SiO<sub>2</sub> must be added to the reactant mixture for zeolite to be converted to higher silica contents with SiO<sub>2</sub>/Al<sub>2</sub>O<sub>3</sub> ratio greater than 2. For example, to produce zeolite X, the reaction mixture may have a composition of 4Na<sub>2</sub>O.Al<sub>2</sub>O<sub>3</sub>.4SiO<sub>2</sub>.16OH<sub>2</sub>O. The additional silica is in the form of sodium silicate.

Another form of synthesizing zeolites with high SiO<sub>2</sub>/Al<sub>2</sub>O<sub>3</sub> ratio from clays involves increasing the ratio in the starting clay by first leaching alumina from the clay by acid treatment e.g., zeolite Y with a SiO<sub>2</sub> / Al<sub>2</sub>O<sub>3</sub> of 4.1 was prepared from acid leached metakaolin using an overall composition of 4.8 Na<sub>2</sub>O.Al<sub>2</sub>O<sub>3</sub>.9.6SiO<sub>2</sub>.192H<sub>2</sub>O. The yield was 95%.

**Table 2.2: Clay Conversion Processes**

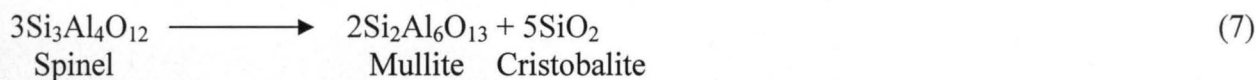
<b>Process</b>	<b>Reactants</b>	<b>Product</b>
Slurry-high purity powder	- Caustic - Metakaolin - Sodium silicate - Allophane	- Type A - Type X - Type Y
In situ crystallization of preform to yield high purity, binderless pellet	- Metakaolin - Caustic - Sodium silicate - Diatomaceous earth	- Type A - Type X - Type Y - Zeolon-Mordenite
Partial, in situ conversion of preformed particle to yield zeolite in clay- derived matrix	- Caustic - Metakaolin - Sodium silicate - Raw kaolin	- Type X - Type Y



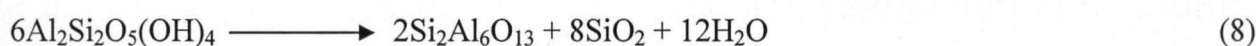
At 800°C the density is only 1.52% less than that of the original kaolin because the interlayer spacing decreases from 7.15 Å to 6.3 Å. As the calcination temperature is raised, the unstable reactive metakaolin becomes stable and rearranges to give defect aluminium – silicon spinel structure normally referred to as gamma alumina phase at 925°C according to the reaction Equation 6.



The so called  $\gamma$  -  $\text{Al}_2\text{O}_3$  phase is not a simple mixture of amorphous silica and alumina but retains some order associated with cubic or hexagonal layers. This spinel phase persists over the temperature range of 925 – 1075°C. The transformation in Equation 6 produces an additional mole of  $\text{SiO}_2$  in a very reactive form. At still higher temperatures, 1050 – 1100°C, the spinel phase converts to a mullite and/or sillimanite of uncertain composition with the additional elimination of  $\text{SiO}_2$  which appears as cristobalite according to the chemical Equation 7.



At higher temperatures, the mullite and cristobalite continue to form. The overall reaction of kaolin to mullite at this elevated temperature is given by the Equation 8 (Breck, 1973).



### 2.3.5 Industrial manufacture of zeolite

The process flow sheet for the manufacture of any zeolite in the form of high purity powder is illustrated in Figure 2.6. This process is based upon the use of kaolin clay that is calcined at 550°C. The type of zeolite produced depends on the reactants, which are mixed in the gel make – up tank. The ambient aging step is also used prior to the crystallization step. Calcined kaolin is the starting material for making several zeolites such as type A, X and Y. Complete conversion of the clay to zeolite powder in high purity is achieved. In order to crystallize zeolite

type X or Y, additional silica is needed to increase the  $\text{SiO}_2 / \text{Al}_2\text{O}_3$  ratio of the reactant mixture. In the preparation of zeolite Y, a larger quantity of additional silica is generally added as sodium silicate. Addition of inorganic salts enhances formation of zeolite Y from kaolin e. g, NaCl may be added to the reactant mixture in the ratio of 2 moles of NaCl per mole of alumina (Barrer, 1982).

### 2.3.6 Synthesis mechanism

Zeolites are synthesized in three steps namely induction period, nucleation, and crystallization (crystal growth). Two theories have been proposed to account for the mechanism of zeolite synthesis, which is:

- In the solid – solid transformation mechanism, crystallization of the zeolite occurs directly from the amorphous gel to the crystalline phase (Zhandov, 1971).
- In the solution crystallization mechanism, nuclei form and grow in the liquid phase (Kerr, 1966).

The latter proposes that equilibrium exists between the solid – gel phase and the solution, and that nucleation occurs in the solution. The gel material dissolves continuously and the dissolved species are transported to the nuclei crystals in the liquid phase. In addition to zeolite formation via either of the two transformations, there is evidence to indicate that both types of transformation can sometimes occur simultaneously. In some cases, zeolite can also be crystallized from a single – solution system containing no secondary solid gel phase (Ueda & Koizumi, 1979). From the single – phase solution studies, it appears that nucleation and subsequent crystallization can occur readily in the solution phase, leading to the possibility that the presence of a solid - gel phase acts only to supply nutrients to the solution. The ease with which the zeolites crystallize is attributed to the high reactivity of the gel, the concentration of

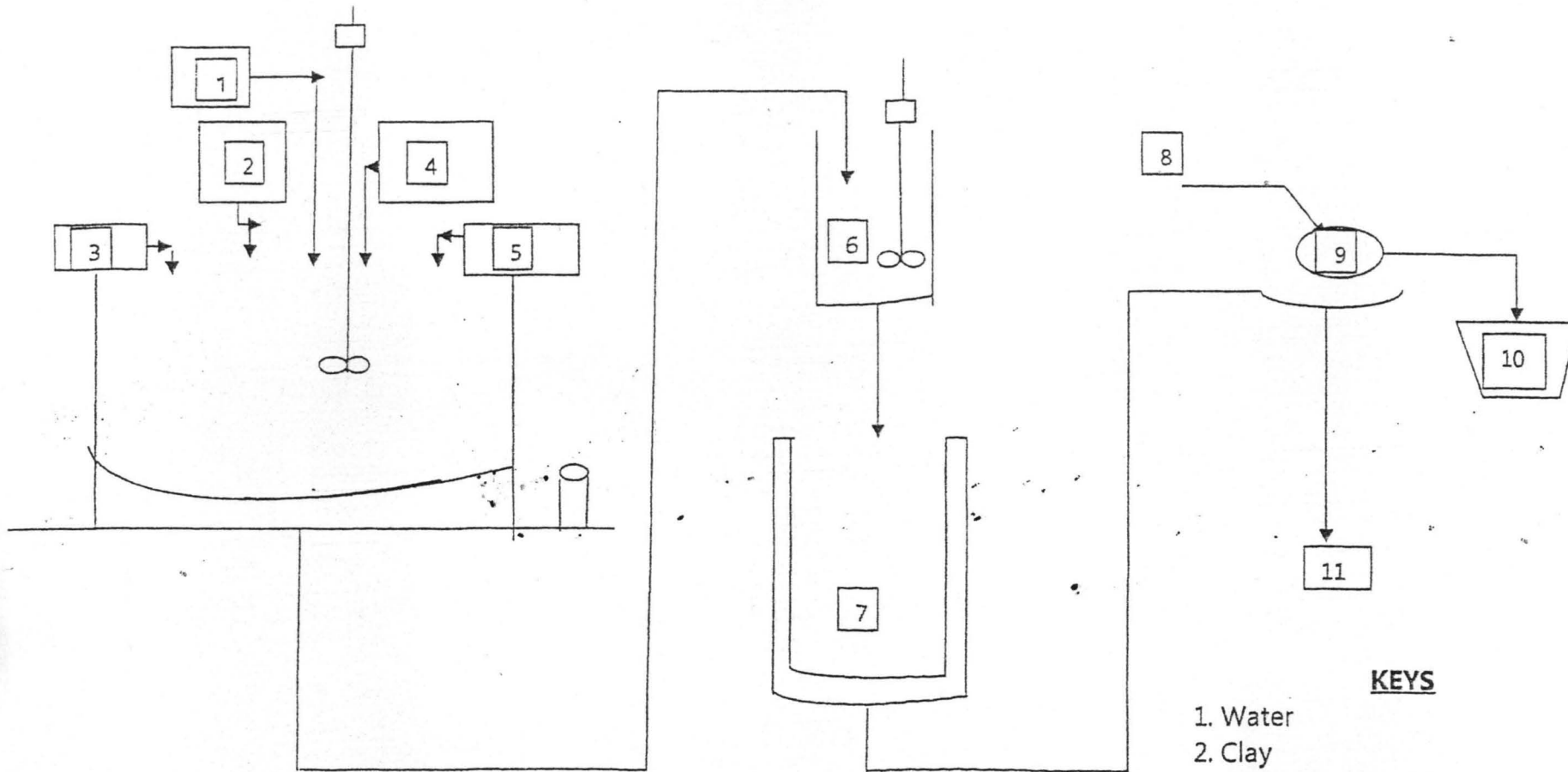


Figure 2.6: Flowsheet for Zeolite Processing

- KEYS**
1. Water
  2. Clay
  3. Sodium Hydroxide
  4. Sodium aluminate
  5. Sodium Silicate
  6. Room Temperature Aging Tank
  7. Autoclave 100°C
  8. H<sub>2</sub>O at 80°C
  9. Filter
  10. Cake
  11. Filtrate to waste treatment

the alkali hydroxide and the high surface activity due to the small particle size of the solid phase concerned (Barrer, 1982).

*a. The induction period* - is the time ( $t$ ) between the notional start of the reaction and the point at which crystalline product is first observed. The period  $\tau$  is divided into a number of subunits:  $\tau = t_r + t_n + t_g$ . (9)

Where  $t_r$  - is referred to as the relaxation time and is the time required for the system to achieve a quasi-steady state distribution of molecular clusters. In zeolite terms, this is equated to equilibration reaction taking place on mixing the reagents and allowing them to reach the reaction temperature during which period the observable distribution of silicate and aluminate ions (and other species) is established.

$t_n$  - the time for the formation of a stable nucleus and

$t_g$  - the time for the nucleus to grow to a detectable size

At the point where the reactants for the zeolite synthesis are initially mixed together, a visible gel is frequently formed which is referred to as the primary amorphous phase (a clear synthesized solution that is colloidal). The primary amorphous phase represents the initial and immediate product from the reactants and is non - equilibrium and probably heterogeneous product containing

- i) precipitated amorphous aluminosilicates,
- ii) coagulated silica and alumina precipitated from starting materials destabilized by the change in pH and increase in salt content and
- iii) unchanged reactants.

After sometimes, either on standing or more rapidly on heating at reaction temperature, the above mixture undergoes changes due to equilibration reactions which occur and is converted

into a pseudo – steady – state intermediate, called secondary amorphous phase. The relationship between the solid and solution phases approaches equilibrium and a characteristic distribution of silicate and aluminosilicate anions is established. A pH measurement will now provide a useful reference point from which, in high silica zeolite synthesis, the progress of the reaction can be monitored by recording subsequent changes. In the final stage of the reaction (usually at elevated temperature for a prolonged period), the secondary amorphous phase is converted into the crystalline zeolite product.

**b) *Zeolite nucleation***

Nucleation takes place after an induction period. Equilibration, which allows the conversion of primary to secondary amorphous phases, forms an extremely important part of the zeolite synthesis process. By this means, the initial gel reacts with solution species to establish (or approach) a pseudo – steady – state distribution of liquid phase species, predominantly ionic. Nucleation (germ nuclei) occurs from very small aggregates of dissolved precursor species that become larger with time (crystal growth) by condensation polymerization mechanism of dissolved species (i.e. the individual silicate and aluminate species) on the growing surface (Barrer, 1982). When solutions of the aluminate and poly – silicate anions are mixed to form hydrous gel, the aluminate anions and silicate anions undoubtedly undergo a polymerization process. The gel structure thus produced is amorphous and its hydrogel composition and structure appear to be controlled by the size and structure of the polymerizing species. Since the silicate may vary in chemical composition and molecular weight distribution, different silicate solutions may lead to differences in the gel structure. Therefore, gelation controls the nucleation of the zeolite crystallites. Primary nucleation may be homogeneous (from solution) or heterogeneous (induced by foreign particles); Secondary nucleation (induced by crystals) may be



considered as a special case of heterogeneous nucleation in which the nucleating particles are crystals of the same phase. The high degree of supersaturation of the ionic species present in the gel lead to rapid and heterogeneous nucleation and the formation of a large number of nuclei.

Zeolite nucleation is therefore a discreet event which could be defined as “a phase transition whereby a critical volume of a semi – ordered gel network is transformed into a structure which is sufficiently well ordered to form a viable growth centre from which the crystal lattice can propagate”. Zeolite nucleation is a summation of complex chain of events such as

- i. mixing of reactants to give a non – equilibrated, inhomogeneous starting material (primary amorphous phase);
- ii. equilibration to form a semi – organized precursor (secondary amorphous phase) containing islands of order or proto – nuclei;
- iii. the establishment of sufficient regular structure within a statistical distribution of ordered sites to enable such structure to propagate (nucleation step itself); and
- iv. the beginnings of crystal growth on the established nuclei.

**c. *Crystallization (crystal growth)***

Crystallization formation has been reported to be a function of time. For this reason, time can be used to determine the final zeolite produced. During crystallization of the gel, the aluminate and silicate components must undergo a rearrangement in order to preform the crystalline structure, which occurs by depolymerization and solubilization of the gel (Colin & Paul, 2005). Figure 2.7 shows the characteristic S – shaped crystallization curve of a molecular sieve, divided into three periods a, b, and c. The “induction period” is part a, during which crystalline nuclei form but no crystalline product is observed. The length of the induction period is reduced by adding crystal seeds to the initial mixture. During the growth period b, crystal



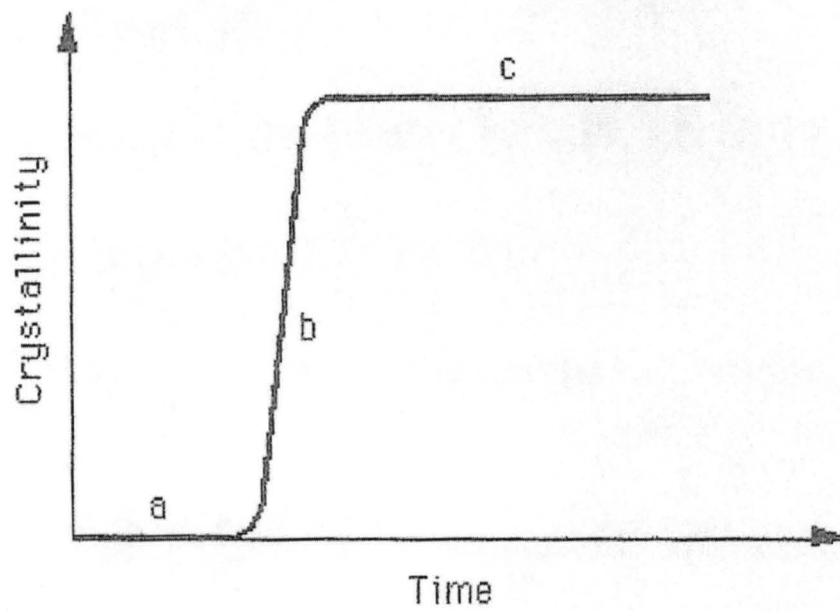


**Figure 2.7: The S – Shaped Crystallization Curve of a Molecular Sieve**

nuclei grow rapidly in size. Finally, during the period c, the crystallization is over, and the products may transform into a more stable phase requiring a longer reaction time.

Specific information concerned with crystallization mechanism and kinetics is rather limited. The rate of growth of zeolite from sodium aluminosilicate gels can be represented by

$$\left(\frac{dWc}{dt}\right)_T = K(\text{OH})^2 \quad (10)$$

Where,  $Wc$  is the degree of conversion. The plots of crystal size against time typically show a constant linear growth rate for most of the reaction with a final tailing off due to nutrient depletion.

### 2.3.7 Factors that affect zeolite crystallization

The main parameters in zeolite crystallization, which can be modified during the synthesis procedure in terms of structure and properties, include:

- the physical and chemical nature of the reactants and their concentrations used in preparing the reaction mixture (its overall chemical composition of the synthesis mixture)
- presence of cations or organic template in the reaction mixture;
- presence of hydroxide (OH);
- silica to alumina ( $\text{SiO}_2/\text{Al}_2\text{O}_3$ ) ratio and level of water ( $\text{H}_2\text{O}$ );
- temperature;
- pH (i.e. the degree of acidic or alkaline character);
- time of crystallization;
- aging, stirring of the reaction mixture, order of mixing, effect of prepolymerization of the silicate.
- the use of seed crystals

It is a common and very useful practice to add seed crystals to zeolite reaction mixtures (Thompson, 1992, Thompson, 1998, Gonthier & Thompson, 1994). The two main effects anticipated are:

- i. a reduction in the synthesis reaction time and
- ii. a “direction” of the synthesis towards a desired phase with consequent reduction in impurities. It is also possible to exert control over product crystal size distribution (Lechert & Kacirek, 1975, Cundy & et al., 1995, Verduijn, 1993, Cundy & Forest, 2003).

The basic action of seed crystals when added effectively is to provide surface area in which the required product can grow. This removes the necessity for such surface to be self-generated by primary nucleation and thus reduces the induction time ( $\tau$ ) since  $t_n$  component is eliminated. If seed crystals are added to a synthesis mixture, the crystals may

- a) remain inert, usually found at the end of the synthesis intact;
- b) dissolve, showing signs of attack. If the added material is unstable in the synthesis medium, it dissolves and influences the course of synthesis if added in sufficient quantity to alter significantly the reaction stoichiometry;
- c) act as pure seeds, in that mass is deposited upon them and they grow and
- d) give rise to secondary nuclei and hence a new crop of crystals.

The balance between seed growth and secondary nucleation depends on the nature of the system, the quantity of material added and the degree of agitation. Secondary nucleation is very reluctant to self-nucleate and therefore the use of seed crystals can be very effective since the response to secondary nucleation is a geometric function of the quantity added (Mullin, 2001, Randolph, 1998).

These factors can modify not only the crystal size and composition, but also the zeolitic structure. The main objective of zeolite synthesis is designing new zeolitic structures by changing the factors involved in the process. The role of organic cations has substantially increased the number of new structures synthesized. These additives are known as structure directing agents (SDAs), and they can change the nature of the final zeolite. Different factors concerning SDAs must also be considered:-

- Size of SDA and temperature at which it is used – the size of the SDA is in direct relation with the cavity or pore size of the obtained zeolite, even though this effect clearly depends on the temperature;
- Flexibility of the SDA – if the SDA has a flexible structure, different zeolites could be synthesized at the same time;
- Polarity of the SDA – the SDA must be soluble enough in the solvent used in the synthesis mixture.

Examples of SDAs are the tetramethylammonium and tetrapropylammonium ions which can be added as bromides or hydroxides. In addition to SDAs, other components or factors in the synthesis mixture that are important are

- The hydroxide ion controls the degree of polymerization of silicates, increasing the crystal growth. The  $\text{OH}^-/\text{SiO}_2$  ratio has also been correlated with the pore size (higher ratios with larger pores). Crystals prepared under normal synthesis conditions are generally rather small;
- Temperature is usually below  $350^\circ\text{C}$ , higher temperatures yield more condensed – phase species;
- The pH of the synthesis mixture is crucial. When it is alkaline, the pH is normally greater than 10 and then it controls the particle size. That also influences polymerization –

depolymerization equilibrium of the gel and the nature of the species in solution. The type of precursor species in solution such as 4 – ring and double 6 – rings will depend upon the pH; as the pH is lowered the precursor units become more complex i.e. change from 4 – ring to a cubic or hexagonal prism unit;

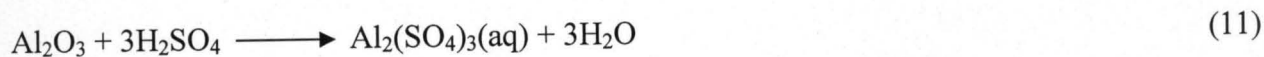
- The reaction time should be optimized because different zeolites or phases can be obtained with the same reaction times; and
- Stirring the reaction mixture also affects the zeolitic structure and the particle size.

After the synthesis procedure, the zeolite should be calcined to remove the organic compounds that are blocking the pores. Calcination entails heating the synthesized zeolite in airflow to a temperature of 350 – 400°C. One common modification is the ion – exchange of the zeolitic structures. Synthetic zeolites are normally obtained in the sodium form, and sometimes it is necessary to exchange sodium for another cation (normally having one or two positive charges) or to obtain the zeolites in their acid form by exchanging the sodium for ammonium and heating in an airflow (Francisco & Rolando, 2003).

### **2.3.8 Dealumination of zeolites**

Zeolites, both synthetic and natural are well known for their roles as solid acid catalysts, adsorbents, and molecular sieves. Of these three areas, the use of zeolites as solid acids concentrates specifically on the modification of the zeolite through dealumination. A dealumination method ranges from chemical treatments to steam calcination. It has been found that the synthesis of silica-rich zeolite types requires Si/Al ratio of 8 – 20 (Zhdanov, 1971) whereas theoretically kaolin clay consists of Si/Al ratio 1:1. Consequently upgrading the theoretical ratio to the required value demands either the addition of make-up silicate externally

or the removal of part of the structural aluminum, represented by the following chemical reaction Equation (11). Alum is the by – product.



While any number of elements can be substituted for silicon in the zeolite framework (Al, Ga, Ti, Zr, V, Fe, Sn etc), the isomorphous substitution of aluminum into the framework is given consideration. The addition of aluminum, a tri-valent cation, into the framework results in a negative charge in the crystal that must be compensated for with a positive charge. This charge compensation can be completed with any cation that is available; however, in order to be of catalytic interest that cation should be hydrogen. The standard synthesis techniques generally use sodium for charge compensation. The completed sodium form of the zeolite which must be converted to acid form is then stirred in a solution containing ammonium ions, which replace the sodium ions at the cation exchange sites in the zeolite. It is first converted to the  $\text{NH}_4^+$  before being converted to acidic form to prevent disintegration of the structure from acid attack. Once all of the sodium has been replaced by ammonium, the zeolite is dried and calcined to liberate ammonia. The resultant is now in its protonic or solid acid form.

Acid catalyzed reactions in organic synthesis, from ring closure to isomerization, all of these reactions benefit from the presence of an acid promoter. The introduction of the solid acid X or Y zeolite and fluid catalytic cracking (FCC) replaces the inefficient free radical based homogeneous thermal process (which produced excessive amounts of coke and light gases) with a heterogeneous process based on carbocation chemistry. In addition to the solid acid nature of the catalyst, the pore system can be vital in the manipulation of selectivity of acid catalyzed reactions. The liquid phase acid catalyzed reactions allow the formation of essentially any transition state while the introduction of a pore system containing the acid site requires the



transition state to be able to fit in the pore system. Any transition states that are too bulky are not formed and thus selectivity can be improved by choosing solid acids with pore systems that are incompatible with by – product transition states.

The five major reasons to be considered in dealumination are

- enhanced thermal stability,
- increased pore size
- increased hydrophobicity
- generation of Lewis acidity and elimination of Bronsted acidity.

In the case of Y zeolite, which has very low silicon to aluminum ratio, the structure is not thermally stable. In order to get Y zeolite to remain stable at elevated temperatures, a significant amount of the aluminum must be removed resulting in ultra stable-Y zeolite (US-Y zeolite). Zeolites with high aluminum contents such as Y zeolite can also have their pore systems sufficiently affected by dealumination, by removing enough aluminum in the pore wall to create larger pores capable of accommodating molecules that were previously too large to enter the original pore system. In terms of hydrophobicity, the more aluminum sites and hence Bronsted acid sites, the more hydrophilic the zeolite. If a reaction requires the migration of a very hydrophobic molecule into the pore system, then dealumination would result in more hydrophobic zeolite and better reaction environment. While aluminum incorporation in the framework results in Bronsted acidity, extra framework aluminum (or more accurately aluminum oxyhydroxides) in the pore system result in Lewis acidity. Reactions that benefit from Lewis acidity would benefit from zeolites containing this extra framework aluminium. The elimination of Bronsted acid sites can serve two primary purposes: decrease in overall acidity or decrease in external acidity. In the cases where a zeolite is just too acidic for the reaction to proceed

efficiently (possibly destroying the desired product before it can leave the pore system), reduction of the Bronsted acid sites via dealumination is warranted. While the pore system of a zeolite in combination with the acid properties results in acid catalyzed reactions with selectivity determined by what transition states can fit in the pore system, a complication is that there are acid sites on the external surface of the zeolite which are accessible to molecules not in the pore system. These molecules will react unselectively since there is no pore wall to prevent unwanted transition states from forming. As a result, selective dealumination of the external surface would benefit reaction selectivity by forcing the reaction to occur only within the confines of the pore system (Bradley, 2004). These de-aluminated materials generate mesopores by extracting aluminum from the lattice and causing partial collapse of the framework and therefore have different uses in catalysis. For example, US-Y zeolite widely used in catalytic cracking helps to overcome diffusional problems in the micropores of zeolites.

## **2.4 Properties of Zeolites**

Molecular sieves have found widespread industrial applications as highly selective adsorbents, ion exchangers and most importantly, catalysts of exceptionally high activity and selectivity in a wide range of reactions (Breck, 1974). Molecular sieves exhibit appreciable Bronsted acidity with shape selective features not available in amorphous catalysts of similar composition.

### **2.4.1 Adsorption and molecular sieve effects**

Molecular sieves are selective, high – capacity adsorbents because of their high intracrystalline surface area and strong interactions with adsorbates. Molecules of different sizes generally have different diffusion properties in the same molecular sieve. Molecules are separated based on size and structure relative to the size and geometry of the apertures of the

sieves. Molecular sieves adsorb molecules, in particular those with a permanent dipole moments, and exhibit other interactions not found in other sorbents. Different polar molecules have a different interaction with the molecular sieve framework and may thus be separated by a particular molecular sieve. This is one of the major uses of zeolites. An example is the separation of  $N_2$  and  $O_2$  in the air on zeolite A, by exploiting different polarities of the two molecules (Breck, 1974).

The quantity of adsorbed gas or liquid depends on pressure, temperature, the nature of the adsorbate and the kind of molecular sieve. Variations in the chemical composition of the sieve also affect adsorption. The adsorbed molecules can be removed by heating and/or evacuation. It is also known that aluminum in materials such as VPI-5 zeolite may possess a higher coordination number than four indicating that chemisorption of water occurs (Davis, 1988, McCusker, 1991). The structure may be changed while the adsorbed water is driven away.

#### **2.4.2 Water sorption/desorption**

The water molecules in the zeolite channels bonded by the forces of dipoles interactions of the cations forming their close surrounding. The water from the zeolite crystals can be removed during thermal treatment, often called bold “thermal activation” or “dehydration”. The dehydration process is equilibric and is depending on the temperature and the partial pressure of water. The curve of the dehydration (water loss versus temperature at constant pressure) gives information on the state of water in the zeolite – the “wide porous zeolite” show wide temperature range of the dehydration starting from room temperature while “narrow porous zeolite show narrow and more distinguishable curves at the beginning of the dehydration process to that at higher temperatures. The overall water content in saturated state and the character of the dehydration depend not only on the zeolite framework type, but also on their cationic

content. During the dehydration process, the frameworks of some zeolites are changed irreversibly. After these changes are observed, the ability of reverse water saturation (rehydration) is lost permanently. That is why some zeolite types are considered as “thermostable” and the temperature of the framework destruction is cited as their thermostability.

The dehydrated stable zeolites are very good water sorbents (water removal); especially at very low partial pressures of water vapour. That is why some zeolites are used as very effective desiccants in several industrial processes to remove volatile organic chemicals from air streams, separate isomers and mixtures of gases. The ring or pore sizes of molecular sieve may be determined by sorption of molecules of different size. Water and nitrogen are two of the smallest molecules, which can easily penetrate almost the entire structures. These two molecules are normally used to determine the crystallinity of molecular sieves by comparing the adsorption volume with that of a standard sample (Breck, 1974).

#### **2.4.3 Silicon to aluminium ratio/ion exchange**

Zeolites with low Si/Al ratios have strong polar anionic frameworks. The exchangeable cations create strong electrostatic fields and interact with polar molecules such as water. The cation – exchange behaviour of zeolites depends on the

- nature of the cation species, the cation size (both anhydrous and hydrated) and cation charge;
  - temperature;
  - concentration of the cationic species in the solution;
  - anion associated with the cation in solution;
  - solvent (most exchange are carried out in aqueous solutions or organics); and
- the structural characteristics of the particular zeolite.

Cation exchange in a zeolite is accompanied by an alteration of stability, adsorption behaviour and selectivity, catalytic activity and other properties. There are two kinds of cations present within the zeolite structure. First, there are exchangeable cations and by the introduction of a larger or smaller cation will decrease or enlarge the pore opening. The location of the cation within the crystal will also contribute to the size of the pore opening. For example, the  $\text{Na}^+$  form of zeolite A has a smaller effective pore dimension than would be expected for its 8-membered ring framework opening. This is due to  $\text{Na}^+$  occupancy of site where it will partially block the 8-membered ring window. When the  $\text{Na}^+$  is exchanged for the large  $\text{K}^+$ , the pore diameter is reduced so that only the very smaller polar molecules will be absorbed. If the divalent  $\text{Ca}^{2+}$  cation is used to balance the framework charge, the effective pore opening widens, as only half the number of cations are needed. These ions occupy sites within the void of the zeolite and do not reduce the effective pore diameter of the 8-membered ring. Secondly, charge imbalance due to the presence of aluminum in the zeolite framework along with  $\text{O}_2$  atoms determine the ion exchange properties of zeolites and induces potential acidic sites. Highly and purely siliceous molecular sieves have virtually neutral frameworks, exhibit a high degree of hydrophobicity and no ion exchange or catalytic properties while low silica zeolite are hydrophilic.

#### **2.4.4 Catalytic properties**

The most important application of molecular sieves is as catalyst. Zeolites are desired catalysts because they combine high concentration of active acid sites, high thermal/hydrothermal stability, high surface area and shape selectivity used to catalyze a variety of hydrocarbon reactions, such as cracking, hydrocracking, alkylation and isomerization. The reactivity and selectivity of zeolites as catalysts are determined by the active sites brought about by a charge imbalance between silicon and aluminum atoms in the framework. Each aluminum



atoms framework induces a potential active acid site. In addition, purely siliceous and  $\text{AlPO}_4$  molecular sieves have Bronsted acid sites whose weak acidity seems to be caused by the presence of terminal – OH bonds on the external surface of the crystal.

Shape selectivity, including reactant shape selectivity, product shape selectivity or transition state shape selectivity, plays an important role in molecular sieve catalysis especially in the petrochemical industry as shown in Figure 2.8. Different sizes of channels and cages promote the diffusion of different reactants, products or transition – state species. The selectivity of zeolites is due to the limited pore sizes (limited diffusivity) which only allow specific molecules either to enter the pores (educt selectivity) or to leave the pores (product selectivity) depending on their sizes. Product shape selectivity occurs when slowly diffusing product molecules cannot rapidly escape from the crystal (leave the pores), and undergo secondary reactions. Furthermore, not every transition state during a reaction might be possible, thus forcing a reaction only into one direction (restricted transition – state shape selectivity). This is a kinetic effect arising from the local environment around the active site and the rate constant for a certain reaction mechanism is reduced if the necessary transition state is too bulky to form readily.

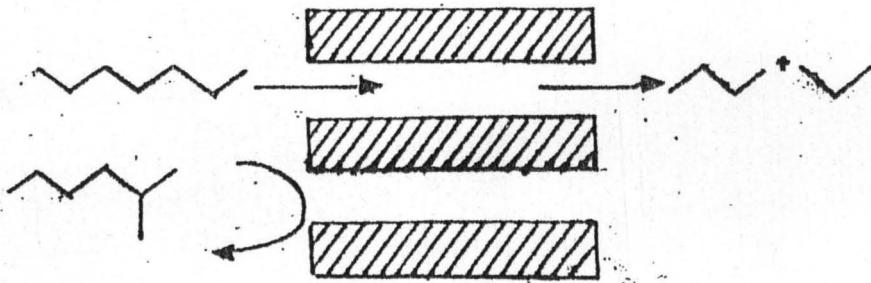
## **2.5 Zeolite Characterization**

Information on the structural, chemical and catalytic characteristics of zeolite is essential for deriving relations between their various chemical and physicochemical properties. In general, characterization of zeolites has to provide information about

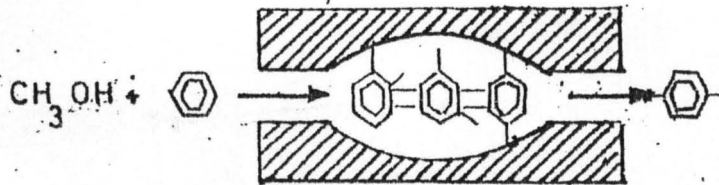
- i) its structure and morphology;
- ii) its chemical composition;
- iii) its ability to sorb and return molecules; and



### Reactant Selectivity



### Product Selectivity



### Restricted transition-state selectivity

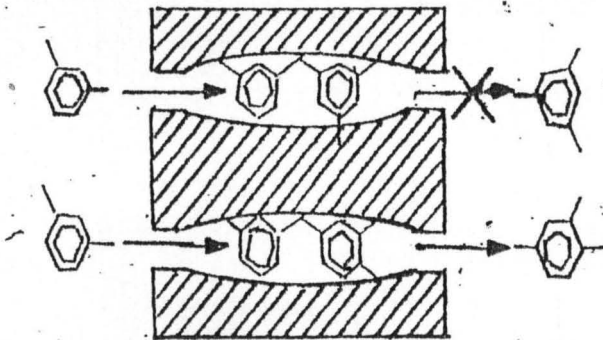


Figure 2.8: Reactant, Product and Restricted Transition-State Shape Selectivity

iv) its ability to chemically convert this molecule (Jentys & Lercher, 2001).

The basic analytical techniques for zeolites characterization are the elemental analysis:- X-ray Fluorescence (XRF), Inductively – Coupled Plasma Emission Spectroscopy (ICPS), Atomic Absorption Spectrometry (AAS), Neutron Activation Analysis (NAA), X-ray Diffraction and Scanning Electron Microscope (SEM) for crystal size. Other analytical techniques, which constitute secondary characterization, include sorptive capacity, ion exchange properties, thermal analysis, IR and NMR etc.

### 2.5.1 X – Ray fluorescence spectroscopy (XRF)

This is widely used for qualitative and quantitative chemical (elemental) analysis of environmental, geological, biological, and industrial samples. Depending on the application, XRF can be produced by using not only X – rays but also other primary excitation sources like alpha particles, protons or higher energy beams. When compared to other techniques such as AAS, ICPS and NAA, XRF has the advantage of being non – destructive, multi – elemental, fast and cost – effective. Furthermore, it provides a fairly uniform detection limit across a large portion of the periodic table and is applicable to a wide range of concentrations from 100% to few parts per million (ppm). The main disadvantage is that the analysis is generally restricted to elements heavier than fluorine.

**Basic principle** – The XRF principle is shown in Figure 2.9. When a primary X-ray excitation source from an X-ray tube or a radioactive source strikes a sample, the X-ray can either be absorbed by the atom or scattered through the material. The process in which an X-ray is absorbed by the atom by transferring all of its energy to an innermost electron is called the “photoelectric effect”. During this process, if the primary X-ray had sufficient energy, electrons are ejected from the inner shells creating vacancies. These vacancies present an unstable

condition for the atom. As the atom returns to its stable condition, electrons from the outer shells are transferred to the inner shells and in the process give off a characteristic X-ray (detector) whose energy is the difference between the two binding energies of the two shells, which appear as an X-ray, emitted by the atom. The signals are processed by computer and because each element has a unique set of energy levels, each element produces X-rays at a unique set of energies, allowing one to non – destructively measure the elemental composition of a sample. The process of emissions of characteristic X-rays is called X- Ray Fluorescence and the analysis using the X-ray fluorescence is called X-Ray Fluorescence Spectroscopy.

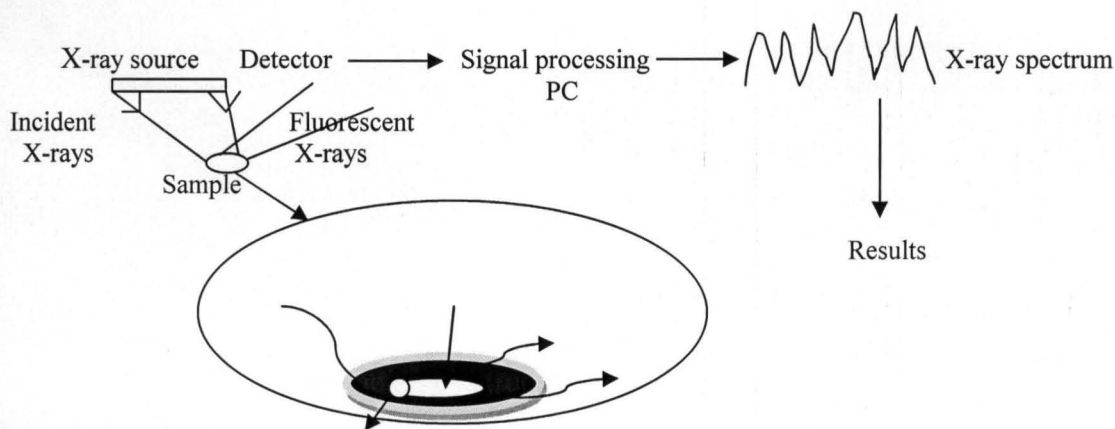


**Figure 2.9: The Principle of XRF and the Typical XRF Detection Arrangement**

An inner shell electron is excited by an incident photon in the X-ray region. During the de-excitation process, an electron is moving from a higher energy level to fill the vacancy. The energy difference between the two shells appears as an X-ray emitted by the atom. The X-ray spectrum acquired during the above process reveals a number of characteristic peaks. The energy of the peaks leads to the identification of the elements present in the sample (qualitative analysis) while the peak intensity provides the relevant or absolute elemental concentration (semi-quantitative or quantitative analysis).

**Sample preparation** - Sample preparation in XRF has two main approaches: Fusion and Pressed pellet methods. In fusion, the sample is fused in a platinum crucible using a ratio of up to 15:1 flux (typically lithium tetraborate) to sample, using automated fusion devices via a muffle furnace or air boosted natural gas burners. The resulting hot melt is poured into a platinum mould and forms a glass disc that is introduced into the XRF. Pressing pulverized samples into pellets is a commonly used sample preparation method in XRF.

### 2.5.2 X – ray diffraction (XRD)

XRD is an analytical technique used to identify and characterize unknown crystalline materials. It is used to determine if the synthesized product corresponds to a zeolite structure by comparison with reference diffractograms. Quantitative calibrations can be used to measure zeolite crystallinity and estimate the unit cell parameter.

In polycrystalline materials each reflection observed at a given angle  $2\theta$  in a powder X-ray diffraction pattern, measured at the wavelength  $\lambda$  is related to lattice planes with a distance  $d$  and an orientation indicated by the Millers indices  $hkl$  as described by the Bragg's law:

$$\lambda = 2d_{(hkl)} \sin \theta \quad (12)$$

For crystals with cubic symmetry, the size of the unit cell  $a_0$  can be determined from the angular positions of the reflections.

$$a_0 = \frac{\lambda \sqrt{h^2 + k^2 + l^2}}{2 \sin \theta} \quad (13)$$

The integrated intensity of selected reflections can be used to determine the crystallinity of the sample by normalizing their intensities to those of standard samples. The crystallinity is defined according to the ASTM standards (Jentys & Lercher, 2001) on catalysis as

$$\text{X-ray crystallinity} = \frac{\text{Intensity of Peak}_{(hkl)} \text{ Sample}}{\text{Intensity of Peak}_{(hkl)} \text{ Standard Sample}} \times 100 \quad (14)$$

The average crystalline size of the element (D) nm is estimated using Scherrer's formula:

$$D = \frac{k\lambda}{\beta \cos \theta} \quad (15)$$

$k$  – the Scherrer constant = 0.89

$\lambda$  – the wavelength of X – ray radiation

$\beta$  – the full width at half maximum (FWHM) of the (111, 200, 220) diffraction line

$\theta$  - the Bragg angle measured in radians at the position of the peaks.

When the unit cell parameter is known, it is possible to determine if an element has been incorporated into the lattice framework position or not.

Monochromatic X-rays are used to determine the interplanar spacing of the unknown materials. Samples are analyzed as powders with grains in random orientations to ensure that the beam samples all crystallographic directions. When the Bragg conditions for constructive interference are obtained and a reflection is produced, the reflective peak height is proportional to the number of grains in a preferred orientation. The X-ray spectra generated by this technique thus provide a structural fingerprint of the unknown. The relative peak heights may be used to obtain semi – quantitative estimates of abundances. Changes in peak position represent either compositional variation (solid solution) or structure state information (order – disorder transitions) that can be detected. Peak positions are reproducible to 0.02 degrees. Data is rapidly generated to determine peak position, relative intensities, and inter-crystalline spacings (d).

**Sample preparation** - Pulverized powder sample, which must be reduced to finer particle size, is used for XRD analysis so as to meet the requirements for an ideal specimen. The requirements for an ideal specimen, which is for the achievement of high degree of accuracy for quantitative XRD, are essentially three and they are total randomness of the crystallite orientations, sufficient



number of crystallites in the experimental specimen to meet statistical requirement, and sufficient diffraction intensity measured to satisfy counting statistics.

Analysis of powders by XRD requires that they be extremely fine grained to achieve good signal to noise ratio (and to avoid fluctuation of intensity), avoid spottiness and minimize preferred orientation. The recommended size range is around 1-5 $\mu\text{m}$ , especially if quantification of various phases is desired. For routine qualitative evaluation of mineral components, the samples are usually ground to pass through a 325-mesh sieve (45  $\mu\text{m}$ ).

**Data collection** – The most important element in data collection for XRD is the peak position. If the pattern is to be indexed, (Miller indices hkl assigned to each of the peaks and thereby the unit cell dimensions extracted from the pattern), it is essential that the peak positions be determined accurately. The instrument's  $2\theta$  scale needs to be carefully calibrated using a standard material such as the NIST silicon standard 640b. The sharper a peak, the better its  $2\theta$  value can be determined.

The second most important parameter is peak intensity. Relative peak intensities are used for mineral identification and structure analysis. Three common factors affect relative peak intensities, these are sample thickness, preferred orientation, and divergence slits. Samples are assumed to be thick enough to allow all the X-rays to interact with the sample (by absorption or diffraction) before they reach the sample holder. In this way, the volume of the sample irradiated remains constant as  $2\theta$  changes. If this is not the case, intensities must be adjusted for the transparency of the sample.

**Identification** – For identification of mineral species, the measured pattern is compared with an existing one from the Powder Diffraction File (PDF) or an in house data file. Several considerations that must be taken for the comparison include making corrections for the peak



intensities, peak position information given in terms of d-values rather than  $2\theta$  values, because d-values are dependent of the X-ray wavelength ( $\lambda$ ) used.

In computer-based programs there is a match program specifically comparing reference patterns to the pattern of the analyzed sample through Boolean operations. A match score is displayed and the “score” quantifies the match between the reference pattern and the sample phase. The higher the score, the higher the probability of the reference phase contained in the sample (Funtua, 2006).

## **2.6 Adsorption Phenomena**

All matter is made up of atoms. In gases, atoms and molecules are free to move about in space. In contrast, atoms in solids are located in fixed positions by electrical forces of attractions among neighbouring atoms. However, the outermost (or surface) atoms in the solid have fewer neighbours than the atoms beneath them. To compensate for their electrical force imbalance, surface atoms seek to attract surrounding gas molecules. The tendency of all solid surfaces to attract surrounding gas molecules gives rise to a process called gas sorption. Monitoring the gas sorption process provides a wealth of useful information about the characteristics of solids. When small amounts of a gas (adsorbate) are admitted in steps into the evacuated sample chamber, adsorbate molecules quickly find their way to the surface of every pore in the solid (the adsorbent). These molecules can either bounce off or stick to the surface. Gas molecules that stick to the surface are said to be adsorbed. The strength with which the adsorbed molecules interact with the surface determines if the adsorption process is to be considered physical (weak) or chemical (strong) in nature.

Adsorption is the preferential concentration of a species at the interface between two phases i.e. adsorbate and adsorbent (Charles, 1977). The surface of a solid represents a

discontinuity of its structure. The forces acting at the surface are unsaturated. Hence, when the solid is exposed to the gas, the gas molecules will form bonds with it and become attached to the surface of the adsorbent. This phenomenon is termed adsorption. This phenomenon is driven by the available surface area (including the pores), pore size, concentration of the adsorbate (in its various forms e.g. vapour pressure), prevailing temperature and the forces among the molecules of the adsorbent and adsorbate. On the other hand, the filling of pores or void volume by the gas molecules is called absorption. Therefore, adsorption process is the preferential partitioning of the substances from the gaseous or liquid phase onto the surface of a solid substrate.

Adsorption also known as adsorptive separation can be simply defined as the concentration of a solute, which may be molecules in a gas stream or a dissolved or suspended substance in a liquid stream, on the surface of a solid. One of three mechanisms by which adsorptive separation can be achieved is either steric, equilibrium or kinetic equilibrium effects. The steric effect is derived from molecular sieving property of zeolites. In this case, only small and properly shaped molecules can diffuse into the adsorbent, whereas other large molecules are totally excluded. The equilibrium mechanism is based on the solid having different abilities to accommodate different species, that is the stronger adsorbing species is preferentially removed by the solid. Kinetic separation is achieved by the virtue of the difference in diffusion rates of different molecules into the pore; thus by controlling the time of exposure the faster diffusing species is preferentially removed by the solid (Duong,1998).

### **2.6.1 Classification of Adsorption Processes**

Adsorption phenomenon is essentially an attraction of adsorbate molecules to an adsorbent surface. The preferential concentration of molecules in the proximity of a surface arises because the surface forces of an adsorbent solid are unsaturated. Both repulsive and

attractive forces become balanced when adsorption occurs and is always an exothermic process.

Adsorption processes can be classified as either a

a) physical adsorption (van der Waals adsorption) or

b) chemical adsorption (chemisorption or activated adsorption) and they can be distinguished from each other depending on which of these two forces plays a bigger role between the adsorbate and the adsorbent (Charles, 1977).

a) **Physical Adsorption (Physisorption)** – is a process where the interactions between the gas (adsorbate) and the solid (atoms) which compose the adsorbent surface are weak (intermolecular forces or van der Waals forces or electrostatic forces), similar to those involved in condensation. Thus, adsorbents are characterized by surface properties such as surface area and polarity. A large specific surface area is preferable for providing large adsorption capacity, but the creation of a large internal surface area in a limited volume inevitably gives rise to large numbers of small sized pores between adsorption surfaces. The size of micropore determines the accessibility of adsorbate molecules to the adsorption surface so the pore size distribution of micropore is another important property of characterizing adsorptivity of adsorbents (Suzuki, 1990). In addition, some adsorbents have larger pores in addition to micropores which result from granulation of fine powders or fine crystals into pellets or originate in the texture of raw materials. These pores called macropores are several  $\mu\text{m}$  in size. The success or failure of adsorption process depends on how the solid performs in both equilibria and kinetics. A solid with good capacity but slow kinetics is not a good choice as it takes adsorbate molecules too long a time to reach the particle interior. This means long gas residence time in a column, hence a low throughput. On the other hand, a solid with fast kinetics but low capacity is not good either as a large amount of solid is required for a given throughput. Thus, a good solid is the one that

provides good adsorptive capacity as well as good kinetics. To satisfy these requirements, the following aspects must be satisfied:

- the solid must have a reasonably high surface area or micropore volume.
- the solid must have relatively large pore network for the transport of molecules to the interior.

To satisfy the first requirement, the porous solid must have small pore size with a reasonable porosity. This suggests that a good solid must have a combination of two pore ranges: the micropore range and the macropore range. The classification of pore size as recommended by IUPAC is often used to delineate the range of pore size as follows:

Micropores  $d < 2 \text{ nm}$  ( $<20 \text{ Angstrom}$ )

Mesopores  $2 < d < 50 \text{ nm}$  ( $20 - 500 \text{ Angstrom}$ )

Macropores  $d > 50 \text{ nm}$  up to  $100 \mu\text{m}$  ( $>500 \text{ Angstrom}$ ) where  $d = 0.3$ .

This classification was developed based on adsorption of nitrogen at its boiling point on a wide range of porous solids such as activated carbon, zeolite, alumina and silica gel. Industries such as Chemical, Petrochemical, Biochemical, Biological and Biomedical that uses these solids are diversified and do satisfy the above two criteria (Duong, 1998).

Surface polarity corresponds to affinity with polar substances such as water. Polar adsorbents are "hydrophilic" and aluminosilicates such as zeolites, porous alumina, silica gel or silica-alumina are examples of adsorbents of this type. On the other hand, non-polar adsorbents are generally "hydrophobic". Carbonaceous adsorbents, polymer adsorbents and silicalite are typical nonpolar adsorbents. These adsorbents have more affinity with oil than water (Suzuki, 1990).

**b) Chemisorption** – is a process, which involves the formation of strong chemical bonds with attendant transfer of electrons between the adsorbate molecules, and specific surface

locations (adsorbent) referred to as chemically active sites. Chemisorption is thus used primarily to count the number of surface active sites, which are likely to promote chemical and catalytic reactions. The solids best suited to adsorption are very porous, and have very large effective surface areas (Charles, 1977).

### **2.6.2 Adsorption isotherms**

Under suitable conditions of temperature and pressure, a gas will adsorb on to a solid, ultimately covering its solid surface entirely. Plots of an amount of material adsorbed versus pressure at a fixed temperature are known as adsorption isotherms. The variation in volume (V) or directly as weight (W) sorbed with change in partial pressure ( $P/P_0$ ) at any constant temperature (T), is a function of the fluid-solid interaction energy and the coverage of the surface. The adsorbate partial pressures (P) are normalized by dividing by the saturation pressure at the temperature in question ( $P_0$ ).

The nitrogen adsorption/desorption isotherms at liquid nitrogen temperature ( $-195.8^\circ\text{C} = 77.34\text{K}$ ) and relative pressures ( $P/P_0$ ) ranging from 0.05 – 1.0. Nitrogen adsorption takes place on the surface while capillary condensation of nitrogen takes place in the pores (Suzuki, 1990).

### **2.6.3 The Brunauer, Emmett, and Teller (BET) isotherm**

Surface area and pore size distribution are important attributes that are used by catalyst manufacturers (quality control tool) and users' especially fluid catalytic cracking to monitor the activity and stability of catalysts. There are different methods used to measure surface area and each method can yield different results. Most methods are based on the isothermal adsorption of nitrogen. Either a single point or multipoint is used to calculate the surface area. At Engelhard, the multipoint BET method is used to measure total surface area of fresh and equilibrium moving bed and fluid catalytic cracking (FCC) catalysts. The BET considers multilayer adsorption and is



the basis of standard methods for determining specific surface areas of heterogeneous catalysts. *Specific surface area* is defined as the accessible area of solid surface per unit mass of material. Methods used to determine SSA are moisture adsorption, N adsorption or BET technique (Assaf et al 1944, Merchant, 1957), nuclear magnetic resonance (Froix and Nelson, 1975) and liquid chromatography (Ladisich et al, 1992). This method can also be used to assess pore size and distribution in the transitional pore range for charcoals, silica, alumina etc. (Giles and De Silva, 1969). The BET approach is essentially an extension of the Langmuir approach. Van der Waals forces are regarded as the dominant forces, and the adsorption of all layers is regarded as physical, not chemical. The rates of adsorption and desorption are set equal to one another, as in the Langmuir case. The kinetic approach to deriving a mathematical expression for the Langmuir isotherm assumes that the rate of adsorption on the surface is proportional to the product of partial pressure of the adsorbate in the gas phase and the fraction of the surface that is bare. Adsorption may occur only when a gas phase molecule strikes an uncovered site. If the fraction of the surface covered by an adsorbed gas A is denoted by  $\theta_A$ , the fraction that is bare (unoccupied) is  $1 - \theta_A$  if no other species are adsorbed. If the partial pressure of A in the gas phase is  $P_A$ , the rate of adsorption is given by

$$R_a = kP_A(1 - \theta) \quad (16)$$

$k$  - is be regarded as a "pseudo rate constant" for the adsorption process.

The rate of desorption depends only on the number of molecules that are adsorbed. Thus

$$R_d = k'\theta_A \quad (17)$$

Where  $k'$  may be regarded as a pseudo rate constant for the desorption process.

At equilibrium the rates adsorption and desorption are equal.

$$kP_A(1 - \theta_A) = k'\theta_A \quad (18)$$



The fraction of the sites occupied by species A is then

$$\theta_A = \frac{kP_A}{k' + kP_A} \quad (19)$$

$$\text{but } K = k/k' \quad (20)$$

If one takes the ratio of the pseudo rate constant for adsorption to that for desorption as an equilibrium constant for adsorption (K) and equation (19) can be written as

$$\theta_A = \frac{\frac{k}{k'} P_A}{1 + \frac{kP_A}{k'}} = \frac{KP_A}{1 + KP_A} \quad (21)$$

The fraction of the sites that are occupied is also equal to the ratio of the volume of gas actually adsorbed (V) to that, which would be adsorbed in a monolayer ( $V_m$ ).

$$\theta_A = \frac{V}{V_m} \quad (\text{Charles, 1977}) \quad (22)$$

The specific surface area of the adsorbents can be determined by applying BET equation

$$\frac{V}{V_m} = \frac{Cx}{(1-x)(1-x + Cx)} \quad (23)$$

Equation (23) can only be used if we can relate x in terms of pressure and other known quantities. When gas phase pressure is equal to the vapour pressure, i.e.  $P = P_0$  occurs when  $x = 1$  thus the variable x is the ratio of the pressure to the vapour pressure at the adsorption temperature.

$$x = P/P_0 \quad (24)$$

With this definition equation (23) become what is now known as the famous BET equation containing two fitting parameters, C and  $V_m$ .

$$\frac{V}{V_m} = \frac{CP}{(P_o - P)[1 + (C-1)(P/P_o)]} \quad (25)$$

Or

$$\frac{P}{V(P_o - P)} = \frac{1}{V_m C} + \left[ \frac{C-1}{V_m C} \right] \frac{P}{P_o} \quad \text{or} \quad \frac{1}{W[(P_o/P)-1]} = \frac{1}{W_m C} + \frac{(C+1)}{W_m C} \frac{P}{P_o} \quad (26)$$

Where V or W is the volume or weight of gas adsorbed on the surface at a given P/P<sub>o</sub>,

V<sub>m</sub> or W<sub>m</sub> is the volume or weight of gas adsorbed in monolayer coverage,

P<sub>o</sub> is the vapour pressure of the gas,

C a constant that is related to the heat of adsorption (proportional to exp (-δH<sub>d</sub>-H<sub>vap</sub>)/RT),

δH<sub>d</sub> is the enthalpy of adsorption in the first layer and H<sub>vap</sub> is the heat of vaporization.

The pressure range of validity of the BET equation is P/P<sub>o</sub> = 0.05 – 0.3. For relative pressures above 0.3, there exists capillary condensation, which is not amenable to multilayer analysis. A linear relationship or plot of the LHS of equation i.e., P/V (P<sub>o</sub>-P) or 1/W [(P<sub>o</sub>/P)] vs (P/P<sub>o</sub>) is required to obtain the quantity of gas adsorbed and would yield a straight line with a slope

$$\text{Slope} = \frac{(C-1)}{CV_m} \quad \text{and an intercept} \quad (27)$$

$$\text{Intercept} = \frac{1}{CV_m} \quad (28)$$

$$V_m = \frac{1}{\text{Slope} + \text{intercept}} \quad (29)$$

The slope and intercept are used to determine the quantity of gas (N<sub>2</sub>) adsorbed in the monolayer.

Once V<sub>m</sub> (mole/g) is obtained from the slope, the surface area is calculated from

$$A = V_m N_A a_m \quad (30)$$

Where  $N_A$  is the Avogadro's number and is equal to  $6.023 \times 10^{23} \text{ mol}^{-1}$ ,

$a_m$  is the molecular projected area, and

$V_m$  is the volume occupied by the monolayer coverage  $V_m$  obtained from the graph. For  $N_2$  molecular projected area is  $T \text{ (K)} = 77$ ,  $P_o \text{ (Pa)} = 1.013 \times 10^5$  and  $a_m = 16$  (Doung, 1998). For a single point method, the intercept is taken as zero or a small positive value, and the slope from the BET plot is used to calculate the surface area.

Internal surface area of microporous adsorbents is often used as one of the measures to describe the degree of development of pores. The concept of Brunauer, Emmett and Teller (BET) adsorption isotherm where the amount adsorbed by monomolecular coverage,  $q_m$ , gives the specific surface area by assuming the molecular sectional area of  $N_2$  to be  $16.2 \text{ \AA}^2/\text{molecule}$ . This corresponds to  $9.76 \times 10^4 \text{ m}^2/\text{mol}$  or  $4.35 \text{ m}^2/\text{Ncm}^3$ .  $q_m$  can be determined from the experimentally obtained data of isotherm, so called BET plot of  $P_r/[q(1-P_s)]$  vs  $P_r$ . Then from the slope and intersect of the straight line obtained in the range of  $0.35 < P_r < 0.5$ ,  $q_m$  is readily obtained (Suzuki, 1990).

#### a) *Equilibrium Relations*

When an adsorbent is in contact with the surrounding fluid of a certain composition, adsorption takes place and after a sufficiently long time, the adsorbent and the surrounding fluid reach equilibrium. In this state the amount of the component adsorbed on the surface mainly of the micropore of the adsorbent is determined as shown in Figure 2.10. The relation between amount adsorbed,  $q$ , and concentration in the fluid phase,  $C$ , at temperature,  $T$ , is called the adsorption isotherm at  $T$ .

$$q = q(C) \text{ at } T$$

(31)

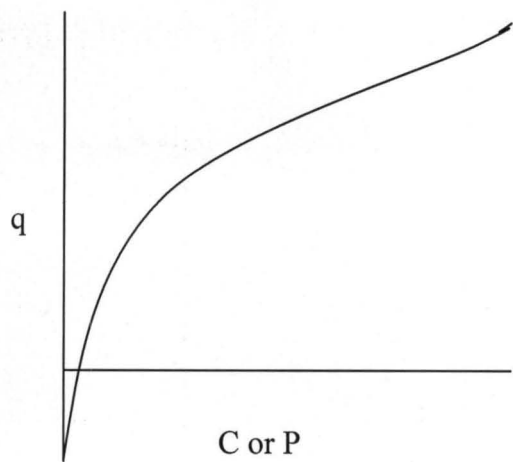


**Figure 2.10: Adsorption Isotherm**

b) **Surface Adsorption**

When surface coverage or fractional filling of the micropore is  $\theta (=q/q_0)$  and the partial pressure in the gas phase,  $P$ , which is to be replaced by  $C (=p/RT)$  when the concentration in the fluid phase is used, the adsorption rate is expressed as  $k_a p (1-\theta)$  assuming first order kinetics with desorption rate given as  $k_d \theta$ . Then equilibrium of adsorption rate and desorption rate gives the equilibrium relation as

$$\theta = KP/(1 + KP) \quad (32)$$

$$P = \frac{1}{K} \left[ \frac{\theta}{1-\theta} \right] \quad (33)$$

The above relation is given by Langmuir, called Langmuir isotherm where  $K = k_a/k_d$  is called the adsorption equilibrium constant. When the amount adsorbed ( $q$ ), is far smaller compared with the adsorption capacity of the adsorbent ( $q_0$ ), equation (32) is reduced to Henry type equation;

$$\theta = KP \quad (34)$$

Further, when the concentration is high enough,  $p \gg 1/K$ , then adsorption sites are saturated and

$$\theta = 1 \quad (35)$$

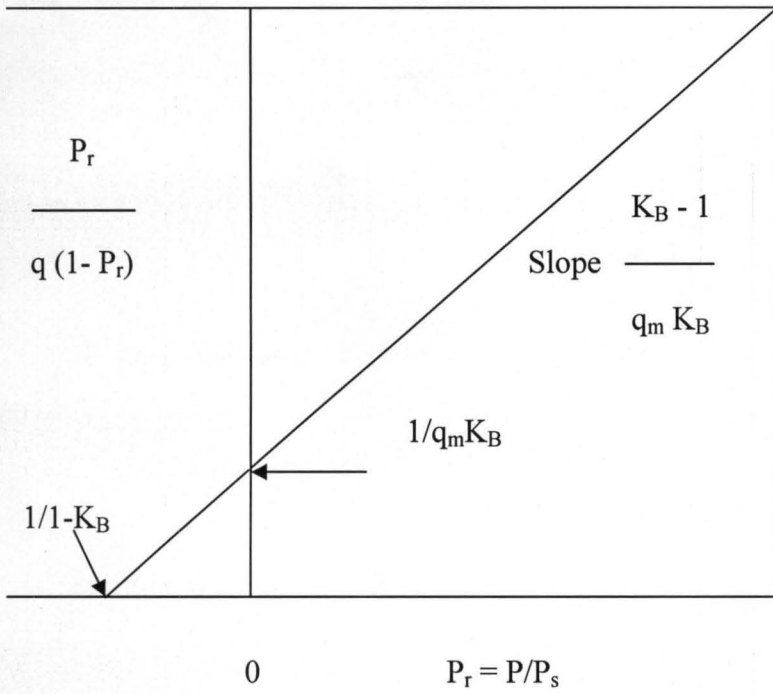


**Figure 2.11: BET plot of gas phase adsorption isotherm**



Where  $P_r$  is the relative pressure ( $=P/P_s$ ) and  $q_m$  represents the amount adsorbed by monomolecular coverage on the surface. From  $N_2$  adsorption at liquid nitrogen temperature, the surface area of the adsorbent is determined by converting  $q_m$  to the surface area. In most cases,  $q_m$  is obtained from the BET plot of the adsorption data as shown in Figure 2.11. It gives a straight line in the range  $0.05 < P_r < 0.35$  and  $q_m$  is readily determined. The surface area of the adsorbent based on nitrogen adsorption can be calculated by multiplying nitrogen surface area of  $3480 \text{ m}^2/\text{g}$  with  $q_m$ .

#### 2.6.4 Physical characteristics of zeolite catalyst

##### a) Catalyst Void (Pore) volume

The simplest method of determining the void volume or the pore volume of a given catalyst sample is to measure the increase in weight that occurs when the pores are filled with a liquid of known density. Water, carbon tetrachloride, and various hydrocarbons have been used successfully. The difference between the wet and dry weights ( $W_{\text{wet}} - W_{\text{dry}}$ ) divided by the density of the imbibed liquid ( $\rho_L$ ) gives the void volume.

$$\epsilon_p = \frac{\delta M_p}{\rho_L} \quad (\text{cm}^3) \quad (36)$$

The void volume per gram of catalyst ( $V_g$ ) is obtained by

$$V_g = \frac{W_{\text{wet}} - W_{\text{dry}}}{\rho_L W_{\text{dry}}} \quad (37)$$

This technique determines the total volume of the pores with radii between approximately 10 and  $1500 \text{ \AA}$ . It is limited in accuracy by the fact that is difficult to dry the external surface of the particles without removing liquid from large pores. Some liquids tend to be retained around the

points of contact between particles. These two sources of error offset one another. Any air retained within the pores after boiling will lead to erroneous results (Charles, 1977).

**b) Porosity** of adsorbents is determined by several alternative methods. When true solid density  $\rho_s$  ( $\text{g}/\text{cm}^3$ ), is known, total porosity,  $\epsilon_t$ , specific pore volume,  $V_p$  ( $\text{cm}^3/\text{g}$ ), is calculated from  $\rho_s$  and particle density,  $\rho_p$  ( $\text{g}/\text{cm}^3$ ), as

$$\epsilon_t = 1 - \rho_p / \rho_s \quad (38)$$

$$V_p = 1 / \rho_p - 1 / \rho_s \quad (39)$$

$\rho_p$  – particle weight/particle volume

$$\rho_p = W_s / [(W_m - W_p + W_s) / \rho_{\text{Hg}}] \quad (40)$$

Where  $W_s$  is the weight of empty glass pycnometer filled with the sample weight.

$W_m$  is the weight of empty glass pycnometer filled with mercury.

$W_p$  is the weight of empty pycnometer filled with mercury after evacuation.

$\rho_{\text{Hg}}$  is the density of mercury at the measurement temperature.

$\rho_p$  is the particle density (Suzuki, 1990).

The porosity of the catalyst pellet ( $\epsilon_p$ ) is defined as the void fraction.

$$\epsilon_p = \frac{\text{Void volume of catalyst particle (V}_v\text{)}}{\text{Total volume of catalyst particle (V}_T\text{)}} \quad \text{no unit} \quad (41)$$

For a particle of mass  $M_p$ ,

$$\epsilon_p = \frac{M_p V_g}{M_p V_g + \frac{M_p}{\rho_{\text{skeletal}}}} \quad (42)$$

where  $\rho_{\text{skeletal}}$  is the true density of the bulk solid and the second term in the denominator is the volume occupied by the solid proper. If porosity is about 0.5 it indicates that the gross particle volume is evenly split between void space and solid material.

$$\varepsilon_p = \rho_b V_v \quad (43)$$

where  $\rho_b$  is the bulk density and  $V_v$  is the void volume (Charles, 1977).

### c) **Bulk (Apparent) Density Determination**

This is a method for determining the packed density of a bed of granular zeolite sample and calculated to be:

$$\text{Bulk density} = \frac{\text{Weight of zeolite sample}}{\text{Weight of equal volume of water}} \quad (44)$$

in (g/ml)

### d) **Pore volume and Pore Size Distribution (PSD)**

Physisorption is the most common type of adsorption. Physisorbed molecules are fairly free to move around the surface of the sample. As more gas molecules are introduced into the system, the adsorbate molecules tend to form a thin layer that covers the entire adsorbent surface. Continued addition of gas molecules beyond monolayer formation leads to the gradual stacking of multiple layers (multi-layers) on top of each other. The formation of multi layers occurs in parallel to capillary condensation. Computational methods such as the one by Barrett, Joyner and Halenda (BJH) allow the computation of pore sizes from equilibrium gas pressures. One can therefore generate experimental curves (or isotherms) linking adsorbed gas volumes with relative saturation pressures at equilibrium, and convert them to cumulative or differential pore size distributions. As the equilibrium adsorbate pressures approach saturation, the pores become completely filled with adsorbate. Knowing the density of the adsorbate, one can calculate the

volume it occupies and, consequently, the total pore volume of the sample. If at this stage the adsorption process is reversed by withdrawing known amounts of gas from the system in steps, desorption isotherms can be generated. Physisorption is limited to the determination of specific surface areas and the distribution of pore sizes within a porous catalyst.

The most common methods to determine pore size distributions are the

- mercury penetration method;
- nitrogen adsorption method; and
- molecular probe method.

In principle either, desorption or an adsorption isotherm may be used but, in practice, desorption isotherm approach is much more widely used when hysteresis effects are observed. A typical adsorption–desorption isotherm of a porous solid usually exhibits a hysteresis over the pressure range where the capillary condensation phenomenon is operating. The onset of the hysteresis loop indicates the start of the capillary condensation mechanism. The desorption curve (AB'C) is always above the adsorption branch (ABC), i.e. for a given loading adsorbate desorbs at a lower pressure than that required for adsorption as shown in Figure 2.12. The basis of this approach is the fact that the BET equation is the most popular equation for the determination of surface area. The range of validity of this equation is that the relative pressure is between 0.05 and 0.35. Adsorption beyond this range will result in filling of mesopores with sorbate liquid through the action of capillary condensation in narrow pores at pressures less than the saturation vapor pressure of the adsorbate. The smaller the radius of the capillary, the greater is the lowering of the vapor pressure and hence in very small pores, vapor will condense to liquid at pressures considerably below the normal vapor pressure.

Investigation of how capillary condensations vary with the pore size, from which useful information is derived about mesopores size distribution from the data volume adsorbed versus pressure. The range of validity for the capillary condensation is that the relative pressure is between 0.35 and 0.99.

The catalysts employed in commercial fixed bed reactors often exhibit a bimodal pore size distribution, sometimes referred to as bidisperse or macro-micro distributions. In these systems the bulk of the catalytic reaction occurs in pores with radii below 200 Å, since this is where the bulk of the surface resides. However, the transport of reactants to these small pores occurs primarily through macropores with radii ranging from 200 to 10,000 Å. This catalyst pellets are prepared by compacting fine porous powders. The micropore region arises from the pore structure within each of the particles of the original powder, while the passageways around the compacted particles form the macropores. As the pelleting pressure is increased, the macropores become successively reduced in size, but the micropores remain unchanged unless the crushing strength is exceeded. The micropores accounted for about 99% of the surface area and 65% of the void volume. Most of these industrial catalysts are deliberately developed with macropore-micropore structure in order to minimize or eliminate pore diffusion limitations on the reaction rate. The macropores serves as expressways that facilitate reactant transport to the internal surface area of the catalyst.

For each pore of radius  $r$ , there exists a threshold pressure for condensation and a threshold pressure for evaporation. This important point can be used to determine the pore size and its distribution. During the adsorption cycle the filling of pore with adsorbate is in a radial fashion, and hence the rise in the amount adsorbed versus pressure is gradual and relates the vapor pressure of the film in terms of the vapor pressure of the bulk liquid and the capillary radius

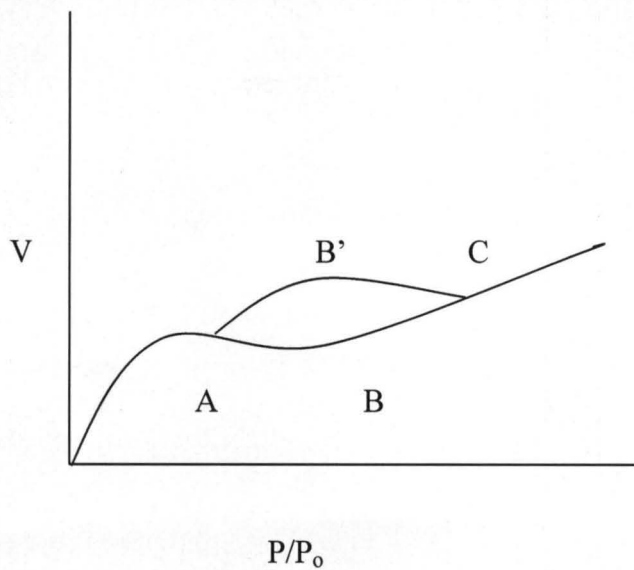


**Figure 2.12: Adsorption isotherm in mesoporous solids**



$$\frac{P_{\text{ads}}}{P_o} = \exp \left[ - \frac{\sigma V_M}{r R_g T} \right] \quad (45)$$

Equation 45 is the required capillary condensation equation for the adsorption branch. After the pore is filled, and when the pressure is reduced the liquid in the pore will remain until the pressure in the gas phase reaches the evaporation pressure governed by equation 46 at which the liquid will instantaneously evaporate, leaving only the adsorbed layer below. As the pressure is reduced further, the amount adsorbed will decrease and relationship between the amount adsorbed and the pressure is dictated by the equilibrium between the two phases.

$$\frac{P_{\text{des}}}{P_o} = \exp \left[ - \frac{2\sigma V_M}{r' R_g T} \right] \quad (46)$$

Knowing this condensation pressure (vertical emptying of the pores occurs during desorption of vapor pressure of the capillary liquid) from the desorption branch, the pore radius can then be calculated from Kelvin equation

$$\frac{P}{P_o} = \exp \left[ - \frac{2\sigma \cos\theta V_M}{R_g T} \cdot \frac{1}{r} \right] \quad (47)$$

Assuming that the liquid molar volume, the contact angle and the surface tension are known, then

$$r = \frac{2\sigma V_M \cos\theta}{R_g T} \ln \left[ \left( \frac{P_o}{P_{\text{des}}} \right)^{-1} \right] \quad (48)$$

Unfortunately, this ideal situation never occurs in practice as all practical porous solids have a distribution of pore size, so there will be a gradual change in the desorption branch rather than an abrupt change as in the case of ideal solids.

e) **Solids exhibiting adsorbed layer prior to condensation**

The analysis in which there is no adsorption occurring on the pore wall prior to the capillary condensation or after the evaporation is applicable to systems such as water adsorption on perfect hydrophobic surface, like graphitized charcoal. The case where adsorption (multilayer adsorption is allowed for) prior to condensation, the so called adsorbed layer will grow with pressure (BET mechanism). This growth in the adsorbed will make the effective pore radius smaller and thus making capillary condensation to occur sooner than the case where we have no layer adsorption. Thus, the difference between this case and that above is the adsorbed layer, which must be allowed for in the calculation of the Kelvin radius.

If we let  $t$  to represent the statistical thickness of the adsorbed layer (which is a function of pressure) then the effective pore radius available for condensation is related to the true pore radius as follows:

$$r_k = r - t \tag{49}$$

where  $r_k$  is called the Kelvin radius, governed by equation 50

$$r_k = \begin{cases} \frac{2V_M\sigma\cos\theta}{R_gT \ln(P_0/P)} & \text{for evaporation} \\ \frac{V_M\sigma}{R_gT \ln(P_0/P)} & \text{for condensation} \end{cases} \tag{50}$$

The statistical film thickness can be determined from either the BET equation

$$t = \frac{V}{V_m} \sigma \tag{51}$$

Where  $\sigma$  is the thickness of one layer or obtain film thickness measured for a non porous reference material or from an estimate for the statistical adsorbed film thickness as a function of pressure for  $N_2$  adsorption at 77K.

$$t \text{ (nm)} = 0.354 \left[ \frac{5}{\ln(P/P_0)} \right]^{1/3} \quad (52)$$

where 0.354nm is the thickness of one nitrogen molecule. With this film thickness given in equation 52 and the Kelvin radius  $r_k$  given in equation 50, the threshold radius corresponding to a gas phase pressure  $P$  is

$$r(P) = \begin{cases} t + \frac{2V_M\sigma\cos\theta}{R_gT \ln(P_0/P)} & \text{for desorption} \\ t + \frac{V_M\sigma}{R_gT \ln(P_0/P)} & \text{for adsorption} \end{cases} \quad (53)$$

**f) *The critical pore radius and statistical film thickness***

To evaluate the volume adsorbed, critical pore radius,  $r_k$ , need be known and the statistical film thickness,  $t$ . Using equation 50 for the Kelvin radius, the critical radius,  $r_k$  is calculated from equation 53. The statistical film thickness may be calculated from equation 52 or from the BET equation, i.e.

$$t_{\text{BET}} = \frac{\theta_{\text{BET}}V_M}{a_m N_A} \quad (54)$$

where  $V_M$  is the liquid molar volume,  $a_m$  is the molecular projected area,  $N_A$  is the Avogadro number equal to  $6.023 \times 10^{23}$  molecules/mole, and  $\theta_{\text{BET}}$  is the fractional loading relative to the monolayer coverage, calculated from the following BET equation

$$\theta_{\text{BET}} = \frac{C(P/P_0)}{(1-P/P_0)[1 + (C-1)P/P_0]} \quad (55)$$

For N<sub>2</sub> as adsorbate at 77K, we have the following values for liquid molar volume and the molecular projected area  $V_M = 34.68$  cc/mole,  $a_m = 16.2$  A<sub>2</sub>/molecule. From these values, the film thickness for one adsorbed layer can be calculated as

$$\left[ \frac{V_M}{a_m N_A} \right]_{N_2} = 0.354 \text{ nm} \quad (56)$$

Thus the statistical film thickness for N<sub>2</sub> calculated from the BET theory is

$$t \text{ (nm)} = 0.354 \times \theta_{\text{BET}} \quad (57)$$

The t-plot method is attributed to Lipens and deBoer in which they determined that the multilayer adsorption curve for N<sub>2</sub> at different pressures and constant temperature is identical for a wide variety of adsorbents, provided no capillary condensation occurs. The statistical film thickness of adsorbed N<sub>2</sub> multilayer is calculated using isotherm equation of Harkins and Jura.

$$t = \left[ \frac{13.99}{\log(P_0/P) + 0.34} \right]^{1/2} \quad (58)$$

## 2.7 Application and Practical Utilization of Zeolites

The four properties of zeolites that make them technologically important are:

- Dehydration and rehydration;
- Adsorption and related molecular sieving;
- Cation exchanger; and
- Catalysis.

Zeolites are widely used as drying agents in separation process (such as n-paraffins from other paraffins and p-xylene from its isomers), in laundry detergents, as catalysts and catalyst supports (e.g. in petroleum refining), in wastewater treatment, nuclear effluent treatment



(Bekkum et al, 1991). Other advanced applications of molecular sieves are as components in membranes and sensors (Behrein and Stucky, 1996).

### **2.7.1 Petroleum refining processes for the production of fuels.**

a) *Catalytic cracking* – The prime goal in petroleum refining is efficient conversion of crude oil into high-quality fuel components. Desired fuel fractions in order of increasing molecular weight are gasoline, aviation jet fuel, and diesel fuel. Gasoil and asphalt with even higher molecular weight, are most often further processed by thermal cracking, catalytic cracking to make gasoline (Hemmler & Tajbl, 1997), and catalytic hydrocracking (to make jet fuel). A lower-boiling fraction, light straight run naphtha, rich in pentanes and hexanes and some butane is further processed by catalytic hydroisomerization.

Strong acid catalytic activity of X and Y zeolites was discovered in 1957 by Rabo and was related to their crystallinity (Rabo & et al, 1960). This discovery laid the basis for zeolites in cracking, hydrocracking, and isomerization of hydrocarbons. From the early 1960s on, use of synthetic zeolites in catalysis and in related adsorption separation processes has dramatically transformed petroleum refining by vastly increasing the yield of high-quality fuels and reducing capital and operating costs, energy requirements, and adverse environmental impact. Zeolites also played a major role in allowing the efficient reformation of gasoline to the present lead-free gasoline.

In modern petroleum refineries, gas oil and other heavier fractions from the crude oil fractionation unit are fed to fluid catalytic cracking units, which use small, fluidizable catalyst particles containing type Y zeolite or other zeolites, or to hydrocracking units, which use fixed beds of larger catalyst particles also containing zeolites. The FCC and hydrocracking units



convert higher molecular weight hydrocarbons to lighter ones suitable for gasoline, light fuel oils, olefins, and other uses.

In both FCC and hydrocracking, zeolite catalysts provide vastly superior combinations of strong acid catalytic sites, uniformity of pore structure, and stability, all of which provide improved selectivity, yield, durability, and cost over non-zeolite alternatives. Zeolites are used as catalysts for FCC process, a process which transforms long-chain alkanes (heavy oil) into shorter ones (petrol), and to enhance the octane number of the petrol by producing branched species. The FCC unit is a continuous process in which the pre-heated zeolite (mainly zeolite Y) is added to the feed stream, which flows upward in the reactor. The alkanes are cracked by the hot zeolite and the product gas stream, containing the short-branched alkanes is transferred to a fractionator. The zeolite is only in contact with the feed for a few seconds during which it is deactivated due to coke formation within the pores. This coke is removed by a calcination step by which the zeolite is regenerated and brought on reaction temperature again. The burn-off of the coke thus delivers the heat, which is needed to initiate the cracking process within the catalyst.

The ZSM-5 when used in FCC units provides refiners with a rapid method to improve gasoline octane number and light olefin yield without affecting dry gas, coke, or unit conversion. ZSM-5 is a 10-membered sieve containing channel openings of 5.1 to 5.6 Å. These openings are smaller than 7 – 8 Å cage openings for a commercial FCC Y zeolite. Hence, access to molecules larger than monomethyl aliphatics into ZSM-5 is restricted, and reaction of molecules with critical diameters greater than 6 Å is severely diffusion controlled. Besides controlling accessibility of hydrocarbons, ZSM-5 contains strong Bronsted acid sites necessary for cracking hydrocarbons and does not catalyze coke formation as readily as a Y zeolite (Chen et al., 1989).



The properties stated above allow ZSM-5 to be used as an FCC additive for boosting gasoline octane number (Schipper, 1988). It also increases C<sub>3</sub> and C<sub>4</sub> LPG selectivity with a concurrent decrease in gasoline selectivity. It should be noted that the increased LPG fraction consists predominantly of olefins. There is essentially no change in dry gas (C<sub>2</sub>-) or coke selectivity; however, there is a significant change in gasoline composition. The effects of ZSM-5 on gasoline structure are (Madon, 1989):

- C<sub>7+</sub> straight chain and branched olefins and paraffins decrease;
- C<sub>5+</sub> hydrocarbons increase and the molecular weight of gasoline decreases;
- The concentration of aromatics and naphthenes increases.

Since the rate of olefin cracking is more than two orders of magnitude greater than paraffin cracking (Haag et al., 1981), the decrease of C<sub>7+</sub> olefins is due to their being cracked to give mainly C<sub>5</sub> – C<sub>5</sub> olefins. In the presence of such reactive olefins, paraffin cracking is substantially reduced. There are several pathways for gasoline paraffin formation during catalytic cracking. One secondary pathway involves hydrogenation of primary olefins. By cracking these primary olefins, ZSM-5 reduces the reactant olefins needed to produce paraffins. Thus, low octane paraffins in gasoline are decreased as a direct result of olefin cracking.

The decrease in gasoline molecular weight and increase in C<sub>5</sub> hydrocarbons are important reasons for the increase in gasoline octane number. There is no incremental formation of aromatics and naphthenes due to the presence of ZSM-5. However, since the total volume of gasoline is reduced due to the decrease in C<sub>7+</sub> aliphatics, the concentration of aromatics and naphthenes in the gasoline being increased, again helps in enhancing gasoline octane numbers. However, the balance between the increase in octane number, C<sub>3</sub> and C<sub>4</sub> olefin yields, and the

decrease in gasoline yield will depend on factors such as feed characteristics, operating conditions, and the type of zeolite catalyst used.

b) **Hydrocracking** – The early 1960s saw increasing demand for high-octane gasoline for the high-compression-ratio engines in new high-performance cars. Demand also grew for diesel fuel for diesel-electric locomotives and low-freeze point jet fuel. Rapid growth in hydrocracking of the more-refractory crude fractions that were not converted to gasoline and lighter products in the catalytic cracking units met these needs. Roland Hanford at Union Oil, now Unocal, pioneered the development of new zeolite-based hydrocracking catalysts, which dramatically improved activity and selectivity (Scherzer, 1996). In hydrocracking, hydrocarbon molecules and hydrogen gas pass over the zeolite catalyst, which converts higher-molecular-weight petroleum fractions to lower-molecular-weight fuels (Bridge, 1997). Universal Oil Product (UOP's) Unicracking process uses base-or noble-metal hydrocarbon-activity promoters impregnated on combinations of zeolite-and amorphous-aluminosilicates for cracking activity (Reno, 1997). The specific metals chosen and the proportions of the metals, zeolite, and non-zeolite aluminosilicates are optimized for the feedstock and desired product balance. The isocracking process of Chevron also uses hydrocracking catalysts, some containing zeolites to increase the cracking function of these dual-function catalysts (Bridge, 1997).

The zeolites most frequently used in commercial hydrocracking catalysts are partially dealuminated and low-sodium, or high silica type Y zeolites in hydrogen or rare earth forms. Other zeolites and mixtures of zeolites are also used. The zeolites are often imbedded in a high-surface-area amorphous matrix, which serves as a binder. They can reside inside the zeolite and on the amorphous matrix.

c) **Catalytic Dewaxing** – This yields various grades of lube oils and fuel components suitable for extreme winter conditions. Paraffinic (waxy) components, which precipitate out at low temperatures are removed. The first stage saturates olefins, desulphurizes and denitrifies the feed via hydrotreating (Genis, 1997). The second stage performs a dual function by using a non-noble-metal zeolite catalyst to selectively adsorb and then selectively hydrocrack the normal and near-normal long chain paraffins to form shorter-chain (non waxy) molecules. Alternatively, Chevron Isodewaxing process isomerizes the linear paraffins to branched paraffins using a SAPO – 11 molecular sieve catalyst containing platinum (Miller, 1994).

d) **Light Paraffin Hydroisomerization** – Lead was added to gasoline to increase its octane number, especially for vehicles in the early 1960s that had modern high-compression – ratio, high performance engines. The subsequent U.S – legislated reduction of lead in gasoline required increased use of catalytic hydroisomerization of the light straight-run naphtha fraction. The hydroisomerization process uses highly active zeolite-based, Pt-containing hydroisomerization catalysts (UOP 1-7) containing modified synthetic (large-pore) mordenite. In the presence of hydrogen at moderate conditions, such catalysts optimize isomerization and minimize hydrocracking (Cusher, 1997). Linear paraffins in the feed convert to branched paraffins with higher octane number. To further increase octane level, products from a hydroisomerization unit can be sent to the Molex (Molecular Extraction Unit) process (simulated moving-bed technology) where the remaining lower-octane, linear paraffins are separated from the other compounds by using a zeolite adsorbent and a liquid desorbent; the Molex process is an example of UOP's Sorbex simulated-moving bed technology (Sohn, 1997). The extracted linear paraffins are recycled to the hydroisomerization unit and the remaining higher-octane fraction is recovered

for gasoline blending. These two processes boost the octane number of a typical feed from 68 – 70 to 89 – 92.

### 2.7.2 Petrochemicals processing for production of aromatics and their derivatives

a) *Ethylbenzene synthesis* - Styrene monomer, made by dehydrogenating ethylbenzene (EB), is the basic chemical for all polystyrene products. Ethylbenzene is made using various catalysts to alkylate benzene with ethylene. In 1980, nearly all the EB were produced by liquid-phase alkylation reactions using aluminium chloride catalyst. In the same year, vapour phase alkylation using a heterogeneous catalyst was introduced to eliminate many problems of waste disposal. In 1990, liquid-phase zeolitic technology began to replace the vapour – phase process, based on ZSM-5 zeolite.

The 1990 Lummus/UOP EB liquid-phase process using highly stable, poison-resistant zeolite catalysts operates at low benzene to olefin ratio and at high selectivity of EB. In 1995, MCM-22 zeolite catalyst was used for liquid-phase alkylation and modified MFI catalyst for vapour-phase transalkylation of polyethylbenzene and cracking of C<sub>6</sub> and C<sub>7</sub> naphthenes (Jeanneret, 1997).

b) *Cumene synthesis* – Cumene is the principal chemical for production of phenol and its byproduct (acetone). The phenol yields phenolic resins, bisphenol-A, caprolactam, and other products. Phenolic resins are used extensively to bond plywood and composition board. Both phenol and acetone are used increasingly in the production of polymers such as epoxy, polycarbonate resins and nylon-6.

Cumene is made by alkylating benzene with propylene over an acid catalyst, mostly solid phosphoric acid and minor AlCl<sub>3</sub>. Recent awareness of the negative environmental impact of spent-catalyst disposal spurred the search for better alternatives. Catalytic condensation process

for production of high purity cumene, which uses inexpensive solid phosphoric acid catalyst, however gave rise to side reactions over the catalyst resulting in a 4-5% loss in cumene yield. QZ-2000 zeolite catalyst for direct alkylation of benzene with propylene which incorporates a second step (transalkylation) to react with the diisopropylbenzene, a by-product of the first step, with benzene to form additional high quality cumene product (>99.97% purity) and overall cumene yield of 99.7% at lower investment cost. Other zeolites are MCM-22 zeolite, 3D-DM catalyst based on dealuminated forms of mordenite and Enichem-a catalyst based on zeolite beta (Wallace et al., 1997).

c) ***Para-xylene production from mixed C<sub>8</sub> aromatics*** – Polyester fibres has revolutionized clothing, which has the advantage of wash-and-wear, and permanent press clothing. Demand has grown in developing countries because of the great comfort of fabrics made from cotton-polyester fibres blended in any proportion for any climate as well as low cost, excellent durability, and ease of washing with little water and detergent. It makes use of the Parex process, which uses the Sorbex technology.

Most p-xylene is used to make purified terephthalic acid which is reacted with ethylene glycol to make poly- (ethylene terephthalate), the basis of polyester fibres. The p-xylene is separated from mixed C<sub>8</sub> aromatics (containing o-, m-, and p-xylenes and EB) by using either crystallization or adsorption processes. Another use is in the manufacture of poly-(ethylene terephthalate) for bottles that are recyclable and environmentally friendly (Jeanneret, 1997). Ion – exchanged forms of synthetic FAU zeolite are used with desorbent liquids to recover >99.9% purity from a raffinate containing EB and o- and m- xylenes.

d) ***Xylene isomerization*** – The raffinate from the Parex unit goes to an Isomer unit for isomerization to a near-equilibrium mixture of xylenes, which are recycled to the Parex unit. The



Isomer unit uses zeolite acid catalysts such as Pt-bearing 1-9 catalyst, which converts EB to xylenes, and the I-100 catalyst, which dealkylates EB to benzene. Both provide efficient EB conversion with excellent xylene retention (Jeanneret, 1997).

### 2.7.3 Disproportionation of toluene and transalkylation of toluene and trimethylbenzenes

a) *Trimethylbenzenes* – The recent demand for p-xylene has begun to exceed the supply of mixed xylenes. Incorporating the Tatoray process into the aromatics complex in a refinery can more than double the yield of p-xylene from a naphtha feedstock (Jeanneret, 1997). The zeolite-based TA-4 catalyst has two principal functions, disproportionation of toluene into the more valuable benzene and mixed xylenes, and transalkylation of toluene and trimethylbenzenes to mixed xylenes. The mixed xylenes are then added to the Parex unit to produce more p-xylene.

b) *P – xylene synthesis from toluene* – Xylenes can be produced from the zeolite – catalyzed disproportionation of toluene alone. Mobil toluene to para-xylene (MTPX) process and Mobil selective toluene disproportionation process (MSTDP) based on ZSM-5 (MFI) “product shape – selective” zeolite catalysts. The toluene disproportionation generates mixed xylenes inside the catalyst but the overall relative yield of p-xylene is greater than the thermodynamic equilibrium allowed because the p-xylene diffuses more rapidly out of the zeolite than do o- and m- xylenes (Olson et al., 1984).

c) *Aromatics from light hydrocarbons* - Cyclic process converts the low-value LPG (propane, butanes) or light feedstocks containing olefins and paraffins to high-value, easily transportable, petrochemical-grade liquid aromatic products, particularly BTX (benzene, toluene and xylenes). It uses a single gallium-modified zeolite catalyst in conjunction with CCR (continuous catalytic regeneration) system (Jeanneret, 1997). Acidic sites on zeolite catalyze



dehydrogenation, oligomerization and cyclization. The shape-selectivity of the zeolite cavities helps promote the cyclization reactions and limits the size of the rings (Gosling, 1991).

d) **M – Forming** – Catalytic reforming produces high octanes liquid reformat product rich in aromatics and hydrogen gas; light hydrocarbon such as LPG and C<sub>6</sub> to C<sub>9</sub> paraffins. M – Forming process selectively hydrocracks linear and single branched paraffins in gasoline reformat fractions to LPG by size selective catalysis by using medium-pore ZSM-5 zeolite (Chen et al., 1987).

#### 2.7.4 Petrochemicals processing for olefins production

a) **Light olefin production by methanol-to-olefins (MTO) process** - Natural gas is processed to make liquefied natural gas at high cost or alternatively they are converted first to Synthesis gas (CO and H<sub>2</sub>) and then to the more valuable, easily shipped methanol. The new UOP/HYDRO MTO process provides the means to efficiently convert methanol to even more valuable light olefins (ethylene, propylene and butenes). This process uses the product-shape selective MTO-100 catalyst based on a unique molecular sieve (Vora & et al, 1997).

b) **Olefin isomerization** - The 1990 Clean Air Act increased the demand for blendable ethers in motor fuels and created a demand for isobutene to make methyl tertiary butyl ether, and for isopentene to make tertiary amyl methyl ether using I – 500 catalyst based on SAPO structure. Butesom for isobutene isomerization and Pentosom for pentene isomerization processes (Gajda, 1993; Ozmen & et al, 1993; Davis, 1997) where coke progressively accumulates on the catalyst and is periodically removed by a simple carbon burn-off process in the reactor. The Lyondell IsoPlus uses a ferrierite (FER) zeolite and medium pore zeolite (ZSM-5) catalyst for the isomerization of olefins to isoolefins (Chen and et al., 1992).

c) **Oxygenate removal unit** – Zeolite adsorbents are used in an oxygenate removal unit down to >1ppm total of trace oxygenates {e.g. dimethyl ether (DME), methanol, and methyl tertiary butyl ether} from C<sub>4</sub> streams. Depending on the flow scheme, the C<sub>4</sub> stream generally goes to a motor fuel alkylation (H<sub>2</sub>SO<sub>4</sub> or HF acid) process or is recycled to a dehydrogenation – etherification complex that has an Oleflex unit and a methyl tertiary butyl ether unit. The advantages of the oxygenate removal unit is that it minimizes the acid consumption otherwise associated with these oxygenates, thus minimizing the acid neutralization wastes, a significant environmental benefit. In dehydrogenation, the oxygenate removal unit improves catalyst stability and lowers costs of methyl tertiary butyl ether production.

### 2.7.5 Petrochemicals processing for detergents production

a) **Linear paraffins for biodegradable detergents** – Petroleum derivatives account for most of the total surfactant production and household detergents. During the 1940s and 1950s, sodium dodecylbenzene sulfonate was the most widely used synthetic detergent. However, dodecyl paraffin side group on the benzene ring is highly branched and not easily biodegraded. In 1960s, environmental concerns led to the development of linear alkylbenzene sulfonate (LAS) detergents, which are biodegradable and cost-effective. The key to the manufacture of the linear paraffins required to make linear alkylbenzene (LAB) and hence, LAS is the use of size-selective synthetic zeolites that adsorb linear paraffins but exclude branched paraffins, naphthenes, and aromatics, from mixtures spanning a range of boiling points as in kerosene (C<sub>12</sub> – C<sub>18</sub>). Two different processes are employed; one vapour phase and the other liquid phase are used.

The vapour-phase IsoSiv process was developed at Union Carbide originally for octane improvement. To produce linear paraffins for detergents, kerosene feed pretreated to acceptable

quality and the desired carbon number range, passes at elevated temperature and over atmospheric pressure through a bed of zeolite adsorbent, which adsorbs just the linear paraffins. Enough hexane vapour follows the kerosene feed to displace the non-adsorbed feed and isomeric hydrocarbons from the void spaces in the adsorber vessel. The effluent from this step is combined with the adsorption effluent stream. The linear paraffins adsorbed in the zeolite are adsorbed by purging the bed in the opposite direction with hexane. The hexane in the effluent is separated by distillation and is recycled. The remaining linear paraffins comprise of the desired product.

The liquid-phase Molex process is most often used to produce plasticizers ( $C_6 - C_{10}$ ), LABs ( $C_{10} - C_{15}$ ) and detergent alcohols ( $C_{13} - C_{22+}$ , but usually heavier than  $C_{16}$ ). To make linear paraffins for LAB, increased linearity and low aromatics content are desired. This process improves product purity to 99.7% and reduced aromatics content to 0.05 wt %. ADS-34 zeolite adsorbed provides improved long-term separation performance in the Molex process. Molex process is sent to Pacol (Paraffin Conversion to Olefins) and DeFine processes for catalytic conversion to mono-olefins. This pass to a UOP's Detergent Alkylate process (Vora, 1985), which uses hydrofluoric acid catalyst or to a Detal process which uses a more environmentally friendly solid heterogeneous catalyst to produce LAB from the mono-olefins plus benzene. Unreacted linear paraffins are recycled to the Pacol and DeFine units for conversion to extinction. The catalytic processes use nonzeolite catalysts.

**b) *Linear olefins for detergent alcohols*** – Detergent alcohols are made from  $C_{10}-C_{15}$  alpha olefins derived from ethylene or from  $C_{10}-C_{15}$  internal olefins derived from lower-cost kerosene feed. Linear paraffins from the high-purity Molex zeolite adsorption process are sent to the Pacol and DeFine processes to convert them to a mixture of mono-olefins plus unreacted linear

paraffins. The mixture is fed to Olex process unit, which uses a zeolite adsorbent in a Sorbex simulated-moving-bed process to separate the linear olefins, and the unreacted paraffin, which are recycled back to the Pacol and DeFine units to extinction. The Olex process uses ADS-32 zeolite adsorbent, which provides improved capacity and rates. The linear olefins product has improved product purity (reduced aromatics and diolefins) as a result of improvements in the zeolite adsorbents and in the nonzeolite catalysts and operating conditions in the Molex-Pacol-DeFine Olex sequence of processes.

Other applications include:

#### **2.7.6 Separation and purification process applications**

- Preprocessing of gases before cryogenic separations
- Removal of impurities from gases and liquids down to low levels
- Air separation by swing adsorption (PSA) process

#### **2.7.7 Manufacturing industries and consumer products application**

- Small Oxygen Concentrators for Medical Use (Medox)
- Automotive Air-Conditioning and Stationary Refrigerant Drying
- Air Brake Dryers for Heavy Trucks and Locomotives
- Insulated Glass Windows

#### **2.7.8 Environmental protection applications**

- Builders for Phosphate-Free Laundry Detergents
- Automotive Emissions Control
- Radioactive Waste Management

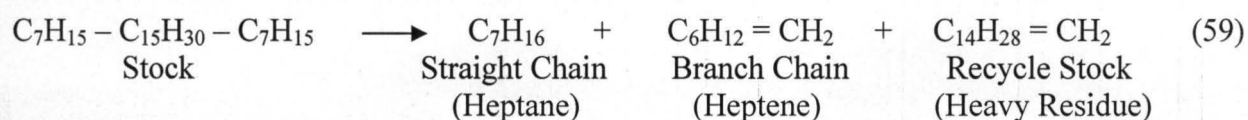


## 2.8 Chemistry of Catalytic Processes

Catalysis is a term used to describe the influence of certain substances on the nature of diverse reactions, the substances themselves apparently being unchanged by the reaction. Berzelius in 1835 imbued these materials with a catalytic force capable of awakening the potential for chemical reaction between species that would normally be nonreactive at a given temperature. Therefore, a catalyst is a substance that affects the rate or direction of a chemical reaction, but is not appreciably consumed in the process. There are three important aspects from the definition above, firstly, a catalyst may increase or decrease the reaction rate. Secondly, a catalyst may influence the direction or selectivity of a reaction. Thirdly, the amount of catalyst consumed by the reaction is negligible compared to the consumption of reactants. A catalyst cannot change the ultimate point set by thermodynamics, but it can affect the rate at which this point is approached. However, it can facilitate approach to equilibrium with respect to a desired reaction while not influencing the rates of other less desirable reactions. In optimizing yields of desired products, chemical engineers are very concerned with the selectivity or specificity of a catalyst. For commercial applications, selectivity is often more important than activity per se. The idea that a catalyst remains unaltered by the reaction it catalyzes is naïve and misleading. Physical and chemical changes can and do occur either during or as a result of the catalytic processes. Many commercial catalysts are gradually deactivated by poisoning reactions that accompany the main reaction process.

Catalytic reactions are often classified as homogeneous or heterogeneous. Homogeneous catalysis takes place when the catalyst and the reactants are both present in the same fluid phase. The term heterogeneous catalysis is a catalytic phenomenon involving a solid catalyst and reactants in a gas or liquid phase and is sometimes referred to as contact catalysis.

Cracking is the process of converting or breaking down of large hydrocarbon molecules into smaller molecules by the action of heat, catalyst or both e.g. cracking of heavy gas oil obtained as a heavy (distillates) fraction of straight run distillation of crude oil which can be converted into an appreciable proportion of such fractions into lower molecular weight hydrocarbons boiling in the motor-spirit range.



Cracking predominantly takes place in the vapour phase in the presence of a catalyst which may be in pellet or powdered form. It has the ability to enhance the rate of cracking reactions and selectively promote certain reactions.

### 2.8.1 Types of cracking processes

There are three main cracking processes namely: thermal cracking, hydrocracking and fluid catalytic cracking (Ahmed, 2007). The most important types of catalytic conversion processes are those which change the carbon number, are catalytic cracking, hydrocracking and polymerization. Carbon to hydrogen ratio is changed by hydrogenation and dehydrogenation while isomerization is the process that neither changes the carbon number, the C-H ratio nor the amount of isomerate, but only changes the shape of the molecules along with the quality of the isomerate.

These processes use catalyst and may involve the reactions which are important in thermal conversion processes. A catalyst usually consists of an active substance (which determines the course of desirable reactions) applied onto a carrier substance (mostly alumina) having a largely extended surface. In some cases, some other substances (promoters) are added to improve the characteristics of the catalytic conversion process. The particles (granules) of a



catalyst possess an enormous porosity and therefore a very large internal surface area. The activity of a catalyst is due mainly to the surface of pores rather than to their external surface. The name of a catalyst depends on the process where it is to be used e.g. cracking catalysts, reforming catalysts etc.

### 2.8.2 Hydrocracking catalysts

A catalyst is a substance that increases the rate at which a chemical reaction approaches equilibrium without itself becoming permanently involved in the reaction. Gasoline and distillates are usually the higher – priced refinery products and therefore refinery processing units are designed to maximize conversion of crude oil to these products. To be commercially successful, the catalyst must possess three properties: activity, selectivity and stability.

Activity is a term which denotes how well a catalyst can perform with respect to reaction rate, temperature or space velocity. The higher the reaction rate, the higher the activity of the catalyst.

Selectivity is the percentage of the desired product yielded from the feedstock. Stability is the ability of a catalyst to maintain its activity and selectivity over a reasonable period.

Note:

- A catalyst having very high activity and excellent selectivity will be of no use to the refiner unless it has stability.
- A catalyst that operates for a long time with little or no loss in activity or selectivity has good stability and therefore has a long cycle life between regenerations whereas a catalyst that loses activity or selectivity has poor stability.

Hydrocracking process needs dual functional catalysts. They have a hydrogenation/dehydrogenation function as well as acidic/cracking function. Active component

and promoters provide hydrogenation – dehydrogenation catalyst activity due to metals loaded and the support whereas the cracking activity is controlled by the support that is acidic in nature.

Active components are commonly transition metal sulphides of an element in group VIB (i.e. molybdenum (Mo) or tungsten (W)) that is responsible for the principal chemical reaction. The active component saturates aromatics in the feed, saturates olefins formed in the cracking and protects the catalyst from poisoning by the coke. A promoter is a chemical compound such as nickel (Ni) and cobalt (Co) which when added results in desirable activity, selectivity or stability effects. With addition of the promoter, the strength of Lewis sites and the number of Brønsted sites are increased, and the enhancement in catalytic cracking is significant. The role of the promoter is to increase the number of sulphur vacancies and to modify the acid-base properties of the catalyst.

Supports provide the cracking functions, where cracking takes place on strong acid sites in the supports. The most important function of support is maintenance of high surface area for the active component and acidity for hydrocracking reactions. A support is chosen for a particular application on the basis of several important characteristics such as:

- Inertness to undesired side reactions,
- Appropriate mechanical properties (attrition resistance, strength etc),
- Stability under reaction conditions,
- A surface area and pore size distribution appropriate for the desired reaction and
- Its cost.

Zeolites with rare earth exchanged ions added to amorphous matrix are widely used as catalyst support and play an important role in the catalysts used in hydrocracking process to improve

their catalytic activity, selectivity or stability by imparting shape selectivity. X and Y zeolites explored commercially for cracking operation and are represented by the formula



where p ranges from 96 – 74 for X, 74 – 48 for Y and g is between the range 250 – 270 as aluminum decreases.

Zeolites have been successful because of their

- Crystallinity
- High surface area
- Adsorption capacity and
- Uniform size distribution which enable shape selectivity.

The techno-economical characteristics of a catalytic process are determined by the quality of the feedstock and the process conditions as well as the properties of the catalyst used. The capability of a catalyst (zeolites) to accelerate the desirable reactions and to retain the rate of undesirable ones at a constant low level is called selectivity. Activity is another important characteristic of a catalysts estimated in terms of the yield of the end product relative to the use of the starting material. In particular, the catalyst activity in catalytic cracking is determined as the yield of gasoline (end product).

Catalysts can participate in process reactions in a stationary (fixed-bed) or moving (circulating) state. In both cases, they gradually lose their activity and selectivity owing to ageing called normal ageing. Along with the normal ageing, quick ageing of a catalyst may also take place when the process is run under abnormal conditions say at an excessively high temperature. Certain substances like S, N<sub>2</sub>, and heavy metals (V, Ni and others) and water in the feed stocks can affect many of the catalysts.

Catalysts can be regenerated to restore their activity and partially the selectivity usually done by removal (burning off) of the coke deposited on catalyst particles during operation or gradually raising the temperature in the reactor.

### **2.8.3 Hydrocracking process**

The three methods of hydrocarbon cracking or conversion of heavy petroleum fraction into valuable products has been achieved mainly by pyrolysis or thermal cracking, catalytic cracking and hydrocracking (Ahmed, 2007). Thermal cracking is the breaking up of heavy oil molecules into lighter fractions by the use of high temperature without the aid of a catalyst. In thermal cracking process, hydrocarbons with higher molecular weight in heavy oils can be transformed to lighter hydrocarbon products by thermolysis at a higher temperature, which is accompanied with the formation of coke. The development of thermal cracking process for producing middle distillates has been limited because large amounts of gas and naphtha with lower quality are produced due to over cracking. Thermal cracking processes are commonly used to convert petroleum residue oil into distillable products, although thermal cracking processes as used in the early refineries are no longer used and the modern thermal cracking processes is visbreaking. The objective of visbreaking is to reduce the viscosity of heavy feedstock and to increase the hydrogen-carbon atomic ratio

Hydrocracking offers several advantages over thermal cracking such as

- Higher gasoline yield
- Better gasoline octane quality
- Improved balance of gasoline and distillate production
- Higher yield of isobutene in the butane fraction.

The development of thermal cracking process for producing middle distillates has been limited because large amounts of gas and naphtha with lower quality are produced due to over cracking.

Catalytic cracking is different from thermal cracking because carbon-carbon (C-C) bond cleavage of hydrocarbons in the former occurs on a solid acid catalyst. However, the absence of high partial pressure of  $H_2$  in the catalytic cracking process not only makes possible the rapid buildup of coke on the catalyst but also results in products containing a significant amount of olefinic and aromatic compounds. This not only accounts for the high-octane rating of the catalytic cracking gasoline, but also for the poor quality of middle distillates obtained in the catalytic cracking.

In petroleum refining, hydrocracking of heavy hydrocarbons has been carried out to produce high quality gasoline, jet fuel and diesel. Hydrocracking is the process of breaking up heavier hydrocarbon molecules into lighter hydrocarbon fractions by using heat and catalysts in the presence of hydrogen (Ahmed, 2007). In this process, the use of higher partial pressure of  $H_2$  and relatively low temperatures decreases the rate of coke formation and favours the hydrogenation of olefins and aromatic compounds.

#### **2.8.4 Hydrocracking reactions and mechanisms**

It is an endothermic reaction, provides olefins and other unsaturates for hydrogenation while hydrogenation, an exothermic reaction, provides heat for cracking (Ahmed, 2007). This process increases the yield of gasoline from crude oil. During hydrocracking, the feed is treated with  $H_2$  which makes it  $H_2$  consuming reaction over a dual function catalyst i.e. a catalyst with both hydrogenation and cracking activity, at about  $340 - 470^\circ C$  and  $65 - 135$  atm with extremely high  $H_2$  to oil ratio ( $\sim 1000$ ). The cracking function of the catalyst is provided by silica – alumina



or zeolite catalysts and the hydrogenation component may be provided by nickel, platinum or palladium. During hydrocracking, the primary reaction is the cracking (same as catalytic cracking) where scission of a carbon-carbon single bond occurs and the secondary reaction is hydrogenation of olefins (C-C double bond) into alkanes. The olefinic materials produced during cracking are saturated before they can contribute to coke formation. The feedstock is thermally cracked and hydrogenated to yield products with increased H/C atomic ratio, reduced S and N<sub>2</sub> content. An increase in reaction temperature results in an increase in reaction rate but has no significant effect on the conversion. The hydrocracking process converts the heavy feed such as vacuum gas oil to lower weight products. The process also allows removal of organic sulphur and nitrogen compounds, and saturation of olefins and aromatics. Organic sulphur compounds are transformed into H<sub>2</sub>S, while organic nitrogen compounds are transformed into NH<sub>3</sub>.

The main types of reactions that take place during hydrocracking unit can be categorized into two types: Cracking reactions and hydrotreating reactions.

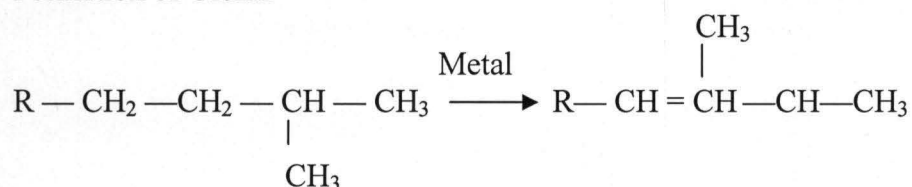
The hydrocracking reactions proceed through a bifunctional mechanism, requiring both types of catalytic sites – acidic and metal sites to catalyze separated steps in the reaction sequence of cracking and hydro/dehydrogenation. There are many of simultaneous reactions occurring in the hydrocracking, but in general, the mechanism of hydrocracking is that of catalytic cracking with hydrogenation superimposed. Moreover, cracking and hydrogenation are complementary; cracking provides olefins for hydrogenation while hydrogenation in turn provides heat for cracking. The overall reaction is exothermic, as the heat by the exothermic hydrogenation reactions is much higher than the amount of heat consumed by the endothermic cracking reactions. The postulated mechanism of hydrocracking reactions starts with the generation of an olefin or cycleolefin on a metal site of the catalyst. Then, an acid site adds a proton to the formed



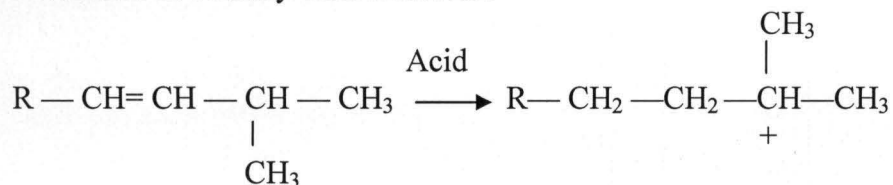
olefin, leading to the formation of a carbenium ion, which tends to crack, to give a smaller carbenium and a new olefin, also smaller than the initial called primary cracking products. These products can react further to produce smaller secondary products, and so on, until the abstraction of a proton from the carbenium ion to form an olefin at an acid site; and its saturation at a metal site (Susana, 2009). Chemical Equations 61 and 62 are the main types of reactions that take place during hydrocracking while figures 2.13(a-d) gives the detailed mechanism involved in the hydrocracking of paraffins.



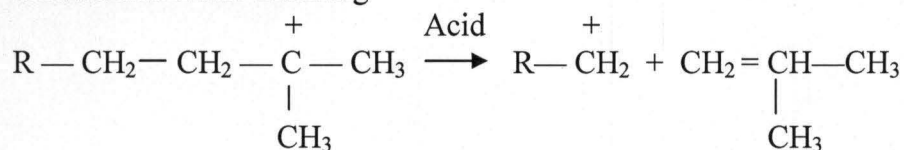
(a) Formation of Olefin



(b) Formation of Tertiary Carbenium Ion



(c) Isomerization and Cracking



(d) Olefin Hydrogenation

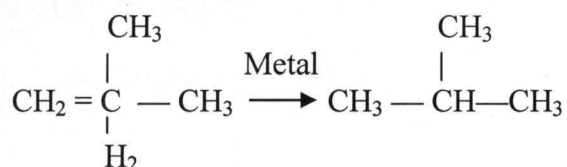


**Figure 2.13: Hydrocracking mechanism of n-paraffins**

The gasoline obtained from the hydrocracking process has a lower octane number and has to be catalytically reformed before use in motor engines. It is useful for cracking products above the gasoline boiling range. They contain high proportions of polynuclear aromatic hydrocarbon resistant to further cracking. It is also useful where it is desired to minimize heavy fuel oil production.

Hydrotreating reactions are desired reactions for sulphur removal (HDS), nitrogen removal (HDN), aromatic removal (HDA), and halides removal (HDM). Depending on the source of the feed, these compounds are present though in variable amounts. Hydrogen is consumed in all hydrotreating reactions, as in the hydrodesulphurization (equation 63) and hydrodenitrogenation as shown in Chemical Equation 65 below.

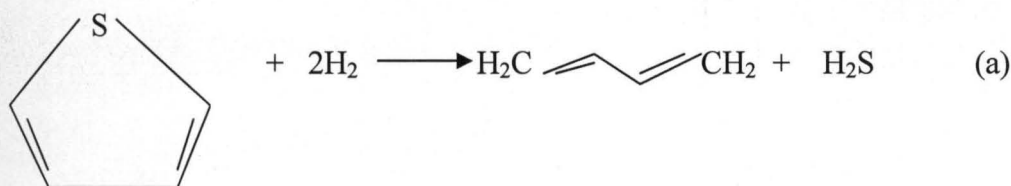
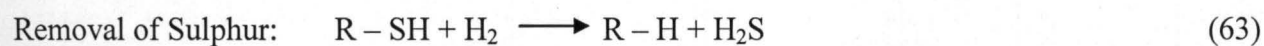
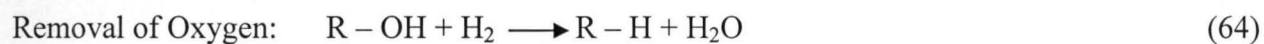
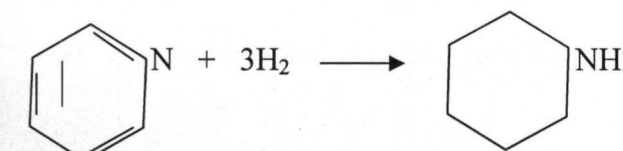
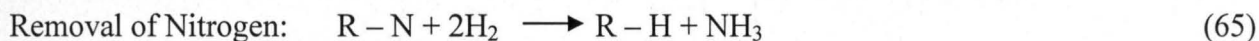


**Figure 2.14: Generally accepted desulphurization mechanism**

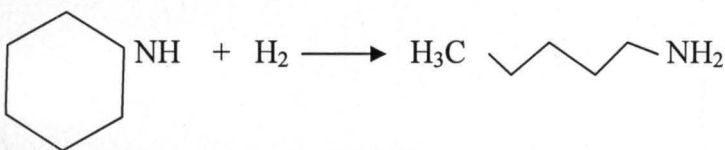
In the hydrodesulphurization process, the sulphur is removed from the initial molecule, and is formed an intermediate olefin and  $\text{H}_2\text{S}$ . The olefin is hydrogenated to form a paraffin, or other molecules depending on the organic sulphur compound as shown in figures 2.14a and 2.14b, respectively. Once the hydrocracking process runs under high  $\text{H}_2$  pressure, the feed desulphurization is almost complete (Susana, 2009).



Hydrodenitrogenation removes  $N_2$  from the feed of the process, proceeding through a different path. The aromatic hydrogenation occurs first followed by hydrogenolysis and, finally, denitrogenation releasing ammonia as shown in figure 2.14 a-c below:



(a) Aromatic Hydrogenation



(b) Hydrogenolysis



(c) Denitrogenation

Figure 2.15: Typical mechanisms of HDN



Catalysts that decrease reaction rates are usually referred to as inhibitors and the aromatic compounds may have substantial inhibiting effects over the catalyst as coke precursors and their levels have to be controlled. Their cracking reaction is very complex, requiring hydrogenation prior to cracking, but is necessary for cracking cyclic hydrocarbons. Hydrocracking and hydrotreating are first order reactions with hydrocracking as the rate controlling step, and kinetic data of the reaction follow Langmuir Hinshellwood approach (Ahmed, 2007).

### 2.8.5 Coke formation

Coke is a high carbon-content residue remaining from the destructive distillation of petroleum residue. Coking is a process for thermally converting and upgrading heavy residual into lighter products and by-product petroleum coke.

Besides hydrotreating and hydrocracking reactions, there are several other possible reactions occurring simultaneously, such as aromatic saturation, coke precursor's formation or even coke formation. These reactions can take place either in the hydrotreating or in the hydrocracking sections. In fact, the aromatic saturation is the only reaction, which is limited at higher temperatures, reached by the catalyst deactivation. This leads to an incomplete aromatic saturation that will react from different ways to form coke. The coke molecules will at first deactivate the acid sites in the supercages of the catalyst, due either to the poisoning of the sites or to the blocked access to the reagents. However, even if there is no coke molecules inside a pore, there is the possibility to an acid site being blocked by the incrustation of coke molecules from the outside, blocking in the same way the access of reagent molecules. Normally, the hydrocracking unit (HCU) feed contains polynuclear aromatics (PNA), and due to the catalyst deactivation will be restraint to saturate, leading to important, though undesirable large PNA formation. The result of operating HCU with recycle of the unconverted feed is the creation of PNA, which may deactivate the catalyst. The coking process also needs the retention of the coke precursors under the catalyst hence coke formation occurs inside the zeolite pores (Susana, 2009).

## CHAPTER THREE

### 3.0 MATERIALS AND METHODS

This chapter comprises of materials, equipments, and experimental procedure used in carrying out this research work.

#### 3.1 Materials and Equipment

The materials and equipment used for this research are presented in the Tables 3.1 and 3.2, respectively.

**Table 3.1: List of Materials used for the Experiment**

MATERIALS	SOURCE	COMMENT/REMARK
Ahoko Clay	Ahoko Village, Kogi LGA, Kogi State, Nigeria.	-Solid clay materials rich in kaolin.
Sodium Hydrogen Carbonate	Pharmacos Ltd, Essex, England	-For deflocculation purposes
Sodium Hexametaphosphate	BDH Chemicals, Poole, England	- “
Sodium Hydroxide	Merck , Darmstadt, Germany	- Preparation of zeolitic materials
Sodium Aluminate	Produced in the laboratory	- “
Sodium Silicate	BDH Chemicals, Poole, England	- “
Hydrated Aluminium Sulphate	“	- “
Ammonium Sulphate	BDH Chemicals, Poole, England	- “
Rare Earth Chloride	Aldrich Chemical Co, Wisconsin	- “
Flux (66% Lithium Tetraborate & 34% Lithium Metaborate)	Socachim-XRF Scientific, Belgium	-Solid used in fusion of sample for XRF analysis
25% Lithium Bromide	“	-Liquid used with flux
Tetraoxo Sulphate VI Acid	Eagle Scientific Ltd, England	-For dealumination purpose

**Table 3.2: List of Equipment used for the Experiment**

<b>EQUIPMENT</b>	<b>SOURCE</b>	<b>COMMENTS</b>
Top Loading Balance.	Denver Instrument, XP3000.	-Used for weighing materials.
Stirrer	Gallenkamp, England Electrical	-Used for maintaining high degree of homogeneity.
Vibratory Shaker and Sieves.	Endecotts Ltd, London England	-For particle size separation.
Centrifuge	Gallenkamp	-Separation of suspended solids.
Drying Oven	Salvis LAB Thermocenter, Swiss	- Drying of materials.
XRF	PANalytical AxoisCem	-Fusion equipment used for making glass beads.
XRF	Phoenix, PX-VFD 4000	-Qualitative & quantitative chemical analysis of samples.
Swing Mill	Herzog, HSM 100 H.	-Grinding of solid materials.
Pellet Machine	Herzog, HTP 40.	-For Pressed Pellet making.
Brabender Moisture Content.	Germany, MT-C 2008.	-Measurement & Control systems
Furnace	Carbolite, England	-Activation of kaolin clay to a more reactive form.
Dessicator	SEDI, Minna, Nigeria	- cooling samples
Magnetic Stirrer	USA	- dilution & reaction of solid chemicals
Autoclave	India	- For zeolite synthesis
XRD	PANalytical X'Pert	-Identification & characterization of unknown crystalline materials.
Tristar	3000 V6.05 A	-Adsorption/Desorption Analysis.
ACMEL LABO	Toni Technik, BSA 1, France	-To measure surface area & porosity



## **3.2 Experimental Procedure**

This section entails the procurement and pretreatment of the Ahoko clay: beneficiation and centrifugation, and particle size reduction of the clay; calcination of the clay and development of zeolite samples. The samples were subsequently subjected to X-ray Fluorescence (XRF) Spectroscopy, X-ray Diffractometry (XRD) Spectroscopy, Nitrogen Adsorption measurement and Catalyst Performance Evaluation.

### **3.2.1 Procurement and pretreatment of the Ahoko clay**

The raw clay material used for the experiment was procured from Ahoko village, Kogi L.G.A., Kogi State, Nigeria and was pretreated by screening out all the unwanted materials present in the clay. The pretreated clay material was subsequently subjected to beneficiation and centrifugation as well as other treatments, as necessary for the formulation of the treated kaolin clay materials into various zeolite samples.

### **3.2.2 Beneficiation of the clay**

Beneficiation of the clay was carried out to remove impurities such as stones, plant remains and other unwanted materials present. This was done by weighing out 1000 g of the clay sample divided into two equal portions and was poured into two small plastic buckets. Subsequently, one of the portion of the clay was soaked in excess of water and the mixture was stirred vigorously and intermittently for 3 days. The resulting mixture was passed through a 70  $\mu\text{m}$  sieve to obtain the fine particles, allowed to settle and the water decanted before centrifugation. To the other portion, 2 litres of 2:8 sodium hydrogen carbonate and sodium hexametaphosphate solution was added and mixed for deflocculation purposes. It was allowed to stand for 8hrs after which the supernatant fluid with its suspended particles were decanted and washed thoroughly with distilled water to remove excess deflocculant before centrifugation.

### 3.2.3 Centrifugation of the clay

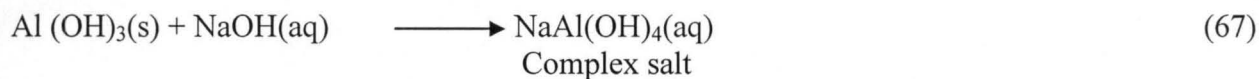
Equal amounts of beneficiated clays were poured into a centrifuge tube and placed in the cups of the Gallenkamp centrifuge machine to remove water. The machine was operated at 1500 rpm for 10 minutes per run. For every run the machine stops automatically, the tubes were removed and the wet lumped clay was scupped out and was collected into a plastic tray. The recovered clays were dried overnight in an oven at 120°C to liberate completely the physical water content and to obtain the beneficiated clay (cake). The samples were then ready for calcinations after the particle size reduction in which the cake formed was crushed, milled to +70 µm particle size using a micro sieve.

### 3.2.4 Calcination of the clay

This was carried out by putting a given quantity of the clay in a porcelain dish. The calcination of the beneficiated clay involved heating at an elevated temperature of about 600°C for a period of 6hrs in a furnace. The samples were then removed, placed in desiccators to cool and was subsequently packaged for use in zeolite synthesis.

### 3.2.5 Preparation of sodium aluminate for zeolite Y synthesis

The sodium tetra hydroxide aluminate 111 (sodium aluminate) used for the preparation of zeolitic materials was prepared in the laboratory using either aluminum hydroxide or aluminum oxide according to the reaction equation shown below:



### 3.3 Preparation of Zeolitic Materials

This entails preparation of zeolitic materials from pure chemicals without the addition of clay marked ZY1 while others have clays and chemicals added to the composition in different amounts and marked ZY2 – ZY7. Samples ZY5 – ZY7 were subjected to dealumination method using varying amounts of chemicals and clay.

#### 3.3.1 Synthesis of zeolitic Materials

The procedure adopted by Ginter, 2001 for the synthesis of zeolite Y was used. The zeolite was synthesized from a sodium hydroxide, sodium aluminate and sodium silicate reaction mixture. Generally, a solution A1 was first prepared by weighing out 4.0 g NaOH, 2.1 g NaAl(OH)<sub>4</sub> and they were dissolved in 20 g deionised H<sub>2</sub>O in a 100 ml beaker. Then a 23 g aliquot of Na<sub>2</sub>SiO<sub>3</sub> was added, the mixture was stirred for 15 minutes, left for 24 hours at room temperature for aging. Another mixture marked B1 was prepared by weighing 0.14 g NaOH, 13.1 g NaAl(OH)<sub>4</sub>, and then they were dissolved in 131 g deionised H<sub>2</sub>O and mixed vigorously in a 250 ml beaker. Mixtures A1 and B1 were again mixed under high shear stress using a magnetic stirrer was left for another 24 hours at room temperature, followed by heating in an autoclave at 100°C for 22 hours. The product known as ZY1 was centrifuged, filtered, washed with deionized water and was subsequently dried at 110°C, which contained no clay as shown in Figure 3.1. The same procedure was followed with the appropriate quantities of reactants for ZY2, ZY3, and ZY4 with the addition of clay before aging and crystallization as given in Table 3.3.

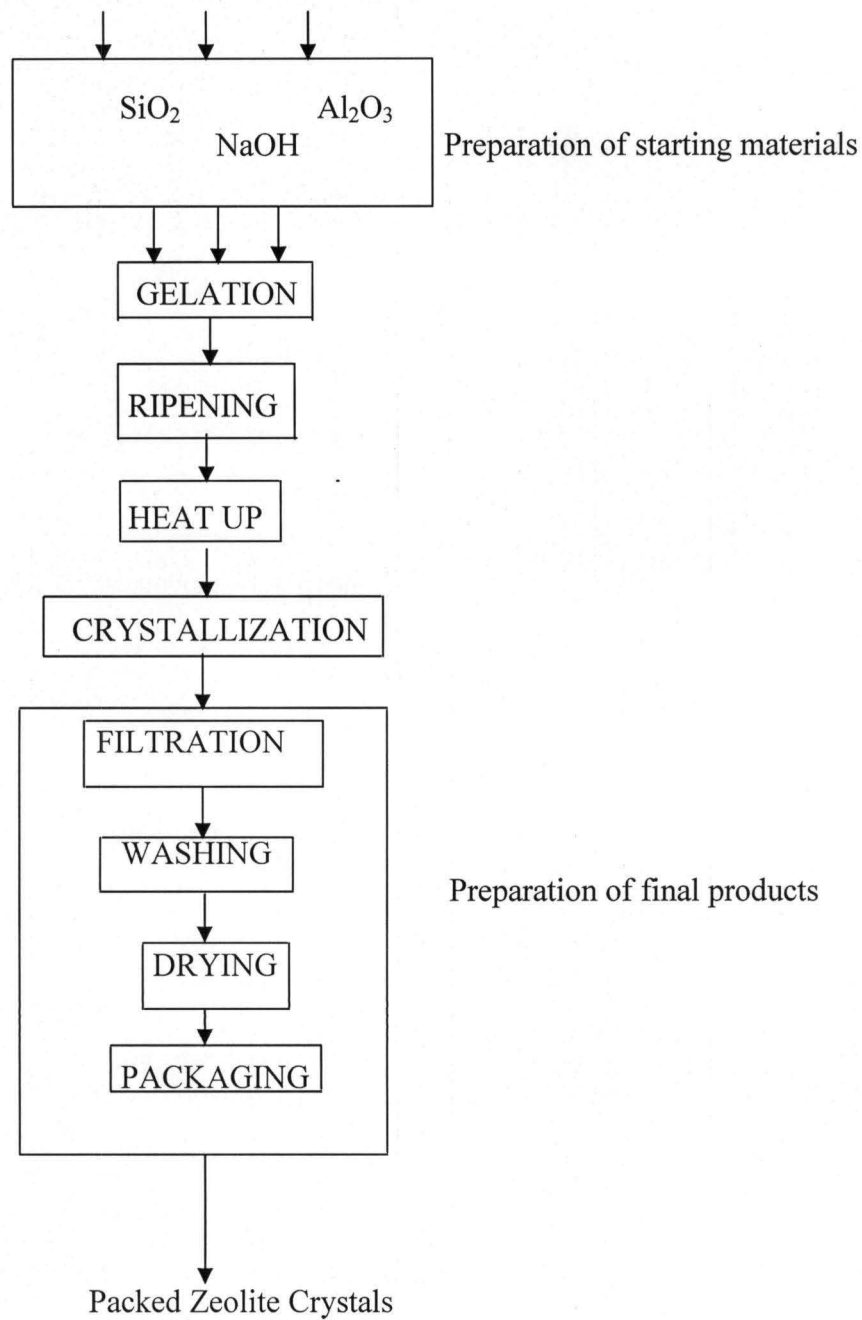


**Figure 3.1: Synthesis of Zeolitic Materials**

**Table 3.3: Reaction Mixture Composition of Zeolitic Materials**

Sample	Reactant Quantity (g)/Synthesis Condition						
	H <sub>2</sub> O	NaOH	NaAl(OH) <sub>4</sub>	Na <sub>2</sub> SiO <sub>3</sub>	Aging Time (RT, hr)	Kaolin	Crystallization Time (CT, hr)
ZY1,(A1)	20.00	4.00	2.10	23.00	24	-	22 and dried
(B1)	131.00	0.14	13.10	-	24	NK	later at 110°C
ZY2,(A2)	20.00	4.00	2.10	23.00	24	-	
(B2)	131.00	0.14	13.10	-	24	58.00	“
ZY3,(A3)	20.00	8.00	2.10	23.00	24	-	
(B3)	131.00	0.28	13.10	-	24	59.20	“
ZY4,(A4)	20.00	4.00	2.10	46.00	24	-	
(B4)	131.00	0.14	13.10	46.00	24	64.90	“

NB: RT – Room Temp. = 25°C, CT – Crystallization Temp. = 100°C, NK – No Kaolin.

### 3.3.2 Preparation of zeolite Y

Seed solutions which acted as nucleation centres, were prepared by diluting 3.6 g  $\text{NaSiO}_3$  with 3.3 g deionised  $\text{H}_2\text{O}$  and 0.3 g of  $\text{NaAl(OH)}_4$  and 0.9 g  $\text{NaOH}$  were dissolved in 2.7 g of deionised  $\text{H}_2\text{O}$  and this mixture was added drop-wise with stirring to the sodium silicate solution. The stirring continued for 5 minutes, aged for 24 hours at RT, and was kept for future use. Forty eight point one eight gram of sodium silicate was diluted with 12.12 g of deionised  $\text{H}_2\text{O}$  marked A. Another solution was prepared by dissolving 3.4 g of  $\text{NaOH}$  pellets in 10.6 g of deionised  $\text{H}_2\text{O}$  marked B which was added to A and was stirred continuously to form sodium silicate-alkali solution. Sixteen point eight two gram of hydrated  $\text{Al}_2\text{SO}_4$  was dissolved in 33.33 g of deionised  $\text{H}_2\text{O}$  marked C and was added dropwise to the mixture of A & B (sodium silicate-alkali solution) with constant stirring. Then the prepared seed solution was slowly added with stirring to the A, B, and C mixture and was heated in an autoclave at  $100^\circ\text{C}$  for 22 hours. The crystallized product was filtered out, washed with boiling deionised  $\text{H}_2\text{O}$  and was dried in an oven at  $110^\circ\text{C}$  and was marked ZY5. The same procedure was followed for ZY6 and ZY7 as given in Table 3.4. ZY5, ZY6 and ZY7 samples were subsequently subjected to dealumination method in section 3.3.3.



**Table 3.4: Reaction Mixture Composition of Zeolite Y Catalyst**

Sample	Reactant Quantity (g)/Synthesis Condition					
	H <sub>2</sub> O	Na <sub>2</sub> SiO <sub>3</sub>	NaOH	Al <sub>2</sub> SO <sub>4</sub>	Aging Time (RT, hr)	Crystallization Time (CT, hr)
ZY5,(A)	12.12	48.18	-	-	-	22 and dried later at 110°C.
(B)	10.60	-	3.40	-	-	
(C)	33.33	-	-	16.82	24	
ZY6,(A)	12.12	24.09	-	-	-	“
(B)	10.60	-	3.40	-	-	
(C)	33.33	-	-	16.82	24	
ZY7,(A)	12.12	48.18	-	-	-	“
(B)	10.60	-	6.80	-	-	
(C)	33.33	-	-	16.82	24	

NB: RT – Room Temp. = 25°C, CT – Crystallization Temp. = 100°C, NK – No Kaolin

### **3.3.3 Dealumination and Catalyst enhancement for Evaluation**

Twelve point one two gram of 30% H<sub>2</sub>SO<sub>4</sub> was measured and kept under stirring while 6.42 g of calcined clay was added while stirring. This was followed by the addition of 19.94 g sodium silicate-alkali solution resulting in a fine clay-silica solution. Four gram oven dried zeolite from section 3.3.2 was weighed, milled and the equivalent weight of distilled water was added to make fine slurry. The pH of this slurry was brought down to 4.0 using 10 wt. % H<sub>2</sub>SO<sub>4</sub> and then was added to the already prepared silica-clay solution under vigorous stirring to obtain a pH of 2.95. The product was dried a little and then was washed twice with hot deionized water and then was exchanged with 5 wt. % NH<sub>2</sub>SO<sub>4</sub> solution at 85°C for 30 minutes. Ammonium exchanged product was separated by filtration. NH<sub>2</sub>SO<sub>4</sub> exchange step was repeated two more times with a fresh solution of NH<sub>2</sub>SO<sub>4</sub> each time. This procedure was applied to ZY5, ZY6 and ZY7. Finally, the ammonium-exchanged catalyst was contacted with rare earth chloride solution at 65°C for loading with 2 wt. % rare earth oxide. Rare earth exchanged catalyst was washed with deionised water and dried. The zeolite was now ready for catalyst performance evaluation by a micro activity test (MAT) as specified by US Patent, 2002.

### **3.4 Characterization of the Developed Samples**

This entails determining the XRF spectroscopy of the raw Ahoko clay, beneficiated and calcinated clays marked AC-1, AC-2, AC-3, AC-4 and AC-5, the XRF and XRD spectroscopy of the developed zeolite samples were marked ZY1, ZY2, ZY3, ZY4, ZY5, ZY6 and ZY7 and finally the adsorption analysis of ZY1 ZY2, ZY3, ZY4, ZY5, ZY6 and ZY7 respectively.

#### **3.4.1 Determination of chemical composition of raw materials and products**

The moisture content of the samples was first determined using a Brabender Moisture Content Equipment at 110°C for 1 hour before pelletization of the samples. XRF sample

preparation has two main approaches: Fusion and pressed pellet methods. In fusion, the sample was fused in a platinum crucible using a ratio of 8:1 flux typical of 66% lithium tetraborate and 34% lithium metaborate composition to sample. The flux and the zeolite samples were thoroughly mixed, and 1ml of lithium bromide was added to each of the mixture and was fixed to an automated fusion device (PANalytical Axios fusion Equipment), air boosted natural gas burners where it was strongly heated to red hot until it melts. The resulting hot melt was poured into a platinum mold to form a glass disc and was allowed to cool.

#### **3.4.2 X – ray diffraction (XRD) analysis**

Powdered X – ray diffraction (XRD) patterns of the zeolite samples were recorded with a Philips PW 1710 X' Pert X – ray diffractometer using graphite monochromatized CuK $\alpha$  radiation ( $\lambda = 1.5418$  nm). The equipment was operated at a generator voltage of 40 kV and a tube current of 50 mA to collect XRD data in the range  $2\theta$  values varying from  $0 - 40^\circ$  at a scan rate of  $0.02^\circ$  steps counting for 1.0 s per step.

#### **3.4.3 Nitrogen adsorption measurement**

Adsorption analysis was carried out on the zeolite samples using a Tristar 3000 V6.05 A analyzer. The developed catalyst samples were dried under vacuum at  $200^\circ\text{C}$  prior to analysis for 2 hours. Approximately 0.3 g of each sample was used for the analysis. The adsorption and desorption isotherms were determined at  $-195.8^\circ\text{C}$  with nitrogen over a range of relative pressures varying from 0.01 to 0.99 for adsorption and 0.99 to 0.11 for desorption, respectively, and were recorded by taking between 72 to 85 points to obtain complete isotherm for each sample. Measurements were taken after the pressure was allowed to equilibrate within 10 seconds. Single point surface area and single point adsorption total pore volumes were obtained

by the amount of physisorbed  $N_2$  for  $P/P_0 = 0.98$  and the BJH method was applied to calculate the pore size distribution.

### **3.5 Catalytic Activity**

Finally  $NH_4$  exchanged catalyst (synthesized ZY4 and ZY5) otherwise known as USY zeolites were contacted with a rare earth chloride solution at  $65^\circ C$  for loading with 2 wt % rare earth oxide. Rare earth exchanged catalysts were washed with water and dried overnight at  $110^\circ C$ , followed by calcinations at  $500^\circ C$  for 3 hours in a muffle furnace. It was then evaluated by a micro activity test for its performance.

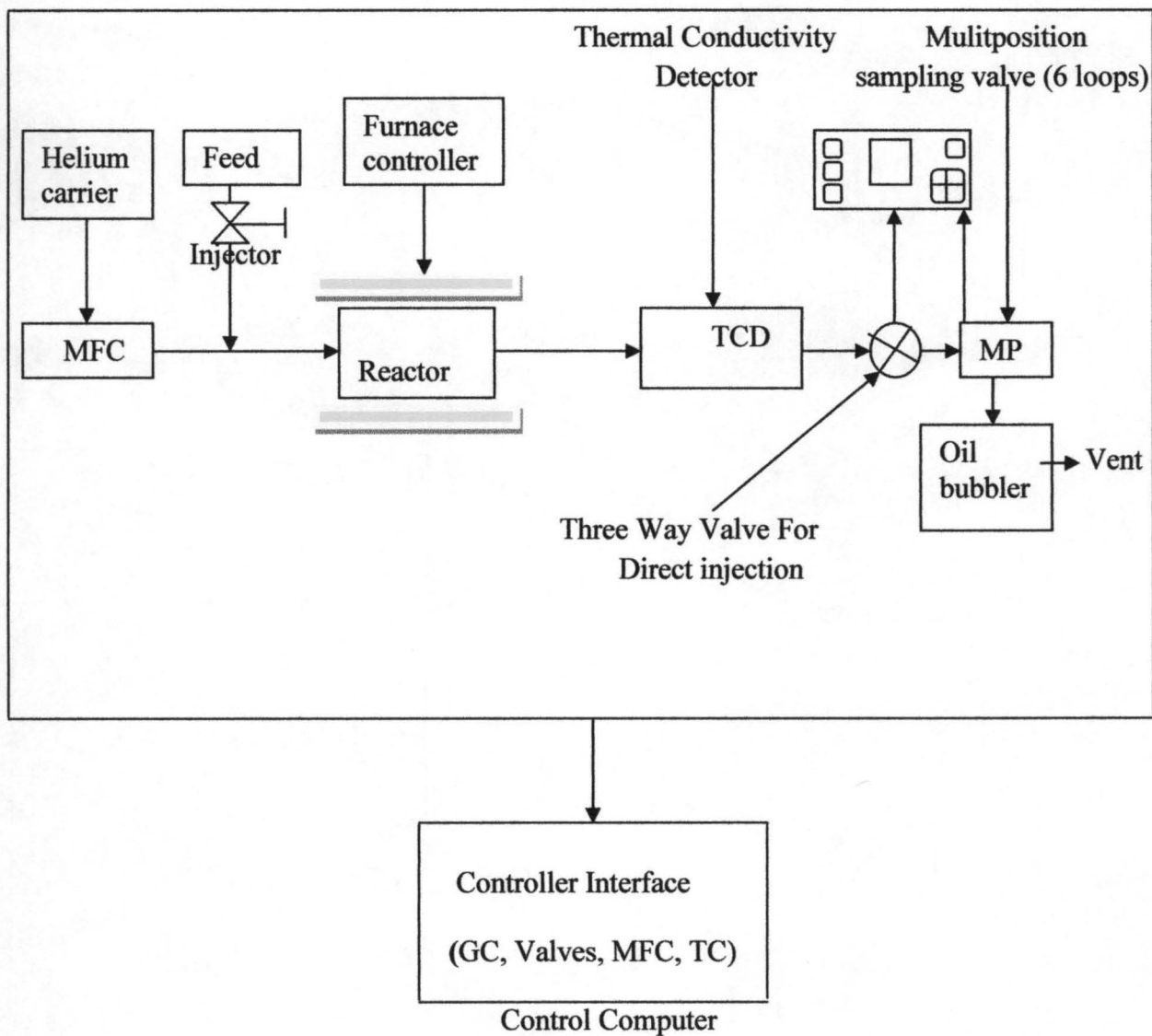


**Figure 3.2: Schematic Representation of Microreactor Configured for a Fixed Catalytic Bed Operation**

Reactor data were collected from an in-built laboratory microreactor system. The system consisted of a valve for loading and injecting the test gas, a stainless steel reactor which was heated in a tube furnace, a thermal conductivity detector (TCD). A second valve after the reactor was used to collect the reactor effluent and was subsequently analyzed offline. A bypass valve before the second valve was used to send the effluent from the reactor straight to the gas chromatograph (GC) for analysis.

About 2 g of the catalyst was placed inside a stainless steel reactor of 9 mm inside diameter and 130 mm length ~~placed~~<sup>placed</sup> which was subsequently inside the tubular programmable temperature furnace. Nitrogen gas was introduced into the system to purge the air completely out of the system. During the purging operation, the programmable temperature furnace was set to give a heating rate of 10°C/min until the temperature of the reactor reached the desired temperature of 360°C. Hydrogen gas was allowed to pass through the system at 40 cm<sup>3</sup>/min for 2 hours.

A distillation unit was used to determine the product boiling range distribution and to investigate the yield of the lighter products after hydrocracking reaction. The volume of the condensate was taken at temperatures of 160, 200 and 240°C. The gaseous products were analyzed using a GC equipped with a flame ionization detector (FID) to identify the resulting GC peaks by injecting standard gases to the FID.

The conversion, product yield and catalyst to gas oil ratio were obtained using the following equations.

$$1. \quad \% \text{ Conversion} = \frac{W_{GO} - W_R}{W_{GO}} \times 100 \quad (69)$$



Where  $W_{GO}$  – is the weight of gas oil and  $W_R$  - weight of unconverted fraction that remained in the liquid product after distillation

$$2. \quad Y_I = \frac{W_I}{W_{GO}} \times 100 \quad (70)$$

Where  $Y_I$  – is the yield of the product (wt %);  $W_I$  – weight of the distillation fraction and  $I$  – is the distillate fraction (gasoline, kerosene, diesel)

$$3. \quad \text{Catalyst to gas oil ratio} = \frac{W_C}{W_{GO}} \quad (71)$$

Where  $W_C$  – is the weight of catalyst loaded

## CHAPTER FOUR

### 4.0 RESULTS

#### 4.1 Determination of chemical composition of raw and pretreated Ahoko clay

Table 4.1 is the chemical composition of the raw Ahoko clay, pretreated through beneficiation, centrifugation or the use of sodium hexametaphosphate (non centrifugated) and calcinations to obtain various samples using XRF spectroscopy equipment as shown below.

**Table 4.1: The Chemical Composition of Ahoko Clay in Mass Percentage**

Composition	SiO <sub>2</sub>	Al <sub>2</sub> O <sub>3</sub>	K <sub>2</sub> O	MgO	CaO	Na <sub>2</sub> O	Fe <sub>2</sub> O <sub>3</sub>	LOI	Total Si/Al Mole Ratio	
Sample	Content (wt %)									
AC-1	67.95	17.60	0.80	0.62	0.36	0.25	1.75	10.67	100.17	6.38
AC-2	67.82	17.68	0.81	0.62	0.30	0.25	1.75	10.77	99.98	6.46
AC-3	78.57	11.14	0.73	0.52	0.28	0.36	1.47	6.93	99.72	11.62
AC-4	70.90	18.82	0.80	0.64	0.34	0.27	1.66	6.57	99.75	6.38
AC-5	79.58	12.01	0.81	0.60	0.52	0.49	1.41	4.58	99.78	11.41

KEY

AC-1 – Raw Clay

AC-2 – Beneficiated-Centrifugated Clay

AC-3 – Calcinated Beneficiated Centifugated Clay

AC-4 – Beneficiated Non-Centrifugated Clay

AC-5 – Calcinated Beneficiated Non-Centrifugated Clay

## 4.2 Determination of Chemical Composition of Developed Zeolitic Materials

Table 4.2 is the chemical composition of zeolitic materials developed from Ahoko clay through synthesis, dealumination and preparation methods using various unit operations such as filtration, drying and crystallization.

**Table 4.2: The Chemical Composition of Developed Zeolite Samples**

Composition	SiO <sub>2</sub>	Al <sub>2</sub> O <sub>3</sub>	K <sub>2</sub> O	MgO	CaO	Na <sub>2</sub> O	Fe <sub>2</sub> O <sub>3</sub>	LOI	Total	Si/Al Mole Ratio
Sample	Content (wt %)									
ZY1	24.90	49.90	0.22	0.12	0.64	8.13	0.12	13.44	97.47	0.83
ZY2	52.27	21.26	0.33	0.11	0.64	9.55	1.26	12.03	97.45	4.01
ZY3	50.97	24.32	0.34	0.13	0.61	8.42	1.28	11.99	98.06	3.58
ZY4	50.27	22.55	0.42	0.12	0.77	9.88	1.34	13.07	98.42	3.72
ZY5	45.92	30.54	0.39	0.21	0.56	7.12	1.22	13.02	98.98	2.57
ZY6	73.34	9.24	0.37	0.01	0.28	0.99	0.97	14.80	100.00	13.09
ZY7	71.50	10.70	0.43	0.05	0.27	0.97	0.95	15.13	100.00	11.41

### 4.3 XRD patterns of developed zeolitic materials

Figure 4.1 shows the graphical representations of the relative peak intensities of the X-ray spectra generated by the developed zeolitic material samples ZY1 – ZY7 on the instrument's  $2\theta$  scale for quantification and identification of the mineral species.

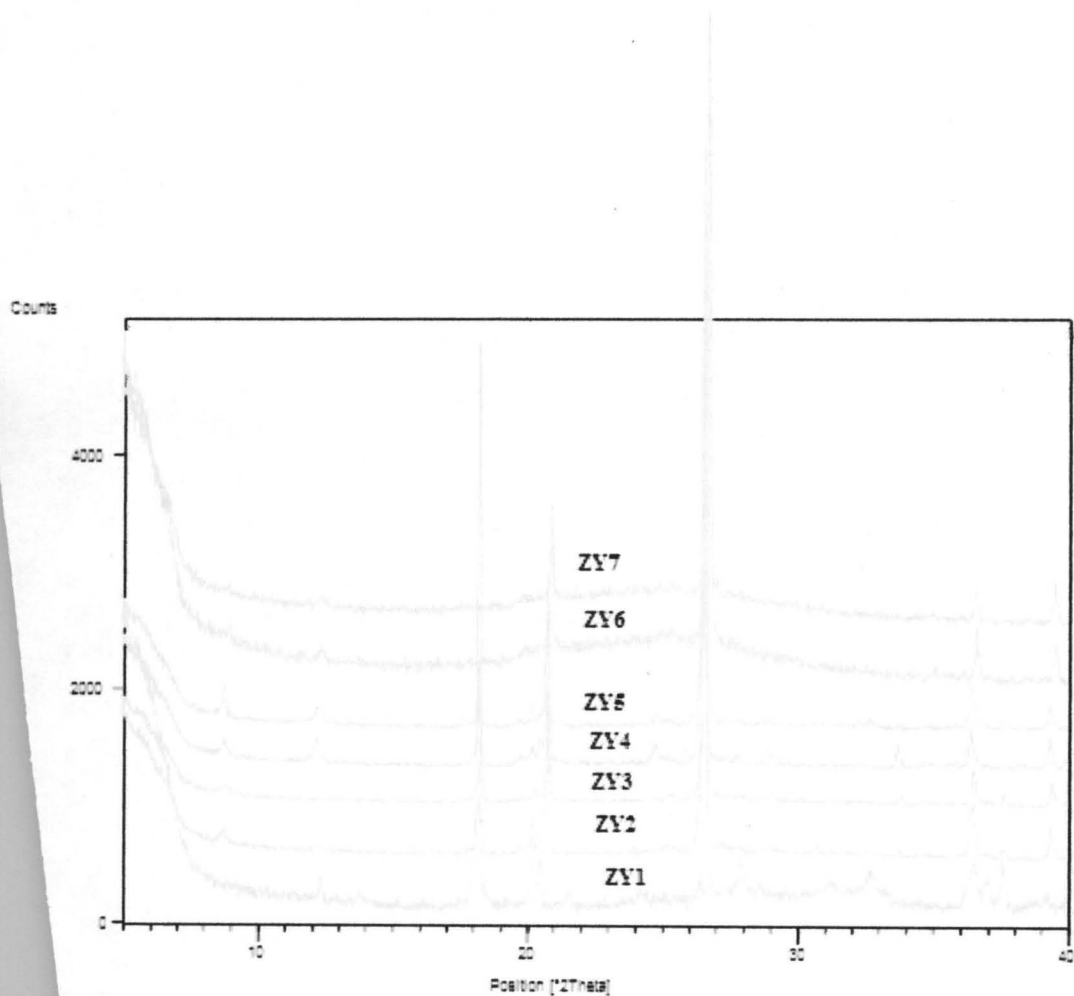


**Figure 4.1: Graphical Representation of XRD Patterns for ZY1-ZY7**

#### 4.4 XRD analysis of the developed zeolitic materials

Table 4.3 gives the data generated for the peak position, relative intensities and inter-crystalline spacing for developed samples ZY1-ZY7 for comparison with the reference sample which is zeolite Y

**Table 4.3: XRD Analysis of Developed Zeolite Samples and Reference Sample**

ZY1		ZY2		ZY3		ZY4		ZY5		ZY6		ZY7		Zeolite Y	
d	I	d	I	d	I	d	I	d	I	d	I	d	I	d	I
15.04	33.93	13.16	1.05	15.02	17.05	15.06	16.42	13.16	1.09	15.83	40.84	17.24	32.75	14.29	100
7.13	2.41	9.93	1.01	13.09	10.07	13.18	9.46	10.05	5.13	13.11	19.19	13.17	13.45	8.75	9
4.85	100.00	4.84	12.07	10.02	3.13	10.06	3.64	7.20	2.71	4.23	25.05	7.11	1.15	7.46	24
4.39	14.41	4.37	2.16	7.20	0.55	7.20	4.15	4.87	10.65	3.53	1.92	4.24	16.51	5.68	44
4.32	11.05	4.25	15.46	4.86	9.61	4.86	15.36	4.39	3.70	3.33	100.00	3.33	100.00	4.76	23
4.11	2.46	3.52	0.87	4.39	2.93	4.39	3.24	4.27	21.39	2.45	9.28	2.45	5.42	4.38	35
3.67	1.35	3.34	100.00	4.26	28.08	4.27	33.90	3.59	1.51	2.28	6.36	2.28	5.64	3.91	12
3.35	5.23	3.19	1.04	3.52	1.03	3.59	3.27	3.35	100.00					3.77	47
3.19	6.96	3.07	1.39	3.35	100.00	3.35	100.00	2.74	0.71					3.57	4
2.86	2.71	2.65	1.54	2.91	1.11	3.25	1.73	2.46	7.61					3.47	9
2.73	4.70	2.46	5.99	2.65	0.89	3.08	3.22	2.39	0.79					3.31	37
2.45	8.43	2.39	1.61	2.46	8.72	2.75	0.40	2.29	3.98					3.22	8
2.43	4.56	2.28	3.86	2.39	1.21	2.65	4.07							3.04	16
2.39	10.40			2.29	5.41	2.57	0.70							2.92	21
						2.46	6.39							2.86	48
						2.39	1.04							2.77	20
						2.35	0.63								
						2.29	1.10								

#### 4.5 Identified phases of XRD patterns of developed zeolitic samples

Table 4.4 gives match scores quantified between the reference pattern and the sample phase from the powder diffraction file for product identification of samples ZY1 – ZY7.

**Table 4.4: Identified Phases of XRD Patterns**

Sample	SiO <sub>2</sub> /Al <sub>2</sub> O <sub>3</sub> Score		Chemical Formula	Product Identification	Reference Code
ZY1	0.50	11	Ca <sub>5</sub> Na <sub>2</sub> Al <sub>12</sub> Si <sub>12</sub> O <sub>48</sub>	Zeolite 5A, synthesize	01 – 077 – 1334
		19	Ca(SiO <sub>4</sub> )	Calcium Silicate	01 – 087 – 1258
		28	K <sub>4</sub> Si <sub>23</sub>	Potassium Silicon	01 – 065 – 3350
ZY2	2.46	73	SiO <sub>2</sub>	Quartz	01 – 083 – 0539
		44	Fe <sub>2</sub> O <sub>3</sub>	Hematite	01 – 001 – 1053
		42	KO <sub>2</sub>	Potassium Oxide	00 – 010 – 0235
ZY3	2.09	12	K <sub>24</sub> (Al <sub>24</sub> Si <sub>84</sub> O <sub>216</sub> )	Zeolite ZSM-10, synthesized	00 – 087 – 1614
		71	SiO <sub>2</sub>	Quartz	01 – 075 – 0443
		51	Al <sub>2</sub> O <sub>3</sub>	Corundum – synthetic	01 – 089 – 3072
		29	Fe <sub>2</sub> O <sub>3</sub>	Hematite, synthesized	01 – 089 – 0599
ZY4	2.23	18	K <sub>24</sub> (Al <sub>24</sub> Si <sub>84</sub> O <sub>216</sub> )	Zeolite ZSM-10, Synthesized	01 – 087 – 1614
		68	SiO <sub>2</sub>	Quartz	01 – 085 – 0930
		30	K(AlSi <sub>3</sub> O <sub>8</sub> )	Microcline	01 – 087 – 1791
		17	Si <sub>7</sub> Al <sub>3</sub> O <sub>2</sub>	Zeolite Y, Synthesized	01 – 077 – 1549
		16	KMg <sub>2</sub> AlSi <sub>4</sub> O <sub>12</sub>	Potassium Magnesium Aluminum Silicate	01 – 050 – 0459
ZY5	1.5	75	SiO <sub>2</sub>	Quartz	01 – 083 – 0539
		39	Al <sub>2</sub> O <sub>3</sub>	Aluminum Oxide	01 – 001 – 1303
		12	(Al <sub>6</sub> Al <sub>3</sub> Si <sub>11.3</sub> O <sub>24</sub> ) <sub>9</sub>	Zeolite Y (dealuminated), Synthesized	01 – 088 – 2288
		30	Na <sub>2</sub> O <sub>2</sub>	Sodium Oxide	00 – 015 – 0068
		6	KMg <sub>2</sub> AlSi <sub>4</sub> O <sub>12</sub>	Potassium Magnesium Aluminum Silicate	00 – 050 – 0459
		19	Fe <sub>2</sub> O <sub>3</sub>	Iron Oxide	00 – 052 – 1449
ZY6		87	SiO <sub>2</sub>	Quartz	01 – 079 – 1906
ZY7		86	SiO <sub>2</sub>	Quartz	01 – 085 – 0796



#### 4.6 Adsorption – desorption isotherm of the developed zeolitic samples

Figures 4.2 (a – g) are plots of material adsorbed on to samples ZY1 – ZY7 versus pressure at a fixed temperature at  $-195.8^{\circ}\text{C}$  with nitrogen gas over a range of relative pressures varying 0.01 – 0.99 for adsorption and 0.99 – 0.11 for desorption, respectively, taking between 72 – 85 points.

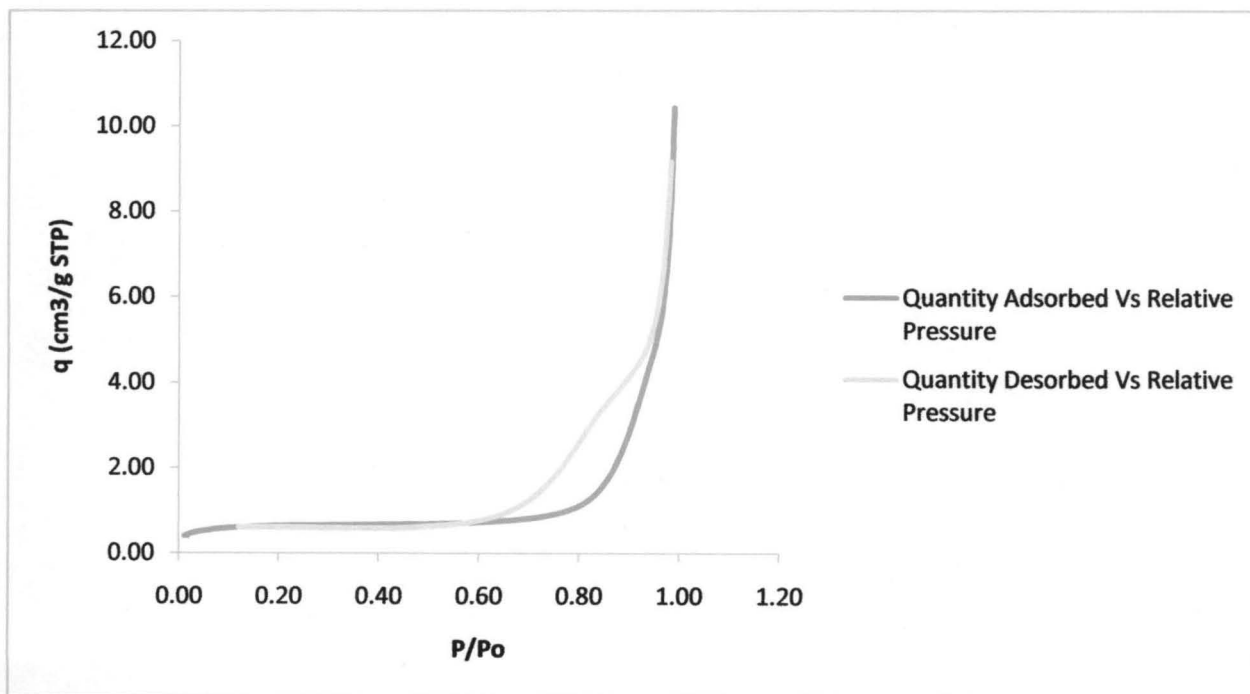


Figure 4.2a: Plot of Adsorption – Desorption Isotherm for ZY1

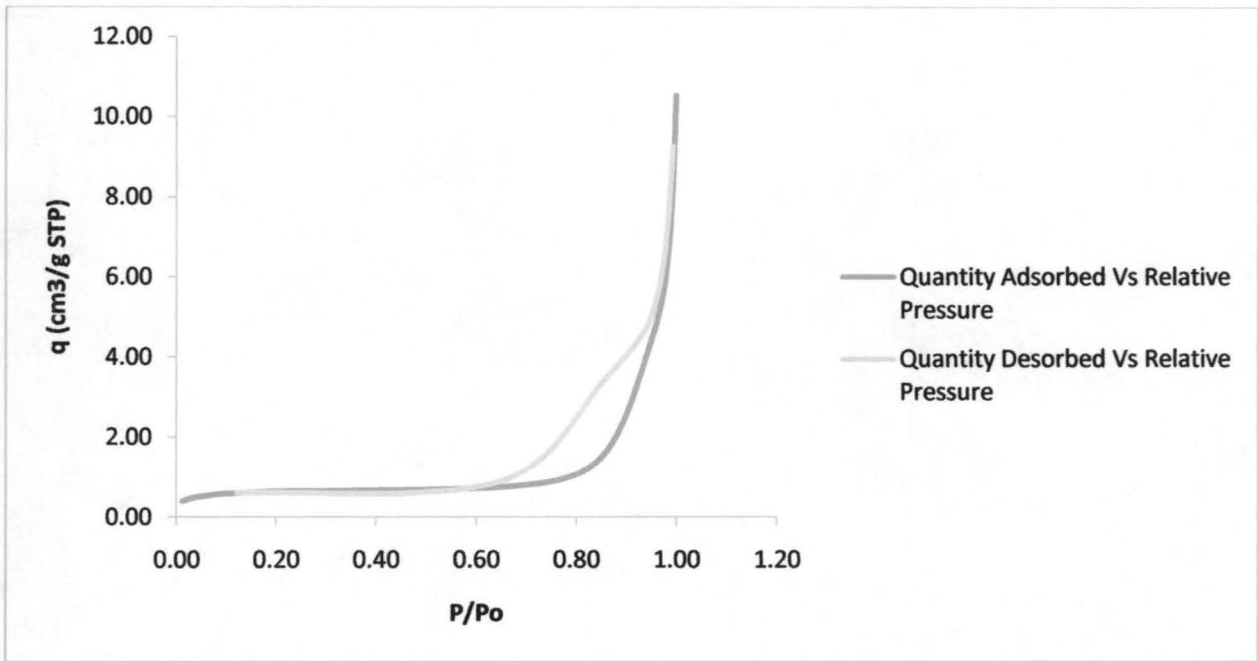
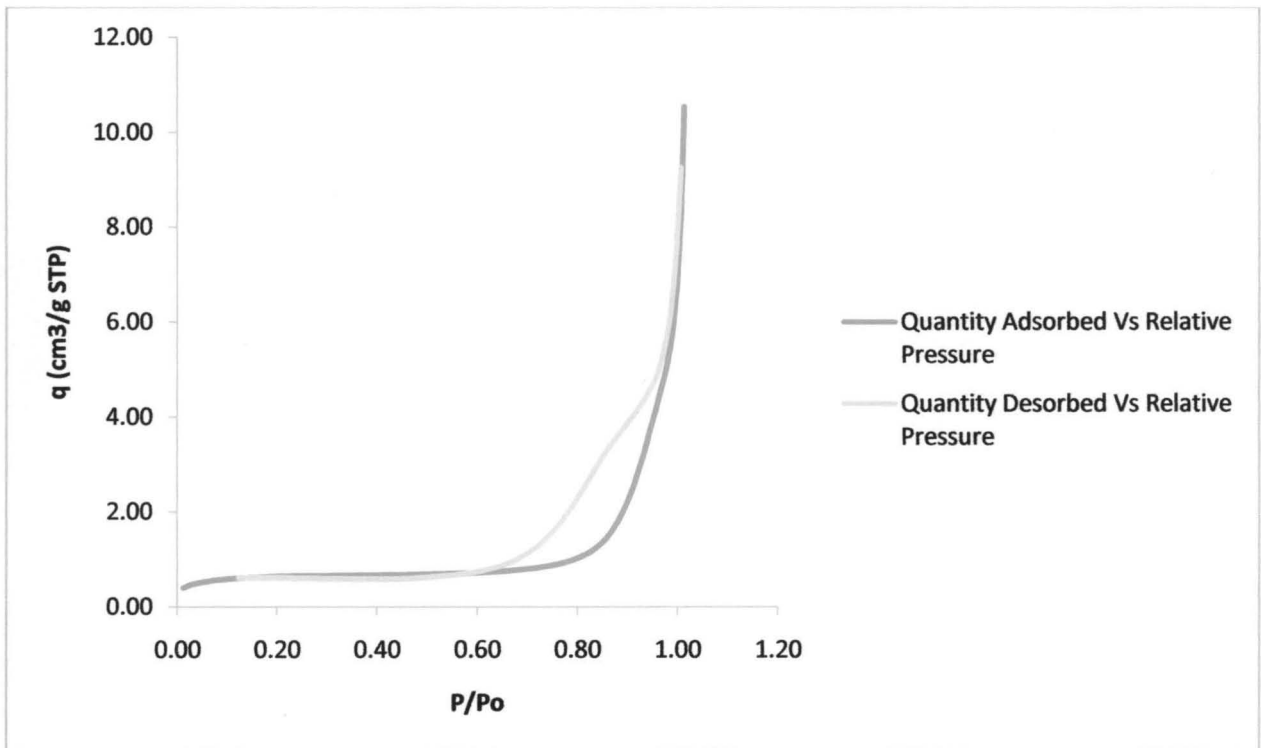
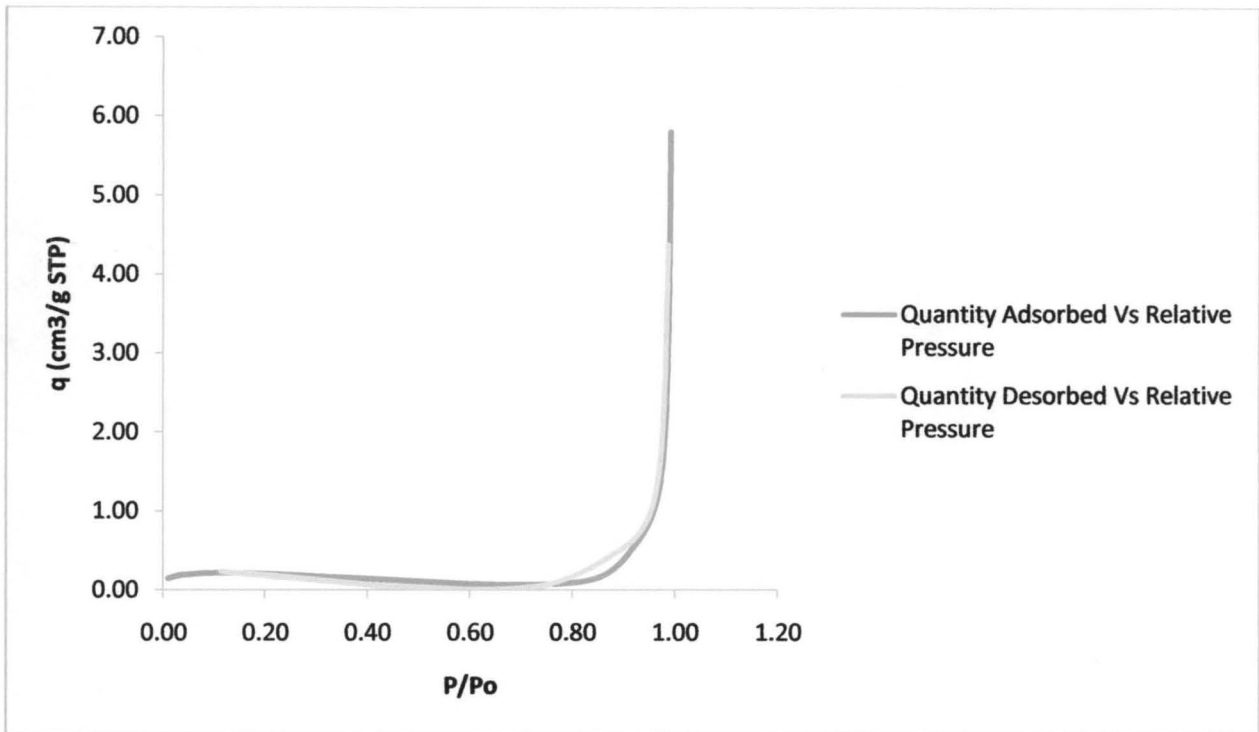


Figure 4.2b: Plot of Adsorption – Desorption Isotherm for ZY2



**Figure 4.2c: Plot of Adsorption – Desorption Isotherm for ZY3**



**Figure 4.2d: Plot of Adsorption – Desorption Isotherm for ZY4**

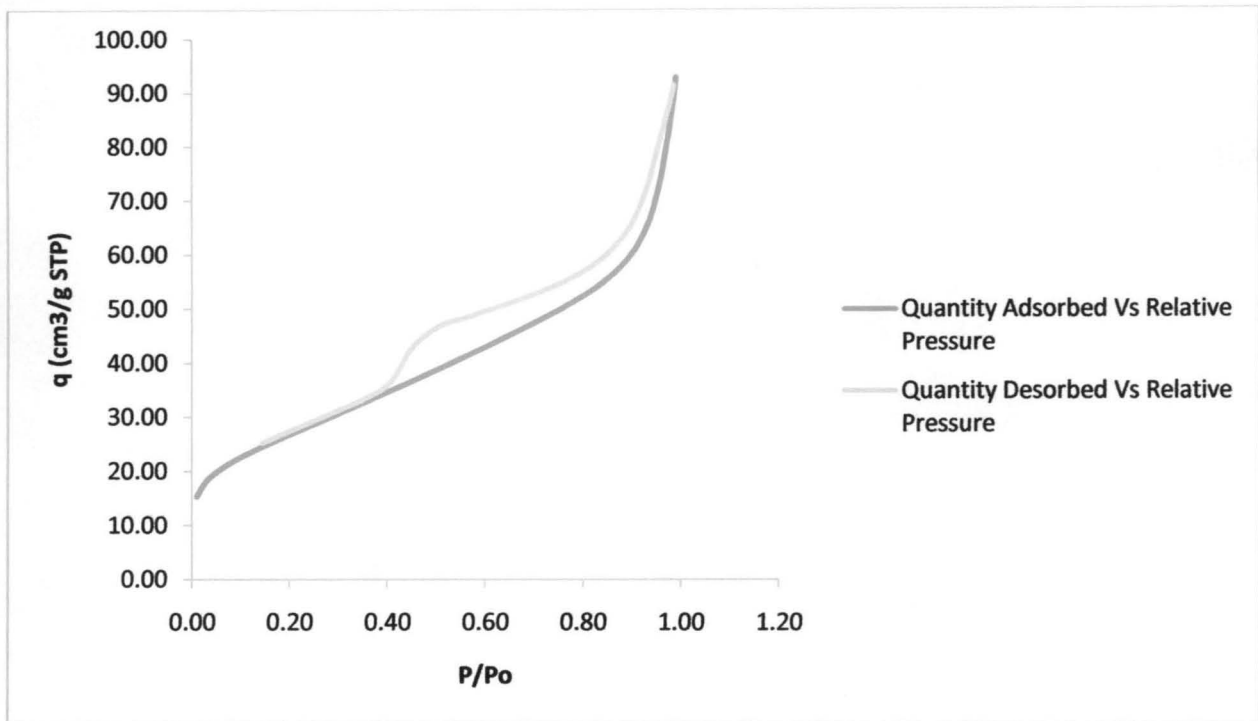


Figure 4.2e: Plot of Adsorption – Desorption Isotherm for ZY5

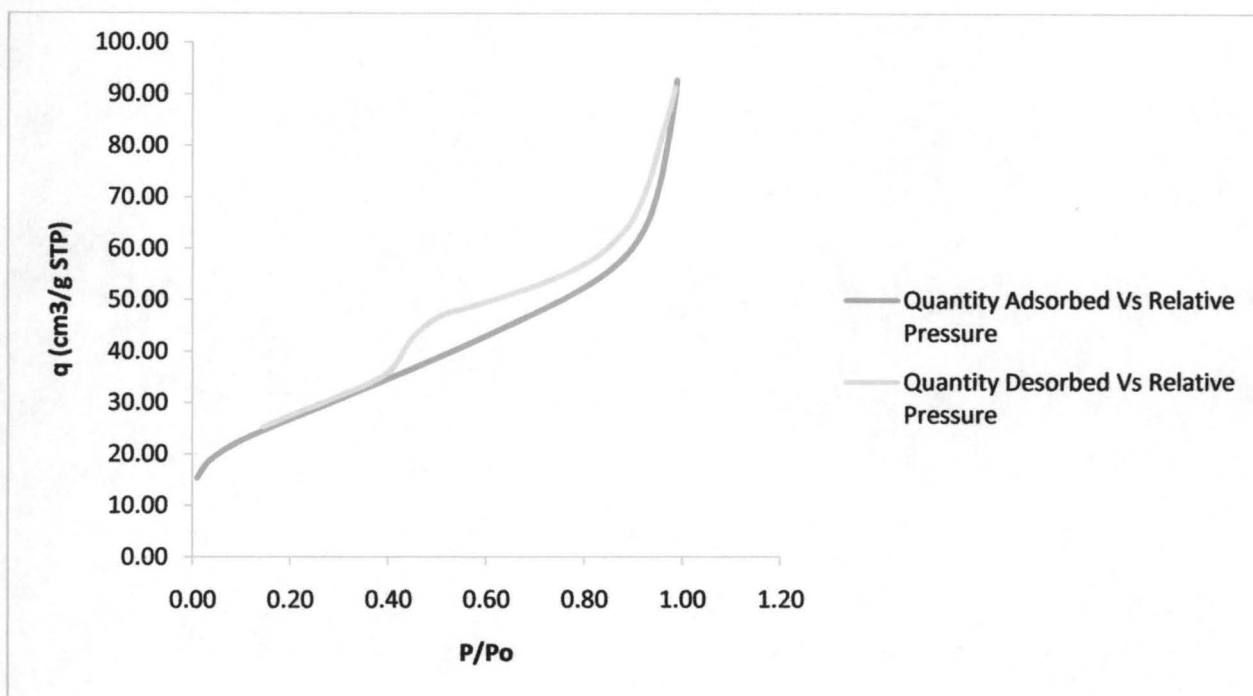
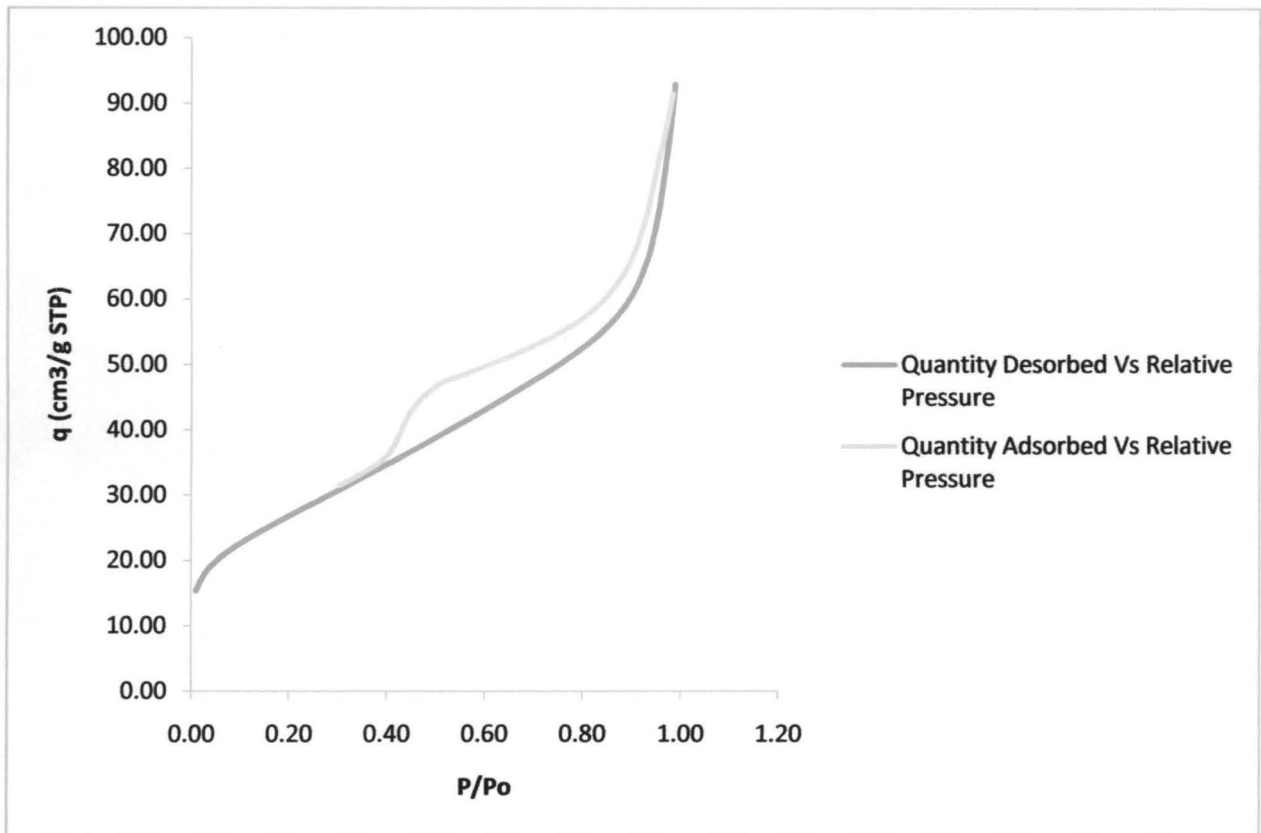


Figure 4.2f: Plot of Adsorption – Desorption Isotherm for ZY6





**Figure 4.2g: Plot of Adsorption – Desorption Isotherm for ZY7**

#### 4.7 Determination of surface area and pore size distribution

Table 4.5 shows the surface area of BET and Langmuir, the total pore volume and the BJH adsorption- desorption average pore diameters and width of the developed zeolite samples

**Table 4.5: Surface Area and Pore Size Distribution**

Zeolite Sample	Surface Area (m <sup>2</sup> /g)		Total Pore Volume V <sub>t</sub> (cm <sup>3</sup> /g)	Porosity (ε)	BJH Adsorption	BJH Desorption	BJH Adsorption Average	
	BET	Langmuir			Average Pore Diameter (4V/A) A <sup>o</sup>	Average Pore Diameter (4V/A) A <sup>o</sup>	Pore Width (4V/A by BET) A <sup>o</sup>	
ZY1	2.4	2.7	0.013	0.5	341.6	194.8	223.8	
ZY2	4.6	2.7	0.043	0.5	341.6	194.8	223.8	
ZY3	22.8	2.7	0.061	0.5	341.6	194.8	223.8	
ZY4	0.9	1.0	0.005	0.5	762.8	553.7	236.2	
ZY5	58.7	104.1	0.101	0.5	64.3	58.0	60.4	121
ZY6	74.4	104.1	0.120	0.5	64.3	58.0	60.4	
ZY7	91.8	104.1	0.139	0.5	64.3	58.0	60.4	

#### 4.8 Physical properties and product distribution of the gas oil

Table 4.7 shows the effect of activity performance on the total conversion and product distribution when the petroleum gas oil is hydrocracked over developed ZY4 and ZY5 catalysts at a reaction temperature of 450°C, contact time of 90 minutes and catalyst to gas oil ratio of 0.04.

**Table 4.6: Testing Conditions**

<b>Physical Properties</b>	
IPB (° C)	235
FBP (° C)	400
Specific Gravity at 15°C (kg/l)	0.8260
Kinematic Viscosity at 40°C (mm <sup>2</sup> /s)	6.3
Pour point (° C)	36
Flash point (° C)	94

**Table 4.7: Product Distribution of Gas Oil Hydrocracking over ZY4 and ZY5**

<b>CATALYST</b>	<b>ZY4</b>	<b>ZY5</b>	<b>USY</b>
[Gas composition (mol. %)]			
CH <sub>4</sub>	0.01	0.02	0.01
C <sub>2</sub> H <sub>4</sub>	1.17	1.15	0.23
C <sub>2</sub> H <sub>6</sub>	35.48	37.72	38.98
C <sub>3</sub> H <sub>6</sub>	2.74	2.50	1.88
C <sub>3</sub> H <sub>8</sub>	29.34	30.75	31.50
C <sub>4</sub> H <sub>10</sub>	19.60	18.82	19.51
C <sub>5</sub> ++	11.66	9.04	7.89
<hr/>			
Conversion (wt. %)	44.91	45.73	47.81
Total Distilled Fuels (wt. %)	35.48	39.39	36.58
Gasoline (wt. %)	11.44	13.24	8.13
Kerosene (wt. %)	3.99	8.57	7.16
Diesel (wt. %)	20.05	17.58	21.29
Gas Yield (wt. %)	4.68	2.62	5.13
Coke yield (wt. %)	4.75	3.72	6.10

## CHAPTER FIVE

### 5.0 DISCUSSION, CONCLUSION AND RECOMMENDATION

#### 5.1 Discussion of results

The results obtained from the various experiments in this work are presented and discussed in this chapter. The results are as follows: Chemical composition of raw and pretreated Ahoko clay; Chemical composition of developed zeolite samples; Diffraction peaks/identified phases of XRD patterns, Analysis of nitrogen adsorption measurement and catalyst performance evaluation.

##### 5.1.1 Chemical and structural composition of kaolin clay

The chemical compositions of raw and pretreated Ahoko clay as prepared are given in Table 4.1. From the table, the major component of kaolin clay is Si and Al<sub>2</sub>, doped with a small quantity of Fe and trace amounts of K, Mg, Ca and Na. The Si-O or Al-O structure in kaolin is inactive which makes it difficult to directly synthesize zeolites. Therefore, kaolin was pre-activated to change this inert structure. The most effective way to activate such natural clay is to thermally transform the inert phase (raw kaolin) into the active phase (metakaolin) at elevated temperature (calcination) of about 600°C in the presence of aqueous alkali metal hydroxide. It was observed that the Silicon to Aluminum (Si/Al) mole ratio of (AC-1) was 6.38, AC-2 was 6.46 and AC-4 was 6.38 while that of AC-3 was 11.62 and AC-5 was 11.41. This implies that for every one mole of aluminum, there is about 6.4 moles of silicon present in AC-1, AC-2 and AC-4. For every one mole of aluminum in AC-3 and AC-5, there is about 11.5 moles of silicon present in the Ahoko clay.

### 5.1.2 Chemical composition of developed zeolite samples

The chosen sample (AC – 2) from the pretreated clay was then developed into zeolite through modification with and/or without dealumination and ion exchange by exchanging the sodium ion out of the zeolite. The sodium was exchanged with ammonium ion and subsequently hydrogen ion. The chemical composition of the developed zeolite samples are given in Table 4.2.

ZY1 showed a significant decrease in the concentration of  $\text{SiO}_2$  while  $\text{Al}_2\text{O}_3$  increased and hence the Si/Al mole ratio of 0.83. ZY2 – ZY5 also showed a departure from ZY1 because  $\text{SiO}_2$  concentrations also increased and there was reduction in  $\text{Al}_2\text{O}_3$  concentration with  $\text{SiO}_2/\text{Al}_2\text{O}_3$  mole ratios ranging from 2.57 – 4.01 while ZY6 and ZY7 Si/Al mole ratio was 13.09 and 11.41 respectively. It showed that  $\text{Na}^+$  was incorporated into the zeolite samples as evidenced in ZY1 to ZY5,  $\text{Ca}^{2+}$  which suggests that they were present either as occluded ions or as precipitate of contaminated salts in ZY1. There was a reduction in concentration of  $\text{Fe}^{3+}$ , which may be due to the partial substitution of the structural aluminum ( $\text{Al}^{3+}$ ) ions or as a free salt.

The present results of chemical composition of the various zeolite samples cannot conclusively be used as a basis of identification of zeolite type, especially, where more than one species were expected.

### 5.1.3 Diffraction Peaks/Identified phases of XRD patterns

After the X – ray scanning of the samples, the background and peak-positions were identified and based on the peak-positions and intensities; a search-match routine was performed using a High Score Plus software for the analysis of the zeolite samples. The analyses of the diffractograms compared reference patterns to the pattern analyzed through Boolean operations. A match score was displayed and this score quantified the match between the reference pattern

and the sample phase. The higher the score, the higher the probability of the reference phase contained in the sample.

The XRD patterns of the synthesized zeolites were given in Figure 4.1. The low background and zeolite strong reflections indicate that the samples are in crystalline forms. Thus, a sample more finely ground will give higher but narrower peaks than the same sample coarsely ground. The diffractograms exhibited many significant peaks at  $2\theta$  ranging from  $8.8^\circ$  to  $39.6^\circ$  as can be read from the spectrometer chart. From these, the relative intensities,  $100I/I_0$  where  $I_0$  is the intensity of the strongest line or peak and the interplanar spacing ( $d$ ) in  $\text{Å}$  were calculated as shown in Table 4.3. Though the interplanar spacings are quite close, the intensities do not agree for ZY4 and ZY5 samples when compared with the literature values for zeolite Y. The presence of zeolite 5A for ZY1, ZSM-10 for ZY2 and ZY3, the synthesized zeolite Y and synthesized dealuminated zeolite Y for ZY4 and ZY5, and pure quartz for ZY6 and ZY7 in the developed samples have very low scores. Therefore, ZY4 and ZY5 cannot be conclusively confirmed to be synthesized zeolite Y and synthesized dealuminated zeolite Y. Other peaks corresponding to other phases emerged confirming the presence of Na, K, Mg, Ca, Si, Al, and  $O_2$  as the elements that make up the zeolite. It is observed that the element Fe is present in the sample as metallic impurity that was chemically bonded with the zeolite. For pure zeolite Y to be produced, there is a need to optimize the parameters for hydrothermal conditions.

#### **5.1.4 Analysis of Adsorption Measurement**

The surface areas and pore size distributions for samples ZY1 – ZY7 were investigated using Tristar 3000 V6.05 A and are given in Table 4.5. Figure 4.2(a – g) depicts the adsorption-desorption isotherms for ZY1 to ZY7. Type II isotherms in physical adsorption were observed common to all the zeolite samples where the isotherm does not reach saturation limit



corresponding to completion of a monolayer. At values of  $P/P_0$  approaching unity, capillary and condensation phenomena occurred. At the Knee of the curve corresponds roughly to completion of a monolayer. A statistical monolayer is built up at relatively low values of  $P/P_0$  of 0.1 – 0.3. All the samples have a porosity of 0.5 which is an indication that the gross particle volume was evenly split between the void space and the solid material. It was seen that zeolites having higher pore volumes and surface areas but smaller average pore diameters adsorbed more nitrogen. Structural changes and pore collapse or blockage led to changes in pore radii and decrease in surface area.

For adsorption-desorption isotherm of ZY1 as shown in Figure 4.2a, the filling of nanopores commence around 0.78 during the adsorption phase. A hysteresis loop typical of this material was also observed at  $P/P_0$  values between 0.60 – 0.97. Sample ZY1 possessed BET surface area of  $2.4\text{m}^2/\text{g}$ , total pore volume of  $0.013\text{cm}^3/\text{g}$  and average BJH adsorption diameter of  $341.6\text{\AA}$ . Introduction of calcium into the sample may be as a result of contaminant during the preparation of the sample before XRD analysis which resulting in the presence of zeolite 5A.

For adsorption-desorption isotherm of ZY2 as shown in Figure 4.2b, the filling of nanopores commence around 0.78 during the adsorption phase. A hysteresis loop typical of this material was also observed at  $P/P_0$  values between 0.60 – 0.98. Sample ZY2 showed BET surface area of  $4.6\text{m}^2/\text{g}$ , total pore volume of  $0.043\text{cm}^3/\text{g}$  and average BJH adsorption diameter of  $341.6\text{\AA}$ . There was a slight increase in the surface area and pore volume while the average pore diameter was constant resulting in synthesized zeolite ZSM-10 type.

For adsorption-desorption isotherm of ZY3 as shown in Figure 4.3c, the filling of nanopores commence around 0.78 during the adsorption phase. A hysteresis loop typical of this material was also observed at  $P/P_0$  values between 0.60 – 0.99. Sample ZY3 showed BET

surface area of  $22.8\text{m}^2/\text{g}$ , total pore volume of  $0.061\text{cm}^3/\text{g}$  and average BJH adsorption diameter of  $341.6\text{\AA}$ . There was a remarkable increase in the surface area and pore volume while the average pore diameter remained constant resulting in synthesized zeolite ZSM-10 type.

For adsorption-desorption isotherm of ZY4 as shown in Figure 4.2d, the filling of nanopores commence around 0.85 during the adsorption phase. A hysteresis loop typical of this material was also observed at  $P/P_0$  values between 0.75 – 0.95. Sample ZY4 shows BET surface area of  $0.87\text{m}^2/\text{g}$ , total pore volume of  $0.005\text{cm}^3/\text{g}$  and average BJH adsorption diameter of  $762.8\text{\AA}$ . There was a remarkable decrease in the surface area and pore volume while the average pore diameter more than doubled that of ZY1 to ZY3 resulting in the presence of synthesized zeolite Y.

For adsorption-desorption isotherm of ZY5 as shown in Figure 4.2e, the filling of nanopores commence around 0.66 during the adsorption phase. A hysteresis loop typical of this material was also observed at  $P/P_0$  values between 0.38 – 0.98. Sample ZY5 showed BET surface area of  $58.7\text{m}^2/\text{g}$ , total pore volume of  $0.101\text{cm}^3/\text{g}$  and average BJH adsorption diameter of  $64.3\text{\AA}$ . There was a remarkable increase in the surface area and pore volume while the average pore diameter decreases tremendously and remains constant for ZY5 resulting in the presence of synthesized dealuminated zeolite Y.

For adsorption-desorption isotherms of ZY6 and ZY7 as shown in Figures 4.2f and 4.2g, the filling of nanopores commences around 0.67 during the adsorption phase. A hysteresis loop typical of this material was also observed at  $P/P_0$  values between 0.35 – 0.99. Sample ZY6 showed BET surface areas of  $74.4\text{m}^2/\text{g}$  and  $91.8\text{m}^2/\text{g}$ , total pore volumes of  $0.12\text{cm}^3/\text{g}$  and  $0.14\text{cm}^3/\text{g}$ , respectively while the average BJH adsorption diameter of  $64.3\text{\AA}$  was constant

resulting in pure quartz. The upward swings of the hysteresis loops are associated with the filling of the mesopores by capillary condensation which is an indication of type IV isotherm.

Surface area and pore size distribution are important attributes of fluid cracking catalysts measured by the use of  $N_2$  adsorption/desorption isotherms at liquid  $N_2$  temperature and relative pressures ( $P/P_0$ ) ranging from 0.05 – 1.0. A typical isotherm for a zeolitic FCC catalyst should have a large uptake of  $N_2$  at low  $P/P_0$  indicating filling of micropores  $< 20 \text{ \AA}$  in the catalyst. The linear portion of the curve represents multilayer adsorption of  $N_2$  on the surface of the catalyst, and the concave upward portion of the curve represents filling of mesopores of between  $20 - 500 \text{ \AA}$  and macropores  $> 500 \text{ \AA}$  (Brunauer, 1938).

### 5.1.5 Product Evaluations

Hydrocracking of petroleum gas oil (PGO) was studied at reaction temperature of  $450^\circ\text{C}$ , contact time of 90 minutes and catalyst to gas oil ratio of 0.04 and was investigated for their activity performance. The effect of the catalyst on the total conversion and product distribution of PGO is shown in Table 4.7.

The two catalysts exhibited a very stable activity for the conversion of gas oil, though ZY5 was somewhat favoured in terms percentage conversion of 45.73. It is interesting therefore to compare the activities of ZY4 and ZY5 enhanced catalysts with that of the commercial USY zeolite. The total conversion and total distillate fuels for ZY4 based catalysts were lower than that of the commercial catalyst by 2.90 and 1.10, while that of ZY5 is 2.08 lower in the conversion and higher by 2.81 for the distillate fuels. Literature reports revealed that the catalyst with the best activity can produce gasoline in the range of 50-65% (Mu Mu & Mya Mya, 2008). Both ZY4 and ZY5 play two important roles of supplying hydrogen to acid sites for continuous hydrocracking and the other is hydrogenation of aliphatic and aromatic compounds to paraffinic

and cycloparaffinic compounds respectively. Among the two catalysts, ZY5 showed more hydrocracking activity when compared to ZY4 in terms of conversion and total distillate products. The hydrocracking activity of the ZY4 and ZY5 samples are therefore in this decreasing order as follows: USY > ZY5 > ZY4. The reason for higher hydrocracking activity may be attributable to its relatively higher surface area with higher pore size and higher acidity which normally favours successive cracking reactions and consequently formation of lighter products. To crack large hydrocarbons, therefore, dual function catalysts with hydrogenation and cracking functions are needed. Supports provide the cracking functions whereas the cracking takes place on acid sites. The results show that the amount of both gas and coke obtained over the different types of the catalysts was between 6 – 12% and the main gaseous products were ethane, propane, butane and C<sub>5</sub>+

## 5.2 Conclusions

It can be concluded that the Ahoko clay used as a principal raw material in this experiment for zeolite development was the kaolinite clay. The ZY4 and ZY5 samples have a SiO<sub>2</sub>/Al<sub>2</sub>O<sub>3</sub> mole ratio of 3.72 and 2.57. They were prepared by activation treatment using NaOH and hydrothermal crystallization under proper conditions of ageing at room temperature for 24 hours and crystallized at 100°C for 22 hours. It was observed that there were apparent competitions between zeolite Y and other phases during the preparation. Ageing temperature therefore becomes an important parameter that must be looked into to reduce the formation of other phases. However, the purity of the adsorbent/dessicants increased after dealumination as evidenced from the absence of other phases in ZY6 and ZY7.

Finally, zeolites 5A, ZSM – 10 and Y were synthesized with other phases, an indication that the zeolite was yet to develop fully while pure silica was also developed. Petroleum gas oil

was converted to distilled fuels (gasoline, kerosene and diesel) by catalytic hydrocracking over zirconium catalyst supported on ZY4 and ZY5 catalysts at reaction temperature of 450°C, contact time of 90 minutes and catalyst to gas oil ratio of 0.04. A maximum value of liquid product (total distillate fuels) was obtained over ZY5/zirconium catalyst for which the total conversion and yield of total distillate fuels were 45.73 and 39.39 wt. %, respectively, when compared to unloaded commercial USY zeolite which has 47.81 and 36.58 wt. % for total conversion and yield of distillate fuels, respectively.

### **5.3 Recommendations**

It is recommended that for the future interest in this work, the researcher should endeavor to investigate the variable parameters such as composition of the starting materials (amount of added water, a silica source, and an aluminate source), ageing temperature, ageing time and crystallization time before developing the final zeolite. Most importantly, it is recommended that the work be studied at pilot plant level.



## REFERENCES

- Ahmed, Mubarak Alsobaai (2007): Development of NiW-Zeolite based Catalysts for Hydrocracking of Gas Oil: Synthesis, Characterization, Activity and Kinetics Studies. A Ph.D Thesis submitted to Universiti Sains, Malaysia.
- Assaf, A. G., R. H. Haas, and C. B. Purves (1944): A new interpretation of the Cellulose-Water Adsorption Isotherm and Data concerning the Effect of Swelling and Drying on Colloidal Surface of Cellulose. *Journal of the American Chemical Society*, **66**, Pp 66 – 67.
- Barrer, R. M. (1945): Classification of Zeolite Minerals. *Journal of the Society of Chemical Industry*, London, Vol. **64**, Pp. 130.
- Barrer, R. M. (1948): Synthesis of Small-Port Mordenite. *Journal of the Society of Chemical Industry*, London, Pp. 2158.
- Barrer, R. M. (1968): Molecular Sieves: Synthesis of Zeolite A as an adsorbent. *Journal of the Society of Chemical Industry*, London, Pp. 1203.
- Barrer, R. M. (1968): Molecular Sieves: General Conditions for Hydrothermal Synthesis. *Journal of the Society of Chemical Industry*, London, Pp. 39.
- Barrer, R. M. (1982): Hydrothermal Chemistry of Zeolites, Academic Press, London, P. 251.
- Behreins, P. & Stucky G. D. (1996): Comprehensive Chemistry, Aiberti G. Bein Eds., Elsevier, Oxford, Vol. **7**, P. 721.
- Bolton, A. P. & Lanewala, M. A. (1970): The Roles Zoelites as Solid Acid Catalysts. *Journal of Catalysis*, Vol. **18**, Pp. 154.
- Bradley, T. (2004): Dealumination of Zeolites, CHE 697M- Nanomaterials Chemistry and Engineering, Sch. of Chem. Engineering, Purdue University.
- Breck, D. W. & Flanigen, E. M. (1968): Molecular Sieves, *Journal of the Society of Chemical Industry*, London, Pp. 47 - 61.
- Breck, D. W. (1974): Zeolite Molecular Sieves, Structure, Chemistry and Use, John Wiley, New York, P. 4, 134 - 188.
- Bridge, A. G., (1997): In Handbook of Petroleum Refining Processes, Ed, Myers, R. A., McGraw-Hill, New York, P. 7.21, 14.15, 14.33.
- Brunauer, Emmett, Teller, (1938): Adsorption Isotherms. *Journal of the American Chemical Society*, Vol. **60**, Pp. 309.



- Charles, G. H., Jr. (1977): An Introduction to Chemical Engineering Kinetics and Reactor Design, John Wiley, NY, P. 167 – 196.
- Chen, N. Y., Garwood, W. E. and Dwyer, F. G. (1989): Shape Selective Catalysis in Industrial Applications, Marcell Dekker Inc., New York, P. 1- 301.
- Chen, N. Y., Garwood, W. E. and Heck, R. H. (1987): M – Forming by Size Selective Catalysis: *Industrial Engineering Chemistry Resources*, Vol.26, Pp.706 – 711.
- Colin, S, C. and Paul, A. C. (2005): The Hydrothermal Synthesis of Zeolites: Precursors, Intermediates and Reaction Mechanism. *Microporous and Mesoporous Materials*, Vol. 82, Pp. 1 – 78.
- Cronstedt, A. (1756): Zeolite Mineral. Akademik. Handling, Stockholm Vol. 18, Pp. 120.
- Cundy, C. S., Forest, J. O., Plaisted, R. J. (2003): Crystallization. *Microporous and Mesoporous Materials*, Vol. 66, Pp. 143.
- Cundy, C. S., Henty, M. S., Plaisted, R. J. (1995): *Zeolites*, Vol. 15, Pp. 353.
- Cusher, N. A. (1997): In Handbook of Petroleum Refining Processes, Ed, Myers, R. A., McGraw-Hill, New York, P. 9.15.
- Davies, M. E., Saldarriaga, C., Montes, C., Garces, J. and Crowder, C. (1988): *Zeolites*, Vol. 8, Pp. 367.
- Davis, S. (1997): In Handbook of Petroleum Refining Processes, Ed, Myers, R. A., McGraw-Hill, New York, p. 10.45.
- Duong, D. D. (1998): Adsorption Analysis: Equilibria and Kinetics, Imperial College Press, London, Pp. 1 – 132.
- Dwyer, J. (1984): Zeolite Synthesis, *Journal of the Society of Chemical Industry*, Pp. 258 - 269.
- Flanigen, E. M. (1991): Molecular Sieve Structures and Composition, *Studies in Surface Science Catalysis*, Vol. 58, Pp. 13 - 34.
- Francisco Marquez – Linares and Rolando Roque – Malherbe (2003): Zeolites, Part 1: Structural Features, Synthesis, Modification, and Characterization, IUMRS Facets.
- Froix, M. F. and Nelson, R. (1975): The Interaction of Water with Cellulose from Nuclear Magnetic Resonance Relaxation Times, Vol. 8, Pp. 726 – 730.
- Funtua, I. I. (2006): Some Analytical Techniques for Zeolites Characterization, Proceedings of the First Nigeria Conference on Zeolite “Zeolite Science and Technology in Nigeria, Pp. 52 – 57.

- Gadja, G. J., and Barger, P. T. (1993): U.S. Patent, Vol. **5**, 191, 146.
- Gates, B. C., Katzer, J. R. & Schuit, G. C. A. (1979): Chemistry of Catalytic Processes, McGraw-Hill, New York, P. 49 - 50.
- Genis, O. (1997): In Handbook of Petroleum Refining Processes, Ed. Myers, R. A., McGraw-Hill, New York, P. 8.49.
- Giles, C. H., and A. P. De Silva (1969): Molecular Sieve Effects of Powders towards Dyes: Measurement of Porosity by Dye Adsorption, *Trans Faraday Society* **65**, 1943 – 1951.
- Gonthier, S. and Thompson, R. W. (1994): In Jansen, J. C., Stocker, M., Karge, H. G., Weitkamp, J. (Eds.), Advanced Zeolite Science and Applications, "Studies in Surface Science and Catalysis", Elsevier, Amsterdam, Vol. **85**, P. 43.
- Gosling, C. D., Wilcher, F. P., Sullivan, L. and Mountford, R. A. (1991): Hydrocarbon Process.
- Haag, W. O., Lago, R., and Weisz, P. B. (1981): *Disc Faraday Society*, Vol. **72**, Pp. 317.
- Hemmler, C. L. and Jabyl, D. G. (1997): In Handbook of Petroleum Refining Processes, Ed. Myers, R. A., McGraw-Hill, New York, P. 3.55.
- Jeanneret, J. J. (1997): In Handbook of Petroleum Refining Processes, Ed. Myers, R. A., McGraw-Hill, New York, P. 2.45, 2.37, 2.55, 2.27.
- Jentys, A. and Lercher, J. A. (2001): In Van Bekkum H., Flanigen, E. M., Jacobs, P. A. Jansen, J. C. (Eds.), Techniques of Zeolite Characterization, "Introduction to Zeolite Science and Practice", Elsevier, Amsterdam, Pp. 345 – 390.
- Kerr, G. T. (1966): Crystallization Mechanism, *Journal of Physical Chemistry*, Vol. **70**, Pp. 1047.
- Ladisch, C. M., Y. Yang, A. Velayudhan, and M. R. Ladsich (1992): A New Approach to the Study of Textile Properties with Liquid Chromatography, *Textile Research Journal*, Vol. **62**, Pp. 361 – 369.
- Lechert, H. and Kacirek, H. (1975): Seed Crystals, *Journal of Physical Chemistry*, Vol. **79**, Pp. 1589.
- Madon, R. J., (1989): Increasing Gasoline Octane Number during Fluid Catalytic Cracking – Role of ZSM-5 and USY, Advances in Catalytic Chemistry IV, Snowbird, Utah.
- McBain, J. W. (1932): The Sorption of Gases and Vapors by Solids, Rutledge, London, Ch.5
- McCusker, L. B., Baerlocher, Ch., Jahn, E., and Bülow, M. (1991): *Zeolites*, Vol. **11**, Pp. 308.

- Merchant, M. V. (1957): A Study of Water Swollen Cellulose fibers which have been Liquid/Exchanged and Dried from Hydrocarbons, TAPPI Vol. **40**, Pp. 771 – 781.
- Miller, S. J. (1994): Studies in Surface Science and Catalysis, Eds. Weitkamp, J., et al. Elsevier Science, Amsterdam, Vol. **84C**, Pp. 2319 – 2326.
- Milton R. M. (1968): Molecular Sieves, *Society of Chemical Industry*, London, Pp. 199 - 203.
- Mu, M. H. and Mya, M. O. (2008): Preparation of Zeolite Y Catalyst for Petroleum Cracking, Proc. of World Academy of Science, Eng. and Tech., Vol. **36** Pp. 859 - 865. ISSN 2070 – 3740.
- Mullin, J. W. (2001): Crystallization, 4<sup>th</sup> Ed., Butterworth Heinemann, Oxford
- Randolph, A.D. & Larson, M.A. (1988): Introduction to the Theory of Crystallization Processes, 2<sup>nd</sup> Ed., Academic Press, London
- Olson, D. H. and Haag, W. O. (1984): Advances in Chemistry Series, Symposium Series, Vol. **248**, Pp. 275.
- Ozmen, S. M., Abrevaya, H., Barger, P., Bentham, M. and Kojima, M. (1993): Fuel Reformulation Vol. **3**, Pp. 54 - 59.
- Rabo, J. A., Pickert, P. E., Stamiros, D. N. and Boyle, J. E. (1960): Proceedings of the Second International Congress on Catalysis Eds. Technology Eds., Paris, P. 2055.
- Reno, M. (1997): In handbook of Petroleum Refining Processes, Ed. Myers, R. A., McGraw-Hill, New York, P. 7.41.
- Scherzer, J. and Gruia, A. J. (1996): Hydrocracking Science and Technology, Dekker, New York
- Schipper, P. H., Dwyer, F. G., Sparrell, P. T., Mizrahi, S., and Herbst, J. A. (1988): Zeolite ZSM-5 in Fluid Catalytic Cracking: Performance, Benefits, and Applications”, Advances Chemistry Series, Symposium Series 375, Ed., M. L. Ocelli, P. 64.
- Sherman, J. D. (1999): Synthetic Zeolites and other Microporous Oxide Molecular Sieves (A paper presented at the National Academy of Sciences Colloquium “Geology, Mineralogy, and Human Welfare,” Nov. 8 - 9, 1998, Irvine, CA.), Vol. **96** Issue 7, Pp. 3471 - 3478.
- Sohn, S. W. (1997): In Handbook of Petroleum Refining Processes, Ed, Myers, R. A., McGraw-Hill, New York, Pp. 10.75.
- Susan, P. (2003): Generation and Application of Radical Cations in Zeolites Pp. 8 - 9.

- Susana, Lopes Silva (2009): Study of Hydrocracking Catalysts based on Modified USY Zeolites at Instituto superior Technico. A research carried out in IFP – A Research and Technologies Development Centre.
- Suzuki, M. (1990): Adsorption Engineering, Kodansha Elsevier Science Publishers, Amsterdam, P. 1 – 42.
- Thompson, R. W. in Catlow, C. R. A., Vetrivel, R. (Eds.), (1992): Modelling and Reactivity in Zeolites, Academic Press, London, Pp. 231.
- Thompson, R. W. in Harge, H. G., Weitkamp J. (Eds.), (1998): Molecular Sieves, Vol. 1, Springer-Verlag, Berlin, Pp. 1.
- Tosheva, L. (1999): Zeolite Macrostructures, Licentiate Thesis, P. 2.
- Ueda, S. and Koizumi, M. (1979): American Miner, Vol. 68, Pp. 172.
- Verduijn, J. P. (1993): World Patent, 9308124
- Vora, B. V. (1985): U. S. Patent, Vol. 4, 523,045 – 523, 048.
- Vora, B. V., Marker, T. L., Barger, P. T., Nilsen, H. R., Kvisle, S. and Fuglerud, T. (1997): Studies in Surface Science catalysis, Vol. 107, Pp. 87 – 98
- Wallace, J. W. and Gimpel, H. E. (1997): In Handbook of Petroleum Refining Processes, Ed, Myers, R. A., McGraw-Hill, New York, P. 1.15.
- Windsor, C. M. (1998): The Chemistry of Zeolites.
- Zhdanov, S. P. (1968): Molecular Sieves, Society of Chemical and Industry, London, P. 62.
- Zhdanov, S. P. (1971): Advances in Chemistry Series, Vol. 101, Pp. 20 - 43